THE UNIVERSITY OF MICHIGAN

COLLEGE OF ENGINEERING
Department of Meteorology and Oceanography

Technical Report

A STUDY OF AGING OF LEAD AEROSOLS

Dale A. Gillette

ORA Project 01173

supported by:

DEPARTMENT OF HEALTH, EDUCATION, AND WELFARE
U. S. PUBLIC HEALTH SERVICE
NATIONAL INSTITUTES OF HEALTH
GRANT NO. AP-00585-02
BETHESDA, MARYLAND

administered through:

OFFICE OF RESEARCH ADMINISTRATION ANN ARBOR

March 1970

ACKNOWLEDGEMENTS

The invaluable help of others made the following work possible. Professor J. W. Winchester suggested the problem and offered guidance. The work of Part II was aided immeasurably by the kind assistance of Professor W. I. Higuchi and Dr. Akira Suzuki. The chemical analysis method was established by W. Matson and P. Harrison. Constructive criticism and guidance on meteorological matters were given by Professor A. L. Cole and Professor D. J. Portman. The research was supported in part by the Air Pollution Traineeship, National Air Pollution Control Administration of the Consumer Protection and Environmental Health Service grant no. T01 AP-00007 (Department of Health Education and Welfare), and by the National Institute of Health, grant AP-00585. For many hours of constant typing and assistance, I thank my wife Barbara Ann.

TABLE OF CONTENTS

APPENDIX

LIST OF TABLES

LIST OF TABLES (CONTINUED)

LIST OF FIGURES

LIST OF FIGURES (CONTINUED)

LIST OF FIGURES (CONTINUED)

LIST OF FIGURES (CONTINUED)

PART I. THE OBSERVATIONAL STUDY OF LEAD AEROSOL

I. INTRODUCTION

Leaded aerosols[1] have long been of concern to air quality researchers, especially since the advent of tetraethyl lead as an anti-knock ingredient in automobile gasoline.

This study was dedicated to investigating part of the history of leaded aerosols. Lead aerosol history is taken from its injection into the atmosphere, its subsequent alteration by atmospheric processes, and its final removal from the atmosphere by atmospheric mechanisms. Of primary interest in this history was the removal, since removal determines whether a build up of a potentially dangerous pollutant or a maintenance of a rather small amount of rapidly removed aerosol will occur. The means of investigating this history was the study of lead aerosol size distributions close to the ground in areas containing sources of lead aerosol and also in areas where the lead aerosol were aged. In this way the history of lead aerosol was studied from zero to about ten hours of aging time.

The initial appearance of lead aerosol (zero hours) has been studied by others and is covered in the survey

---

[1] Leaded aerosols are defined to be aerosols which contain lead whereas lead aerosol is defined to be that part of the total aerosol which is composed of lead.

of literature. The present work sampled lead aerosol in a number of source regions, and differences which could be attributed to differing sources were looked for as in the study of Robinson and Ludwig (1964). The observed great similarity of all source area lead aerosol size distributions proved promising for finding systematic changes as aging proceeded, since any large difference of aged lead spectra would not be obscured by large differences in the original aerosol.

Aged lead size distributions were collected on Lake Michigan where no local sources of lead were present. Samples were grouped by ages and their lead spectra were compared to source area lead spectra.

In addition to an observational study of the aging of lead aerosol, a numerical model was used to predict mechanisms most important in non-precipitative conditions. Parameters which varied in the numerical model were the initial spectrum of lead and the initial spectrum of the unleaded particles.

An attempt to assess the effect of changing weather parameters upon the lead spectrum in a source area was undertaken. A series of twenty-four hour samples taken at a fixed location in a source area were examined for differences due to response to varying weather parameters.

A. Sources of Atmospheric Lead

Lead occurs naturally in the earth's crust in an average concentration of 16 ppm (Goldschmidt, 1935). Coal contains a lead concentration from 2 to 40 ppm for 23 samples of coal found in the Cincinnati area (Cholak et al., 1961). Concentrations of lead in coal soot and

fly ash ranging from 4 to 358 ppm have been reported (Dunn, 1933; Savul, 1958).

An important source of lead is the breakdown by combustion of tetraethyl lead contained in motor-car fuel. An approximate concentration of lead in gasoline is 2 grams per gallon (U.S. Dept. of Health, Education and Welfare, 1965). If only about one half the combusted lead were exhausted during cruising conditions, as suggested by Hirshler (1964), 0.06 grams of lead would reach the air per automobile per mile, providing that the average automobile traveled 15 miles per gallon. This contribution of lead was reflected in high lead concentrations near highways. Other important sources of lead aerosols are industrial emissions. Industries using quantities of lead greater than 100,000 short tons per year are storage battery manufacturers, oil refining, and construction.

Except for the contribution due to natural soil, automobile exhaust is the most omnipresent of lead sources. And with the exception of industrial areas, where industrial sources of lead may be dominant, the automobile is the most important of lead sources.

B. Survey of Literature

1. Lead aerosol studies

Knowledge of the size spectrum of lead aerosols is desirable in assessing the effects of various mechanisms acting to remove particles in the atmosphere and in assessing possible lung retention.[1] Lead aerosol size

---

[1] Toxicological research has shown no hazard due to the use of tetraethyl lead in automobiles. (Cholak et al., 1961; Kehoe, 1963).

distributions have been sampled mostly in urban locations (Ludwig et al., 1963; Ludwig and Robinson, 1964; Lee et al., 1967).

The work of Robinson, Ludwig et al.,(1964) represents the most comprehensive work on urban leaded aerosol size distributions. Size distribution samples were collected in industrial, commercial, and residential locations in the San Francisco Bay Area and the Greater Los Angeles area. The Andersen Sampler and Goetz Aerosol Spectrometer were to be the primary instruments of their study, but when pilot samples showed the leaded aerosol to be primarily sub-micron, the Andersen Sampler work was discontinued.

Goetz Aerosol Spectrometer samples were limited, however, since sizing for any given test could operate in only part of the 0.025 to 4 micron equivalent diameter size range. In order to collect enough material for analysis, sampling periods were hours in duration and since partial size distributions were collected, total size distributions for the sampling period could only be estimated. Days when lead concentration would possibly be low were avoided, in order to obtain sufficiently large samples.

Along with the primary Goetz Aerosol Spectrometer sample, total lead concentration was independently sampled.

A UNICO model 18 two-stage sampler was generally run parallel to the Goetz Aerosol Spectrometer, and gave some estimate of the distribution of lead in the large particles (greater than 0.8 micron.)

Concentrations of leaded aerosols in the samples were generally in the range of 1-5 $\mu g/m^3$ of air. From the two-stage sampler, it was found that particles larger than 0.8μm contained 16 to 45 per cent by weight of the lead mass. A remarkable consistency was seen in the shape of urban lead size distributions. For all samples an average mass median diameter was characterized as 0.3μm. While differing in total concentration, samples obtained near freeways, in the general urban area and a good distance from the urban center showed great similarity in size distribution. The atmospheric lead aerosols sampled in the 14 locations were seen to be primarily submicron in size.

The analytical chemistry method of determining the total lead content of the samples was a modified dithizone technique. The magnitude of the average analytical lead blank was about 2.5μg and the analytic threshold 0.2μg, thus necessitating large total lead concentrations in order to collect meaningful size distributions for short sampling times. Sampling times for the study were four to eight hours. "A typical size distribution might have a mass median equivalent diameter of 0.2μm with 25 per cent of the mass smaller than 0.1μm and another 25 per cent larger

than 0.5μm".[1]

To broaden the range of the sampling program it was extended to areas where industrial atmospheric lead contributions, such as combustion of coal or oil and/or leaded soil contributions, would be significant. A second observational programwas undertaken which added 28 useful size distributions to the more than 50 obtained in the Los Angeles and San Francisco areas. The new areas sampled for air were Chicago; Cincinnati; Philadelphia; Grand Lake of the Cherokees, Oklahoma; and Lake Mojave, Arizona. The purpose of choosing the Cherokee and Mojave sites was to sample in rural areas having perhaps differing sources of lead than urban locations.

In order to maximize the possibility of obtaining significantly differing lead size distributions, sampling sites, with the exception of Cherokee and Mojave, were chosen to be in closest possible proximity to recognized major industrial lead emissions.

The results of the study showed little variation in the size distribution profiles even though sources of lead emissions, atmospheric conditions, and geography were varied. All distributions were approximated by a mean distribution having a mass median equivalent diameter of 0.25μm with 25 per cent of the mass being contained by particles smaller than 0.16 μm and 25 per cent being contained by particles larger than 0.45 μm.

It was concluded that the uniformity of the results indicated that either automobile exhaust is the dominant

---

[1]Robinson, Ludwig et al. (1963) Variations of Atmospheric Lead Concentrations and Type with Particle Size, SRI Project No. PA-4211, p.71.

source of the leaded aerosol or that the ambient size distribution is independent of the nature of the source.

Concentration and particle size distribution information was collected for six metals including lead in Cincinnati and Fairfax, a Cincinnati suburb, by Lee, Patterson, and Wagman (1967). Particulate samples were collected in Cincinnati for 24 hours and for longer periods in Fairfax using Andersen samplers. The samples were then analyzed by atomic absorption spectrophotometry. The mass mean diameter of leaded particles averaged over all samples was extrapolated to be 0.18 micron, in agreement with the range of values found by Robinson and Ludwig in various urban centers. In Cincinnati 75 per cent of the lead by weight was contained by particles smaller than one micron and in Fairfax 65 per cent of the lead was contained by particles smaller than one micron. Weather parameters were recorded for the purpose of correlating changes of size distribution. Humidity was given special attention but little correlation was found between metal size distribution and average humidity.

Studies of the total lead concentration at varying locations in an urban situation were of interest since, by comparison with standard dilution curves for line, area, and point sources one may learn something of local source strength and may therefore conclude the age of sampled leaded aerosol. Such a study was conducted by Cholak, Schafer, and Yeager (1968). Air was monitored for lead content at three locations within Cincinnati at varying distances from a heavily traveled highway: at the highway, within a public park 1300 feet east of the first sampling station in the direction of the prevailing wind, and in

an average residential area about two miles east of the highway sampling station. Arithmetic means of samples taken for a year were: 7.8, 1.7, and 1.1 $\mu g/m^3$ respectively. A mean concentration at the residential station, almost as large as the station 1300 feet from the highway, appeared to be primarily maintained by local source activity. The percentage of lead mass to total particulate mass was about 8 per cent at the highway and 2 per cent at the other stations, indicating that automobile exhaust was at least 4 times more important in contributing to the total particulate load at the highway in comparison with the other stations. Diurnal and seasonal variations of total lead concentration could be traced to traffic loads and meteorological conditions.

Size distribution information was obtained using Andersen Samplers operated for periods of three days. The collected particulates were analyzed by atomic absorption analysis. The average distribution had a mass median equivalent diameter of approximately 0.30 micron and about 70 per cent of lead mass on particles with equivalent diameter of less than one micron.

Lead concentrations in soil and vegetation samples showed that most of the lead mass fallout was contained within 100 feet of the highway. Likewise dust fall measurements at the highway station gave higher concentrations of lead than the other two stations by the ratio 4.5:1. This is in agreement with the work of Hirschler and Gilbert (1964), which states that much of lead mass of automobile emissions is contained by particles formed as the result of "flaking off" of lead plated onto the exhaust system of the automobile.

Additional lead concentration information in central city and outlying areas was furnished by the Survey of Lead in the Atmosphere of Three Urban Communities (U.S. Dept. of Health, Education and Welfare, 1965). Ratios of average city center concentration to outlying area concentration are: 2:1, 3:1, and 3:2 for Cincinnati, Philadelphia, and Los Angeles respectively. One may think of the city and outlying areas as a conglomeration of area sources having varying strengths usually strongest near the densest concentration of traffic or other lead aerosol producing activity. Diurnally, highest lead concentrations were found in the morning before the breakup of the nocturnal inversion. Highest seasonal concentrations were found in autumn and winter when both atmospheric inversion frequency and coal consumption would be expected to be highest.

Interacting studies of leaded aerosol are studies of the size distribution and of the average residence time of lead in the atmosphere. Knowledge of the lead aerosol size distribution and its change in time are needed to make some assessment of the mean residence time of lead. The mechanisms which remove large particles efficiently are different from the mechanisms which remove small particles efficiently, so that the growth of small leaded particles to large leaded particles is of interest. Likewise residence time for each subregion of the spectrum determines the change of the spectrum with time.

Residence time of lead in the atmosphere was commented upon by G. L. Ter Haar, R. B. Holtzman, and H. F. Lucas, Jr. (1967). Lead-210 is derived from the decay of radon-222 (a noble gas) which escapes from the soil and is dispersed in the atmosphere by turbulent transfer. Lead-210 in the

atmosphere was considered to be practically monomolecular and well distributed. Its removal would primarily be through atmospheric precipitation mechanisms. Mean residence times of lead-210, established from the lead-210 daughter assay, were quoted as being about one month (Burton and Stewart, 1960).

Rain water samples were tested for lead and lead-210 for a correlation study. If the atmosphere were well mixed and the ratio of lead to lead-210 were fairly constant the residence time of lead-210 would also be taken as the residence time of lead. Lead analysis was done in triplicate by the standard AOAC spectrophotometric dithizone method and lead-210 concentrations were determined from the beta count of its bismuth-210 daughter.

Lead and lead-210 data yielded a correlation of 0.98 at one location and 0.63 at the other. It was stated that for lead in the part of the atmosphere effectively cleansed by rain (1 to 10 km) lead residence time was on the order of one month.

However, correlation of lead and lead-210 was quoted to be lacking in air samples about 1 meter above ground. Furthermore, while we would suspect lead-210 to originate from a quite uniform areal source and therefore primarily from rural areas having a small background of unleaded dust, lead would have maxima of source concentrations in regions having high dust backgrounds. The size distribution of lead ranges from particles of molecular size to particles having diameters of millimeters (Hirschler, 1957). Lead-210, however, would probably be quite monodisperse and the variety of mechanisms acting upon the total lead content of the air would not necessarily be effective in cleansing lead-210.

Because lead is present in a large concentration of background aerosol in urban locations, growth of the size distribution in time would be greatly different than the growth of a similar lead concentration in a rural location. The study of the leaded aerosol size distribution and its aging are important considerations in the discussion of residence time of lead in the atmosphere.

2. Lead input spectra

In order to comment on the aging of the leaded aerosol one should know about the size distribution of the lead aerosol as it is injected into the atmosphere. One conclusion of the Ludwig and Robinson (1964) survey of urban atmospheric lead was that the greatest source of lead aerosols was combustion, especially the combustion of coal and automobile gasoline. A number of papers concerning the lead content of automobile exhaust are reviewed below. The postulate that the lead combustion aerosols were predominantly submicron is supported by the most recent studies and by some calculations based on the work of W. I. Higuchi (195 9).

The particle size spectrum of automobile exhaust might be thought of as two spectra: a coarse spectrum of rough particles larger than 0.1 μm, and a fine spectrum of a large number of particles of a small size (i.e. smaller than 0.1 μm). The process of combustion produces the fine spectrum. In this process, particles, especially the leaded salts, are produced by combustion processes: 1) by nucleation of the supersaturated vapors, 2) growth of the nucleii by condensation of the supersaturated vapor onto

the nucleus, and 3) thermal coagulation of the particles.

Coarse particles, on the other hand, are produced when the above particles diffuse or impact onto surfaces of the engine or exhaust system. Deposits of exhaust material are built up, then broken up by mechanical or thermal shock and are exhausted.

Leaded particles produced by combustion and deposition are discussed in the literature pertaining to chemical composition and size distribution.

Ethyl fluid is a mixture of tetraethyl lead, $Pb(C_2H_5)_4$; ethylene dichloride, $C_2H_4Cl_2$; and ethylene dibromide, $C_2H_4Br_2$, adjusted to the weight ratios Pb:Cl:Br::1.00:0.34:0.39. Each gallon of gasoline contains about three cubic centimeters of ethyl fluid or about 2 grams of lead. Since the halogen compounds are added as scavengers of lead one would expect to find lead halides as some of the exhaust particulates.

Hirschler and Gilbert (1964) studied leaded particles collected by an electrostatic precipitator which sampled a mixture of clean air and automobile exhaust over a wide variety of engine conditions. Coarse particles, greater than 5 μm, were found to contain more iron and carbon (reflecting exhaust system deposits) than small particles, but the major components of the leaded particles were lead compounds. An elemental analysis is given in Table 1.

The two most abundant compounds found were the normal lead halide PbClBr and binary complexes of PbClBr and NH_4Cl (in 3 forms). For full throttle conditions, when the exhaust gas is hotter than for city driving conditions, the predominant product is PbClBr.

TABLE 1

ELEMENTAL COMPOSITION OF AUTOMOBILE EXHAUST PARTICLES
(AFTER HIRSCHLER AND GILBERT, 1964)

Element	Fine Particles(d<5 μm)	Coarse Particles(d>5 μm)
Lead	58-74	34-60
Chlorine	5.6-16.8	4.5-11.2
Bromine	8.1-21.3	9.12-23.6
Iron	0-1.3	1.2-11.2
Sulfur	0-1.9	0.2-2.3
Carbon	3.5-10.5	4.6-12.1

It was concluded from the data that in both combusted and "motored"[1] engines the lead alkyls were decomposed and that primarily inorganic lead compounds resulted. Tests showed that the ratio of organic lead to unburned hydrocarbons was very small (0.023%-1.7%) in the exhaust gas, implying a rather complete decomposition of tetraethyl lead into inorganic particulates.

Calingaert, Lamb et al. (1949), in studying the lead chloride-lead bromide system, concluded from X-ray diffraction and thermal analyses, conductivity measurements and studies of aqueous preparations that no binary compounds exist in the system other than the preferential replacement structure PbClBr. The PbClBr structure was found to be stable at room temperature but not at the melting point. Thus at high temperatures one would be primarily interested in the formation of $PbCl_2$ and $PbBr_2$.

---

[1] Motored is defined as the operation of the engine without a spark.

A thorough study of lead size distribution over a wide range of engine conditions, including acceleration and deceleration, was reported by D. A. Hirschler et al. (1957). Particles were collected by passing the entire output through an electrostatic precipitator which would extract 90-95 per cent of the lead present in the exhaust gas. The particles were then collected in a solution and sized by successive separations by a centrifuge. Since this method of collection would lead to rapid coagulation, especially of particles smaller than 0.1 μm, the study was of primary value not in establishing detailed size distribution information, but rather in the rate of lead products issuing forth under varying engine conditions. Large particles, in general, would be expected, since a portion of the lead in the exhaust gas deposits onto the surfaces of the exhaust system and is later "flaked off" by increased gas velocity, thermal shocks, etc. as particles of larger size.

At constant speeds, only a fraction of the total lead burned was exhausted. At increasing speeds[1] a larger fraction of lead exhausted to lead burned was recorded and, as might be expected, a larger fraction of total lead particulate was in coarse particles. Tests during a cycled operation of an engine gave a wide variety of the ratio of exhausted lead to burned lead. On the average the ratio could be set 28.2 per cent to 44.8 per cent. On the whole, larger values of the ratio and a

---

[1] Constant speeds of 25, 45, and 60 m.p.h. were used.

larger fraction of coarser particles to fine particles was found for acceleration, deceleration, and high speed driving. This could be explained by "flaking off" of deposited lead from the exhaust system during the conditions of acceleration and high velocity.

A limited number of tests for lead content of automobile exhaust were carried out by McKee et al. (1960). Particulate samples were collected on 20X25 cm (8X10-inch) sheets of glass fiber filter and analyzed for lead by flame photometry. It was found for a 1954 model Plymouth engine, operated under a variety of conditions, that lead compounds collected on the average 60 per cent to 80 per cent by weight of the total particulate except for 30 m.p.h. deceleration (38%) with blowby emitting perhaps 1/3 to 1/2 as much lead as found in the exhaust gas.

Tufts (1959) sampled for lead particulates at three sites and tested the particles on membrane filters with an alcoholic solution of tetrahydroxyquinone which forms a red precipitate with lead. Relations were derived to deduce the original size of the leaded particulate from the spot of precipitate. The three sampling sites represented greatly differing traffic conditions: a busy intersection, a busy highway, and a small shopping district. Results for the three sites showed great similarity in lead particle size distribution. In all cases the largest number of leaded particles was in the size range from 0.01 to 2.7 microns.

The study of lead particle size distribution by Mueller et al. (1962) sampled directly from the exhaust stream using three methods of particle sizing. The sampling, however, was done only for steady state (cruising)

conditions and therefore did not include the conditions that Hirschler et al. (1957) stated would produce large particle sizes: acceleration and deceleration. Three cars were operated on a chassis dynamometer at cruising speeds of 25, 45, and 60 m.p.h. Fuels contained 3 ml tetraethyl lead or 3 ml tetramethyl lead and the lead analysis was conducted using a polarographic method. It was found that those fine particles on the Andersen sampler stage 7 (back up filter) and the Goetz Aerosol Spectrometer did not vary significantly with changing car model, speed, fuel or interaction between car and speed.

Results are summarized in Table 2.

TABLE 2

AUTO EXHAUST ANALYSIS
(AFTER MUELLER ET AL., 1962)

Item	Particle Size (Diameter at Unit Density), μm		
	>2	<2	<0.3
Aerosol concentration, μg per liter	8 to 20	32	>22
Lead concentration, μg per liter	...	13	>8.8
Aerosol lead content, per cent	...	40	40
Size distribution by weight, per cent	20 to 38	62 to 80	>43 to >55

A size distribution of exhaust shortly after leaving the combustion cylinder may be inferred from the work of Zimpell and Graiff (1967). Sampling was done using a time resolution disk revolved by the crank shaft so as to sample

from the end gas region of the engine at a definite position of the piston. Samples were then photographed using an electron microscope. A series of photographs taken during the operation of the engine showed that the size distribution before the arrival of the flame front consisted almost entirely of particles having a diameter of approximately 0.01 μm and having similar morphology. After the arrival of the flame front the size distribution was more disperse and had particles up to the size of 0.1 μm but particles of 0.01 μm diameter were still most numerous.

Indeed, calculations based on the work of Higuchi (1957) indicate that the mean radius of lead combustion aerosols is approximately 0.01 to 0.05 microns. Calculations were based on the assumption that nucleation of leaded particles was not the limiting factor of the agglomeration rate and the mean particle size was expressed in terms of particle concentration. Details are given in Appendix III. Results of the calculation of mean size for Pb, PbO, $PbCl_2$, and $PbBr_2$ for temperatures of 100, 200, 300, 400, 500, and 600°C and for varying initial concentrations of the lead compounds gave remarkably similar results after about one second. A mean radius of 0.01μm to 0.05 μm was inferred for combustion lead aerosols for automobile and for other combustion processes, such as combustion of coal and oil.

C. Statement of Problem

The purpose of this investigation was to study the history of lead aerosol after its injection into the atmosphere of a source region to a period of ten hours. The work of Ludwig and Robinson (1964) showed that lead size distributions in urban areas were very similar. A first step in the present investigation was to check this result using a different collection instrument, the Andersen Sampler. Lead aerosols from source areas, including a large city and cities of population between 100,000-200,000, were collected and lead size distributions compared. Great similarity in the source area size distributions would make obvious upon comparison of aged size distribution samples and source area samples the effects of aging.

A second step was the collection and classification of aged lead aerosols. Aged lead aerosol samples were obtained by sampling the air over Lake Michigan, a large region having no atmospheric lead sources. Aging time was taken to be the travel time of the sampled air over the lake, which was established by backward trajectory analysis. Weather data were taken for all samples to correlate with changes in the lead spectrum.

For comparison of aging effects the above aged lead aerosol size distribution samples were divided into four groups: 1) samples taken in source regions of lead (cities) which were subdivided into urban (Chicago, Calumet Harbor) and city (100,000 to 200,000 population) (Lincoln, Nebraska; Ann Arbor, Michigan) samples; 2) samples of lead aerosol which had been allowed to age by whatever atmospheric processes were present for less than or equal to one hour but

not including samples in group 1, (establishing, when compared to source region samples, whether a rapid change of the mass distribution took place after transport from the source region); 3) samples which had been aged one to six hours, (providing an intermediate aging classification should the short term aging samples and long term aging samples differ greatly) and; 4) samples aged longer than six hours (giving "background size distribution of lead".

Steps 1 and 2 were carried out in largely non-precipitative atmospheric conditions. That is, the aging observed was due to atmospheric processes other than those associated with clouds and precipitation. A third step attempted to assess the effects of changing weather parameters by sampling within a source region on successive days for a month. Weather parameters were recorded and were examined in studying the differing lead spectra.

Finally, a numerical model simulating the leaded aerosol was operated to compare observed aging with aging due to the processes thought most important in the dry atmosphere: i.e. thermal coagulation and gravitational sedimentation. Aging from simulated urban atmospheres and atmospheres perhaps characteristic of a city with a population of 100,000-200,000 was conducted and compared to the observed samples. Aging of several hours in duration was conducted using different input lead spectra and different unleaded (background) spectra. The features of this lead size distribution aging were discussed and compared to observations.

II. THE OBSERVATIONAL TECHNIQUES

A. Data Collection and Presentation

The lead concentration of aerosols sampled is displayed graphically in the results and discussion section and in Appendix II. All size distributions are given in Appendix II in tabular form. Lead concentration is expressed in nanograms per cubic meter of air. Estimated maximum error is given by bars, limiting possible upper and lower values, centered at the measured values. The ordinate, reading from 1 to 8, corresponds to the Andersen Sampler stage. Size fractionation of the aerosol was accomplished using the Andersen Sampler (a cascade impactor) whose stages, given numbers 1 through 8 corresponding to the uppermost stage through a clean up filter, separate decreasingly large particles from the total particulate.

Sampling sites of the lead aerosols were source regions and one source free region on Lake Michigan. Several samples of long duration were taken in Ann Arbor, Michigan. Two sampling sites were used in Ann Arbor, a city having a population of about 100,000, with automobile exhaust as its virtually sole source of lead particulate. One sampling site was in a residential section in south Ann Arbor. The sampler was located at ground level about 30 m from the street. Samples were taken for periods of 24 hours to determine the effect of weather conditions upon the lead size distribution near the source. The other

Ann Arbor sampling site was the East Engineering Building on the University of Michigan campus. Samples were taken on the roof of the building for periods of time corresponding to a significant state of the weather. That is, a sample was changed when a given weather situation significantly changed.

Two sampling sites were used in Chicago. One site was in Calumet Harbor located in south Chicago and surrounded by heavy industry and major highways. The heaviest atmospheric concentrations of lead for all samples were found at this location. The other Chicago location was at the Central Water Filtration Plant located on a man-made peninsula in Lake Michigan.

Samples were taken in a residential section of Lincoln, Nebraska, a city having a population of about 150,000. Samples were taken here for about 24 hours to add to the number of sampling locations. At this location, less industrial than the Great Lakes region where all other sampling took place, differences of the characteristic lead spectrum were sought.

Two other locations, in areas of little industry but significant traffic flow, were also used as sample sites. One site was a residential area in Sidney, New York, about 50 m from a street. The other site was in Ocho Rios, Jamaica, about 100 m from a highway.

In order to ascertain if fast aging of the lead spectrum were taking place, three sampling sites were chosen so that when wind was from the quadrant south to west, aerosol from basically the same source region would be sampled by all three sites but each

CHICAGO AREA MAP

MUNICIPALITIES SUPPLIED FROM CHICAGO WATER WORKS SYSTEM

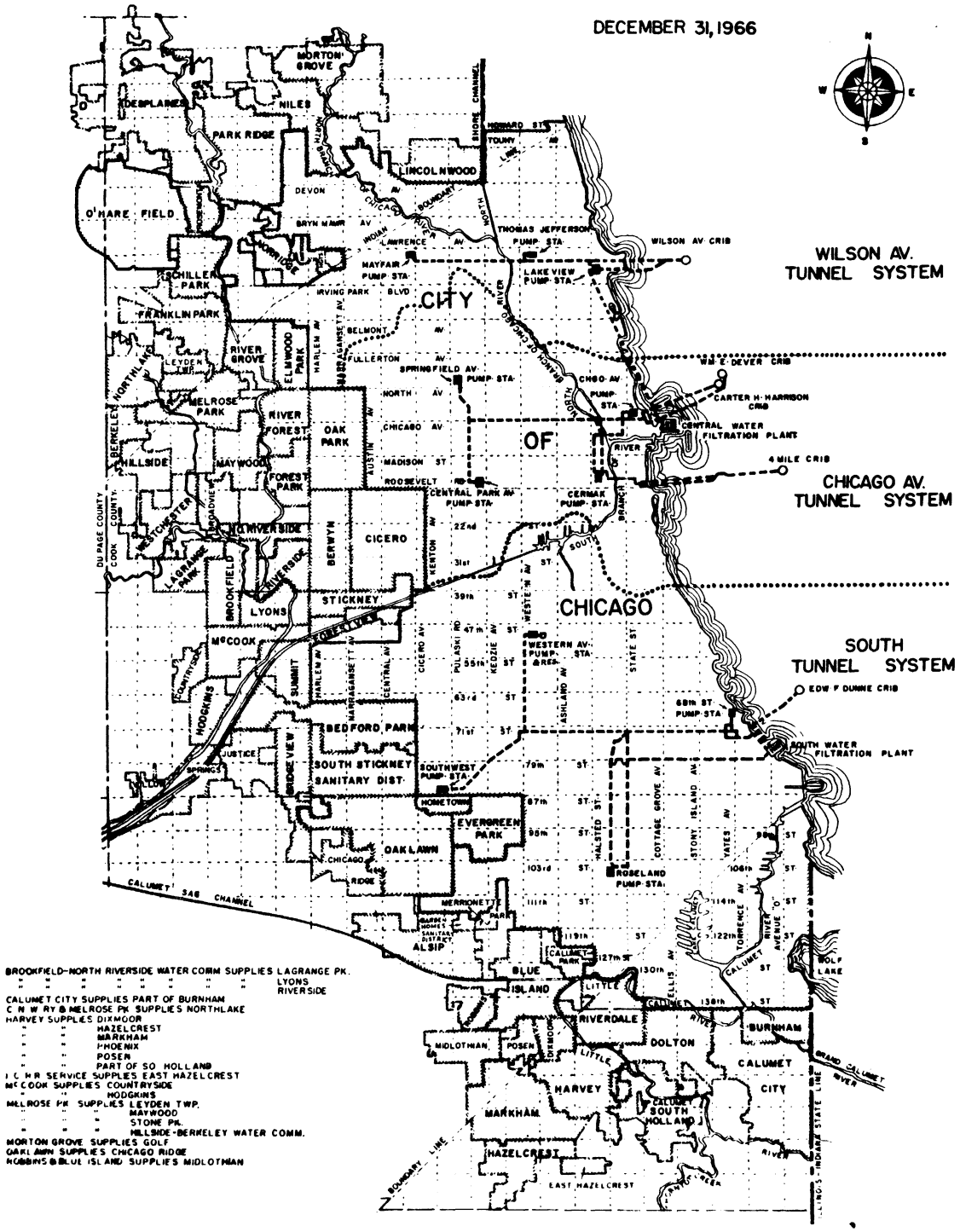

Fig. 1.--Sampling locations were at the Harrison and Dever Cribs, the Central Water Filtration Plant and on Calumet River and approximately 104th Street.

site would correspond to a different travel time over Lake Michigan. The first site or shore site was located at the CentralWater Filtration Plant, as mentioned. The second site, located about 4000 meters from shore, was the combined Wm. E. Dever and Carter H. Harrison water intake cribs. The third site was the deck of the R/V Inland Seas which moved along a path ten to fifteen miles from shore.

The R/V Inland Seas was also used for sampling when the travel time over the water was longer than an hour. One set of samples was taken on the R/V Mysis in an east-west traverse of the lake.

Since the present study was concerned with the aging of aerosol (the travel time of an air parcel after leaving the shore to its being sampled on the ship deck) a trajectory analysis was employed. That is, meteorological(circuit "a") data from stations surrounding Lake Michigan and from ships were plotted each hour on Great Lakes plotting diagrams. Stream lines were deduced from the plotted wind information and were taken as trajectories valid for one hour. Full trajectories were taken to be the sum of the one hour trajectories begun at varying points at the shore at varying times and ending at the particular position of the sampling ship.

In certain cases, however, travel times computed in the above manner did not correspond to reality due to the so called "cold dome" effect (Bellaire, 1965), also called the spring lake anticyclone effect (Strong, 1968). In this situation, which often occurs in the spring, air over the lake is composed of a blanket of cold subsiding air having

little turbulent transfer of horizontal momentum while air moving over this blanket may have a relatively high speed. Polluted air traveling above this blanket or "cold dome" transfers little, if any, of its mass or momentum and thus the air of this "cold dome" may have a travel time from shore much longer than the above trajectory analysis would indicate and have traveled from a different source region.

To test for the"cold dome"effect, pilot balloon ascent readings were recorded and calculated for upper winds. Comparison of these winds to winds at mast height and consideration of the wave height gave some idea of the transfer ofhorizontal momentum. For extremely small momentum transfer a "cold dome" was assumed. For example, if a large wind velocity existed at 100 m, a reduced wind velocity existed at mast height, and the wave heights were negligible, then the presence of the "cold dome" was inferred. If a "cold dome" were deduced to exist for a given sampling period, the travel time of sample air, calculated from the described trajectory analysis, was considered as a lower limit estimate of the travel time.

In addition to trajectory and wind and wave momentum tables, weather information abstracted from shipboard and local weather information are given in Appendix II.

Lead size distributions were normalized by using a size distribution closely approximating the empirical "continental aerosol" distribution of Junge characterizing the naturally occurring aerosol mass-size distributions found over continents. The "Junge" distribution (abbreviated to Std. in the Results and Discussion section) was used to show the shape of the lead aerosol size distribution

in comparison to the size distribution of the total aerosol. E.g., a value greater than one for any stage would indicate that a higher percentage of the total lead mass was found in the size range collected by the impactor stage than would be found in the aerosol as a whole.

The characteristic distribution of continental aerosol was given by Junge (1955, 1964) in Figure 2. The upper limit of the continuous spectrum was given as 20 μm and the lower limit was approximately $4X10^{-3}$ μm. Some discontinuous particle groupings existed below that size.

The remarkable feature of the size distributions observed by Junge is their regularity above r=0.1 μm which is empirically written:

$$\frac{dN}{d(\log r)} = cr^{-\beta}$$

where $\beta \sim 3$

and c = constant.

N is the total number of aerosol particles with radii smaller than r. The number of particles ΔN between the limits of the radius interval Δr is:

$$\Delta N = n(r)\Delta r$$

where $n(r) = dN/dr \quad cm^{-3}$.

Therefore $n(r) = \frac{dN}{dr} = (c/2.30)\, r^{-(\beta+1)}$.

The distribution used ("Junge") was

$n(r) = \text{constant} X r^{-4}$ for 0.1 μm≤r≤20 μm

$n(r) = \text{constant}$ for 0.01 μm≤r≤0.1 μm.

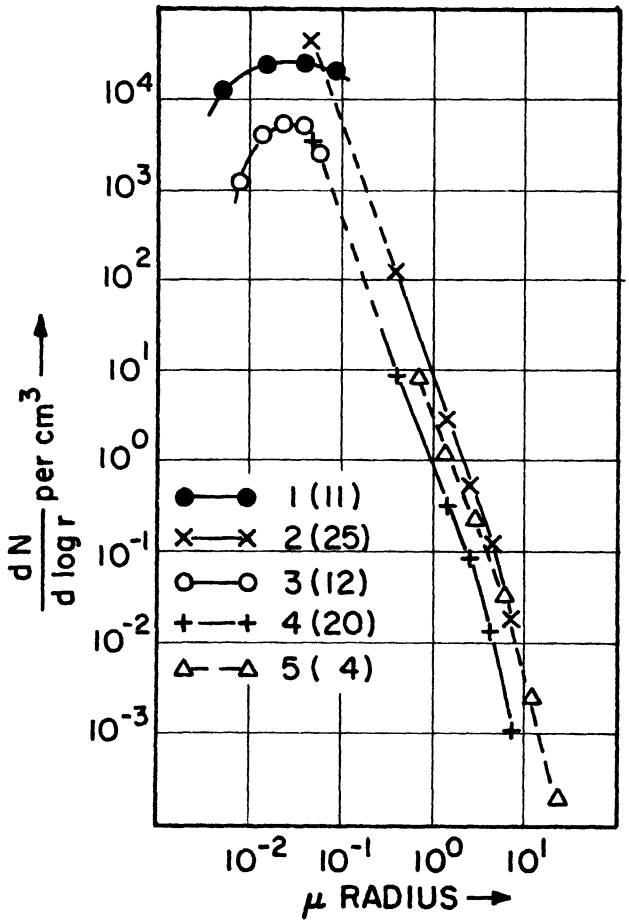

Fig. 2.--Complete size distributions of natural aerosols, average data (after Junge, 1964). Frankfurt/Main, curves 1, 2, and 5. Curve 1, ion counts converted to nuclei numbers. Curve 2, data from impactors. The point below 0.1 μ radius was obtained from the total Aitken nuclei number under the assumption that the radius interval of the Aitken nuclei is $\Delta \log r = 1.0$. Curve 5, average sedimentation data over a period of 11 days. Curves 1, 2, and 5 are not simultaneous. Curves 3 and 4 are simultaneous measurements at the Zugspitze, 3000 meters above s.l., and correspond to curves 1 and 2 for Frankfurt. The figures in parentheses give the number of individual measurements. The dashed curves between 8×10^{-2} and 4×10^{-1} μ are interpolated.

This reference "Junge" mass distribution, as collected by a simulated Andersen Sampler is given in Table 3.

TABLE 3

PERCENT OF TOTAL MASS VS. ANDERSEN SAMPLER STAGE FOR THE "JUNGE" DISTRIBUTION

A.S. Stage	Per Cent of Total Mass
1	25.0
2	9.8
3	9.8
4	9.8
5	11.1
6	9.8
7	8.4
8	16.4

The simulated Andersen Sampler was used in Section II to allow direct comparisons between the observations and the model.

It must be remarked that this standard distribution was based on two parameters. The shape of the "Junge" distribution and the particle size collected on each Andersen Sampler stage were the two parameters needed to compute this distribution. The calibration data of Andersen (1966) were used (page 31) for stages 1 through 5 and the value for stage 6 was taken from values of Flesch et al. (1967), while the stage 7 value was estimated from considerations found in Appendix IV. That is, since jet velocity is estimated to be 43 m/sec. (141.48 ft/sec.) for stage 7 in comparison to 23.2 m/sec. (76.4 ft/sec.) for stage 6, which has an equal orifice diameter, an impaction efficiency of 50 per cent on stage 7 is assumed to correspond to a value of τ 0.54 times

the value of τ on stage 6. Thus an estimated diameter cutoff at stage 7 is approximately 0.4 μm. The cutoff diameter is simply that diameter at which impaction efficiency is placed at 50 per cent. In practice this diameter is used as the minimum size collected by the impactor stage.

The shape of the "Junge" distribution is the other important parameter. Although the distribution used deviates from the empirical distribution of Figure 2 the mass at stage 7 is not sensitive to the choice of the lower limit of the $n(r) \propto r^{-4}$ dependency, since the 50 per cent efficiency limit of the impaction on stage 1 is well above the radius chosen for that lower limit. Actually the detail of the continental aerosol spectrum below r = 0.1 μm was simplified for convenience by the numerical methods of Section II. The lower limit of r = 0.1 μm for the r^{-4} dependency corresponds to the theoretical treatment of aerosol spectra by Friedlander (1960) and to Junge's (1963) lower limit of the r^{-4} dependency, although Junge gives the radius for maximum concentration as r = 0.03 μm. Due to the uncertainty of the empirical distribution in the range $0.01\ \mu m \leq r \leq 0.1\ \mu m$, the given distribution seems to be justified. The upper limit of the distribution, r = 20 μm, is given by Junge (1963). It is seen that the magnitude of the normalized lead distribution stage 8 is a function of both the cutoff diameter of stage 7 and the assumed "Junge" mass distribution in the smallest particles.

A mass median diameter (MMD_7) was determined for the seven impaction stages of the Andersen Sampler. This parameter was found by plotting on probability paper the total distribution of the seven stages using MMD_7 as the diameter corresponding to 50 per cent of the mass. A lead mass distri-

bution showing heavy concentration of lead mass at small diameters would have an MMD_7 smaller than that of a distribution with a smaller concentration of lead mass at small particles. An MMD_7 larger than that of a "Junge" distribution, would have a larger lead mass concentration in large particles than found in the "continental size distribution". The MMD_7 for the "Junge" distribution was found to be ~ 2.5. The ratio of the determined amount of mass on the backup filter (stage 8) to the amount of mass on stage 8, if the mass distribution had been the arbitrary "Junge" distribution, was also determined. That is, the ratio of the percentage of total lead mass on the backup filter (stage 8) to the percentage of mass on stage 8 for the "Junge" distribution was determined as a parameter showing the concentration of the smallest lead particles collected with the Andersen Sampler.

B. Field Sampling Instrumentation

The Andersen Sampler[1] (Model 0203) was used to collect and sort the total aerosol by size fractions. The instrument is known as a cascade impactor because it consists of seven impaction stages, each stage of increasing impaction efficiency for smaller particles.

The impaction process is one in which particles suspended in air deviate from curved air streamlines due to their larger masses. Air particles, in negotiating a sudden change of direction, have sufficient force applied by the pressure gradient to alter their momenta, their trajectories

---

[1] Andersen Air Samplers, 1423 South 2nd West, Salt Lake City, Utah.

thus being identical with the streamlines. An aerosol particle, however, having larger momentum than an equivalent volume of air will depart from the streamline since the force at a given point (pressure gradient, external forces, etc.) is sufficient only to change fluid momentum to follow the streamline.

The curvilinear motion of an aerosol particle for low values of the Reynold number may be written (Fuchs, 1964)

$$m \frac{d\vec{V}}{dt} = -6\pi\eta r \, (\vec{V} - \vec{U}) + \vec{F}$$

where m is the mass of the particle
t is time
η is the viscosity of the medium
$\vec{V}$ is the velocity vector of the particle
$\vec{U}$ is the velocity vector of the medium
and $\vec{F}$ is the external force.

The equation states that the change of momentum of the particle is balanced by the Stokes drag due to the differential velocity of particle and medium.

This equation may be solved for particle trajectories. Davies and Aylward (1951) took air to be an ideal fluid issuing forth in a two dimensional jet onto an infinite plate. From these computed trajectories the efficiency of impaction, defined as the ratio of particles striking the obstacle to the number which would strike it if the streamlines were not diverted by the obstacles (assuming all striking particles stick), was numerically determined. A discussion of impaction efficiency may be found in Appendix IV.

The Andersen Sampler, having improved efficiency for small particles on successive stages was calibrated experimentally by Andersen (1966), Flesch et al. (1967), and May

(quoted in Flesch et al. 1967). Results are given in Table 4. All cutoff diameters were quite similar and the Andersen data were used in this work for stages 1-5 and the Flesch data for stage 6.

TABLE 4

CALIBRATION OF THE ANDERSEN SAMPLER
50% CUT OFF DIAMETERS

Stage	1	2	3	4	5	6	7
Andersen	9.2	5.5	3.3	2.0	1.0	---	---
Flesch (averaged)	---	5.35	3.28	1.76	.89	.54	---
May	---	5.5	3.5	2.6	1.1	---	---

Stage 7, not used in the above calibration, was estimated to have a similar performance to the other stages and was estimated as explained above.

Stage 8 of the Andersen Sampler was an in-line or backup filter. For this work a glass fibre Gelman Type A filter was used. The filter is quoted to have collection efficiency greater than 98 per cent for particles as small as 0.05 μm. 'Specifications manual, Gelman Instrument Co., 1968).[1]

The air flow through the impactor was provided by an electric vacuum pump (Gelman, Cat. No. 25002) at a rate of 28 liters per minute.

---

[1]Gelman Instrument Co., P.O. Box 1448, Ann Arbor, Michigan, 48106.

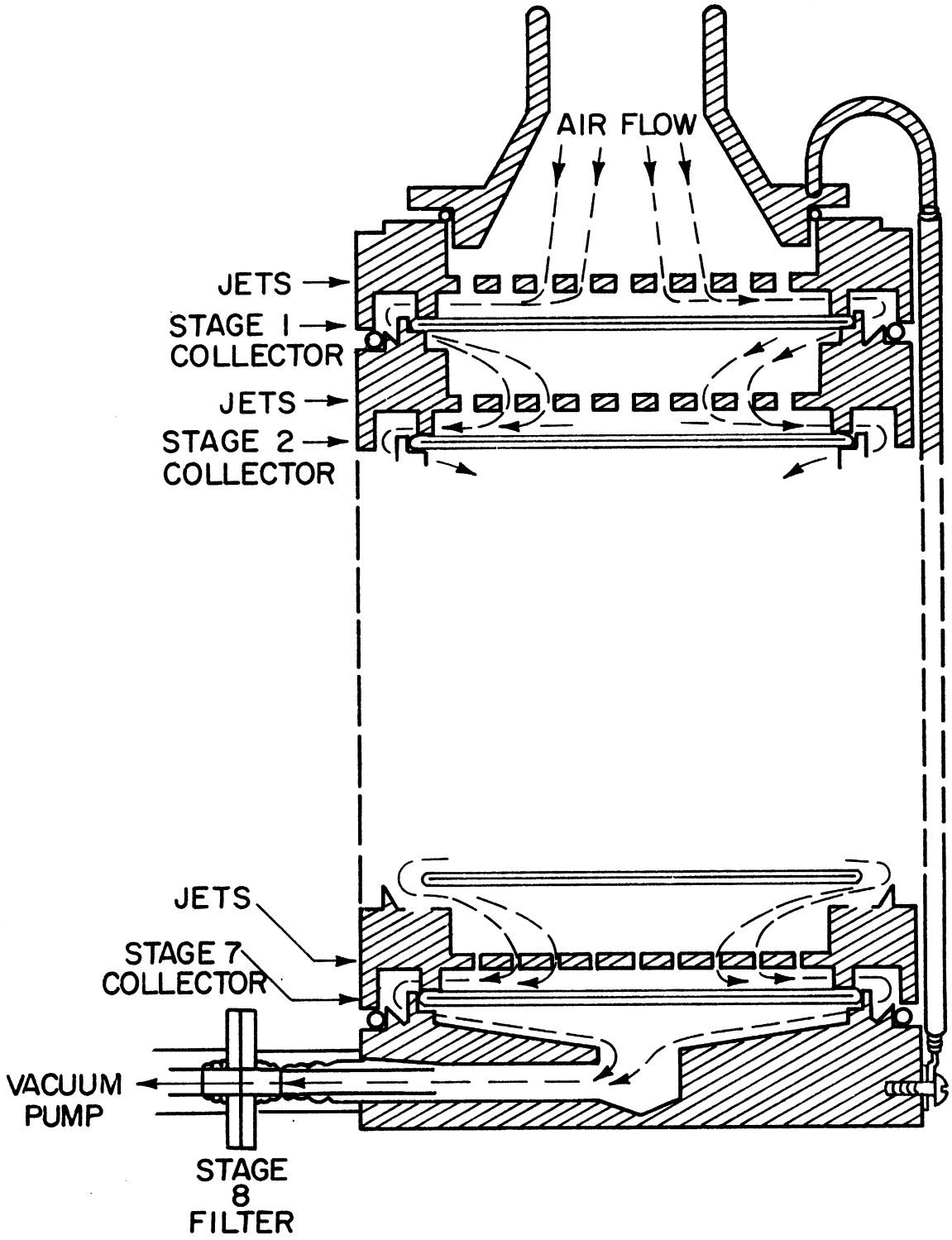

Fig. 3.--Schematic view of the Andersen Sampler Model 0203 Cascade Impactor.

To protect the instrument from direct rainfall a rain shield, consisting of an inverted petri dish, was fitted on top of the sampler. In practice each impaction plate was covered by a thin disk of soft polyethylene to facilitate the sample transfer process and to provide a soft surface on which impaction would take place.

Before each sample run the Andersen Sampler was cleaned and filled with washed polyethylene disks. The disk was washed by placing it in a beaker of triply distilled water and treating it with ultrasonic vibration to remove foreign materials. After a sampling run was completed the polyethylene disks were removed and stored in plastic disposable petri dishes.

C. Chemical Analysis

By the use of anodic stripping voltammetry to test for lead, both urban and rural mass vs. size distributions were studied. This analytical technique with blanks[1] as low as approximately ten nanograms (rather than the thousand nanogram blanks used in other analyses) was used to determine lead aerosol size distributions in regions having low lead concentrations for shorter sampling periods than mentioned in the literature.

---

[1]Blanks are the response of the instrument to a clean or "blank" sample. The signal of a sample is the response to that sample minus the blank so that sensitivity of an instrument is largely a function of the blank.

1. Transfer of sample

Transfer of the collected sample into a 10 ml solution of 0.1 N NaCl solution was accomplished by cutting the polyethylene sample disk in half, submerging one half of the section in the solution, and treating it with ultrasonic vibrations from 3 to 45 minutes. Sample solutions, warmed by the heat of dissipation of fluid motion, were cooled prior to plating. Tests of the sample transfer process showed that more than 90 per cent of total sample was transferred for a variety of sample concentrations (see Appendix I).

2. The analytical method: anodic stripping voltammetry

Anodic stripping voltammetry (abbreviated A.S.V.), a polarographic technique, was useful for determining lead, copper and cadmium mass (Matson, 1966). The method consisted of two steps: 1) plating (reduction of sample cations) and 2) stripping (oxidation of the reduced cations. During the plating step lead ions and other cations were reduced from the sample solution to an amalgam of the mercury layer of a composite mercury-graphite electrode. This electrode was maintained at a potential in the region which corresponded to the diffusion plateau of lead on a polarographic wave. In order to obtain a sufficiently large signal step 1 was longer in duration than step 2. During the stripping step the plated metals were oxidized by increasing the voltage in a linear sweep. The ratio of

plated lead to lead ion as voltage increased may be approximately expressed by the Nernst equation

$$E = E^\circ + \frac{RT}{2F} \ln \frac{[Pb^{++}]}{[Pb(Hg)]}$$

where E is potential difference
E° is the electromotive force for the cell in which the activities of the reactants and products of the cell are each equal to unity
F is the faraday
[ ] is activity
T is temperature
and R is the gas constant.

Voltage was increased linearly with time and as lead ions were stripped current, proportional to the mass of lead plated on the electrode, was recorded.

At the voltage E = E°, the activity of lead ion would be as large as plated lead and E° would be the voltage of the maximum Faradaic current. Since E° values for cadmium, lead, and copper were well separated, three characteristic current vs. voltage curves for each sample could be distinguished. In reality the part of the current vs. voltage curve, up to maximum current, may be approximated by the Nernst equation while the decreasing part of the curve would show the effect of finite numbers of lead ions. A typical curve may be found in Appendix I.

The reaction, which took place at reference electrode, was $AgCl + e^- \rightarrow Ag + Cl^-$. The standard electrode potential of this reaction is +0.222 volts on the electrochemical scale. Standard electrode potentials at 25°C and half cell reactions for those elements encountered in A.S.V. are given in Table 5 (Daniels and Alberty, 1966). The voltage of the test electrode was maintained on a bias to the

reference electrode. E.g. the bias to E° of an element is the difference between the standard electrode potential for the element minus the standard electrode potential for the $AgCl + e^- \rightarrow Ag + Cl^-$ reaction.

TABLE 5

STANDARD ELECTRODE POTENTIALS AT 25°

Electrode	E°	Half Cell Reaction
Cl^-; AgCl(S), Ag	0.2224	$AgCl + e^- \rightarrow Ag + Cl^-$
Cu^{2+}; Cu	0.337	$1/2\ Cu^{2+} + e^- \rightarrow 1/2\ Cu$
Pb^{2+}; Pb	-0.126	$1/2\ Pb^{2+} + e^- \rightarrow 1/2\ Pb$
Cd^{2+}; Cd	-0.403	$1/2\ Cd^{2+} + e^- \rightarrow 1/2\ Cd$

The test electrode was a composite mercury-graphite electrode which was produced by impregnating a graphite rod, properly drilled, with wax. A one cm long tip was left exposed after the remainder of the rod had been covered by a moderately thick coating of wax. A thin layer of mercury was then plated onto the polished tip. The counter electrode was a platinum wire housed in a glass tube and capped by a Vycor plug. The reference electrode was a silver wire housed in a glass tube and capped with a Vycor plug. Mass transfer toward the mercury-graphite electrode was increased by the bubbling of nitrogen gas at a pressure of two psi through the mercury-graphite electrode into the test solution. The A.S.V. cell is shown in Figure 4.

A circuit diagram of the instrumentation used in anodic stripping voltammetry is given in Figure 5. The principal part of the instrumentation is that of box B. The effect of this circuitry is that a sufficient amount of

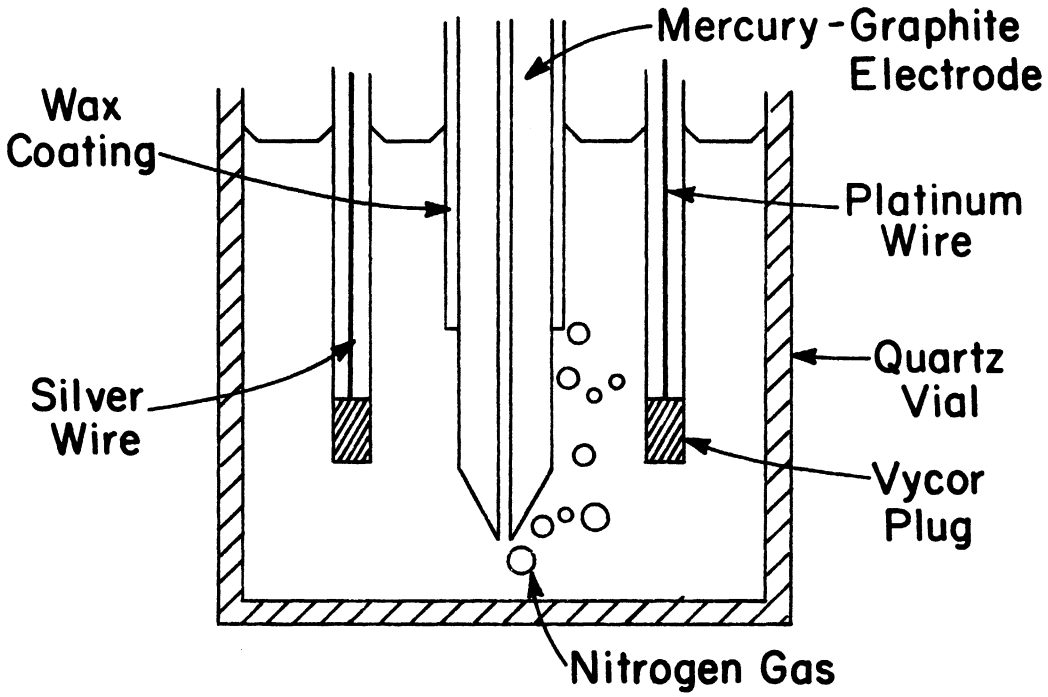

Fig. 4.--Schematic view of the A.S.V. cell.

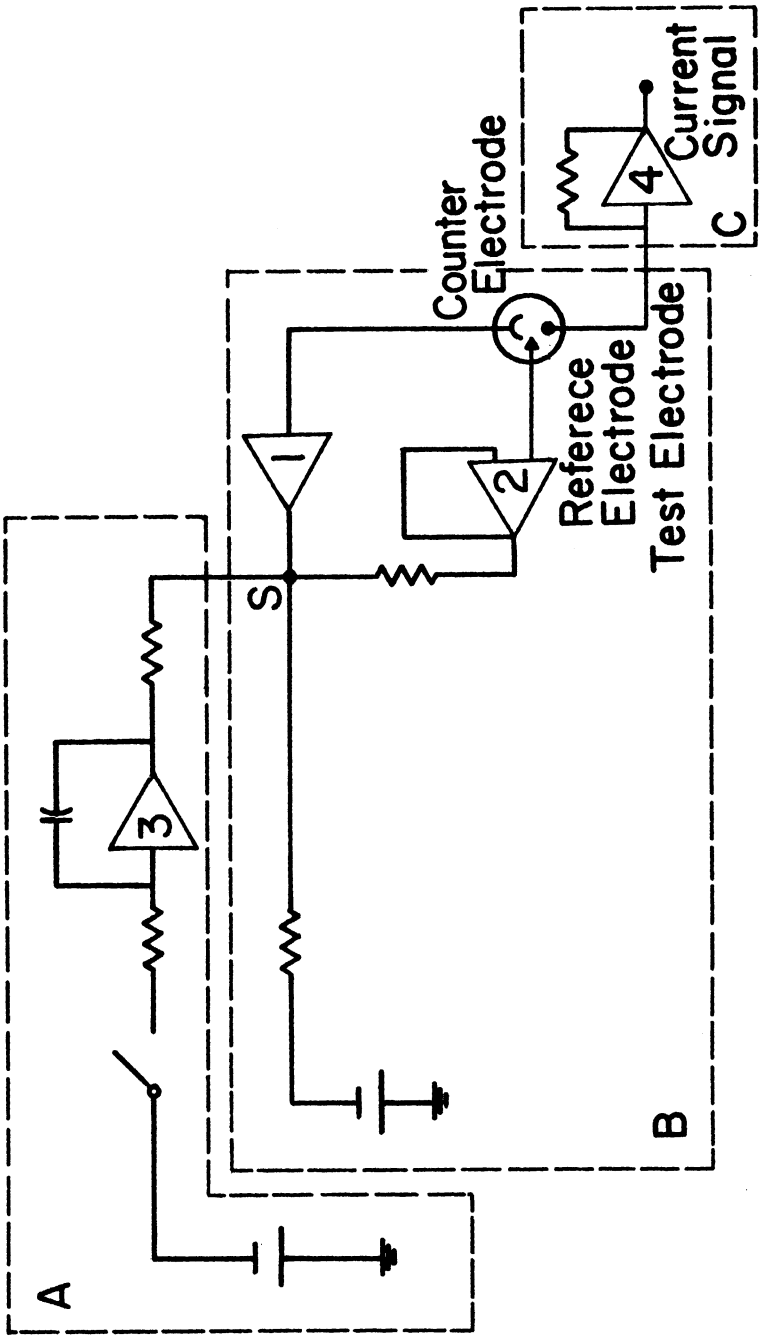

Fig. 5.--Circuitry of A.S.V.

current is applied to the counter electrode to maintain the potential of the test electrode at a desired value with respect to the reference electrode. Since the sum of the current at the summation point junctions must equal zero, amplifier 1 acts as a potentiostat in maintaining the desired potential of the test electrode with respect to the reference electrode. Amplifier 2 in the form of a voltage follower serves to isolate the reference electrode from the rest of the circuit. The reference emf (^{e} var) results in the potential of the test electrode of $^{-e}$ var with respect to the reference electrode. The circuitry of box A simply provides a linear voltage sweep. That is, amplifier 1 in the integrator configuration, with a constant input signal, provides an output voltage which is a linear function of time. The circuit switch, shown in box A, is closed during the stripping step, which occurs after a suitable plating step. During the plating step the test electrode is maintained at a constant potential with respect to the reference electrode. In the stripping step the current is amplified by amplifier 4 (box C) which also holds the test electrode at virtual ground.

3. The experimental technique

The plating step was 10 minutes in duration with the voltage at $\bar{}$0.9 volts, while the stirring mechanism (nitrogen bubbling) was maintained at 2 psi. A standard procedure was adapted which included a blank run for every sample and a calibrating lead standard for every two lead samples.

Blank
Rinse
Sample
Rinse
Blank
Rinse
STANDARD
Rinse
Blank
Rinse
Sample
Rinse

A residue from a sample or standard would not increase a subsequent sample (sample-blank) and if response changed in time to a given lead standard the change would be suitably monitored (see Appendix I). Rinsing was accomplished by spraying electrodes with triply distilled water after the removal of the sample solution vial.

III. RESULTS AND DISCUSSION

A. Source Region Lead Size Distributions

Size distribution samples were taken at a number of locations which were considered as source regions of lead aerosols. Chicago and Calumet Harbor, being industrial areas, were expected to have contributions of lead from coal combustion and other industrial sources. Lincoln, Nebraska and Ann Arbor, Michigan, on the other hand had automobile exhaust as practically their sole source of lead aerosol.

In order to compare lead size distribution results to those obtained by Ludwig and Robinson (1964) and Lee et al., (1968) all samples from a single location were averaged and plotted on probability paper (Figure 6). The Calumet Harbor samples were incorporated with the Chicago samples. A total of ten Chicago samples, fifteen Ann Arbor samples, and three Lincoln samples were used.

The great lakes region averaged lead size distribution samples (Chicago-Calumet Harbor, and Ann Arbor) were similar to the Cincinnati results of Lee et al. (1967). The two averaged source region samples from the great lakes region had similar distributions. The Lincoln, Nebraska results, however, differed from the Chicago and Ann Arbor results principally in the small percentage of mass on the backup filter of the Andersen Sampler. Due to the small number of

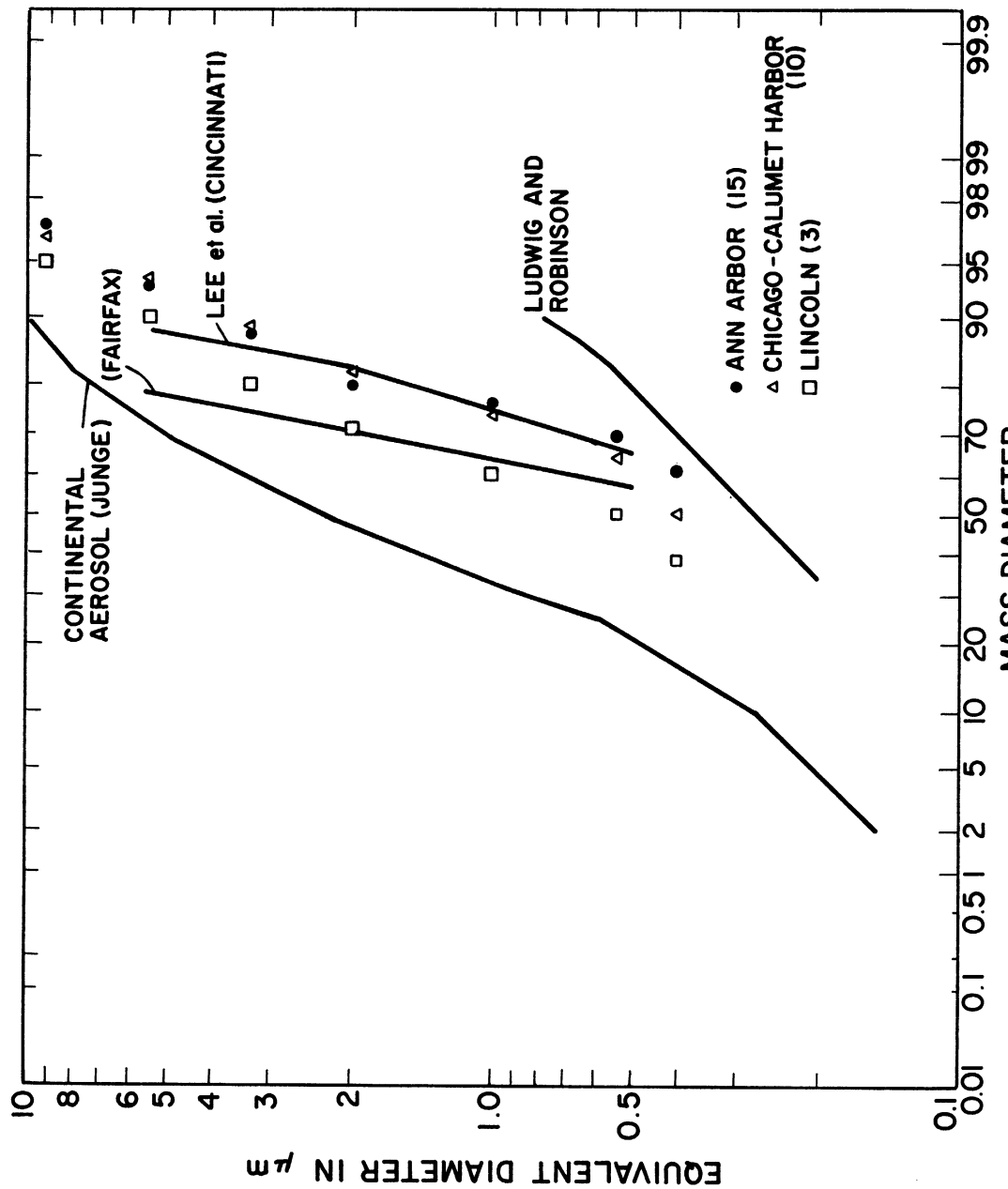

Fig. 6.--Cumulative lead size distributions for averaged samples.

total samples (3) at this location the resulting averaged distribution was not as strongly evident as in the Chicago-Calumet Harbor and Ann Arbor samples, although a likeness with the averaged size distribution from Fairfax (Lee et al. 1968) was noticed. Lead spectra from Ann Arbor and Chicago-Calumet Harbor did not intersect the Robinson and Ludwig (1964) lead spectrum characteristic of urban areas in the United States. Extrapolation of the curves gave mass median equivalent diameters[1] ($\sim$ 0.2 μm for Ann Arbor and $\sim$ 0.4 μm for Chicago-Calumet) which were slightly larger than the MMD range of Robinson and Ludwig. In general the results of Ludwig and Robinson showed a larger concentration of total mass in smaller particles than did the results of the present study or the Cincinnati results. This difference was possibly due to the instruments used for the collection of aerosol: the Andersen Sampler, used for this study and the Cincinnati and Fairfax study; and the Goetz Aerosol Spectrometer, used by Ludwig and Robinson. The Goetz aerosol Spectrometer, as mentioned, has resolution for 0.025 μm $\leq r \leq$ 4.0 μm but cannot sample over that entire range. Most samples were taken, therefore, in a size range below that which is most efficiently sampled by the Andersen Sampler. Resolution is, therefore, not certain for the aerosol spectrometer results for radii larger than $\sim$ 0.5 microns and for the Andersen Sampler results for radii smaller than 0.6 microns.

The size distribution results for Ann Arbor; Chicago-Calumet Harbor; and Lincoln, Nebraska all fall within the

---

[1] Equivalent diameter refers to the diameter of a spherical particle of unit density having the Stokes' velocity of the actual particle.

limits of the auto exhaust aerosol lead size distribution of Mueller et al. (1962). The lead size distributions of these source regions thus show the strong influence of automobile exhaust. The lead mass differed from the natural "continental" aerosol distribution of Junge (see Figure 6) in having a higher percentage of mass in particles of small radius ($r < 1.0$ μm). A plot of the lead mass distribution and standard deviations vs. the Andersen Sampler stage is given in Figure 7. This plot again showed the great similarity of lead mass distributions in lead source regions.

Chicago and Calumet Harbor samples showed a great similarity in size distribution shapes. Ann Arbor samples were also quite similar to Chicago and Calumet Harbor samples. All three had a higher concentration of small particles and smaller concentration of large particles than the samples from Lincoln, Nebraska. The distribution was seen to differ from the "Junge" (Std) mass distribution, in having a greater percentage of its mass in small particles, succeedingly large particles containing monotonically smaller amounts of the total lead mass in comparison to the "Junge" distribution.

A list of the statistics MMD_7 and stage 8/stage 8 (Junge) for all the lead mass vs. size distributions used in the main body of the work is given in Table II-3 in Appendix II. As described, MMD_7 implies a slope of the mass distribution for particles larger than about d = 0.45 μm. Stage 8/stage 8 ("Junge") is the ratio of the percentage of lead mass for particles collected on stage 8 to the percentage of lead mass for these particles if the size distribution were the "Junge" distribution.

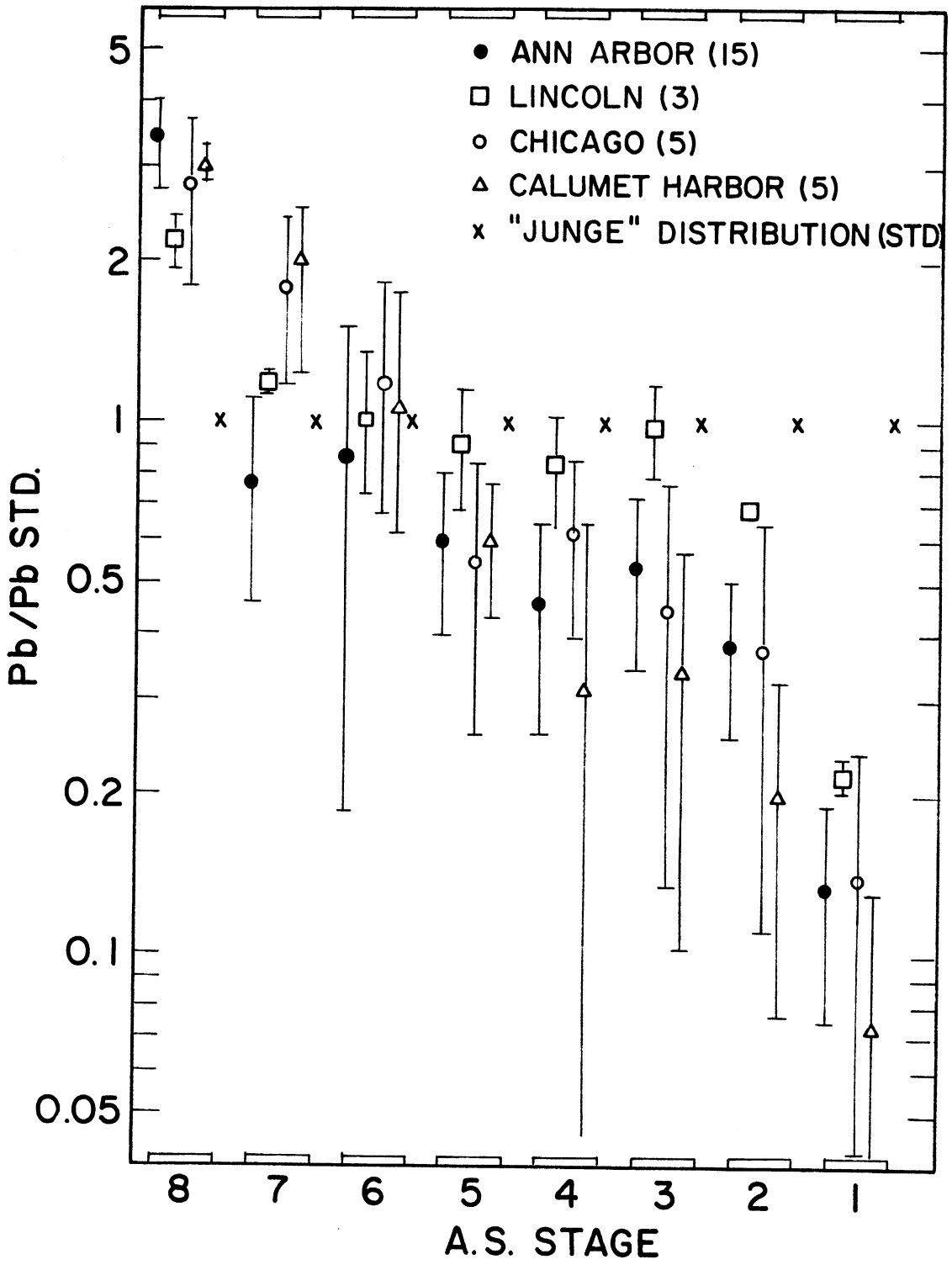

Fig. 7.--Ratio of lead mass percentage to mass percentage of the standard distribution for Andersen Sample Stage. Averaged Ann Arbor, Lincoln, Chicago, Calumet and the standard distribution are shown.

Although individual spectra are given in Appendix II, differences of whole groups of parameters may be pointed out. In Table 6 average MMD_7's are given according to sampling groups. σMMD_7 and $\sigma 8/8$ (Junge) are the estimated standard deviations of the mass median diameter and stage 8/stage 8 (Junge). These statistics are functions of the fractionation of mass by the Andersen Sampler and not of the normalizing "Junge" distribution.

TABLE 6

AVERAGE STATISTICS FOR SAMPLING LOCATIONS

Samples	MMD_7	σMMD_7	$\frac{\text{Stage 8}}{\text{Stage 8 (Junge)}}$	$\sigma 8/8$(Junge)
Lake Michigan (except Chicago Network)	1.0	0.4	2.8	0.9
Ann Arbor	1.8	0.8	3.8	0.7
Calumet Harbor	1.0	0.6	3.4	0.3
Lincoln, Nebraska	~2.0	-	2.4	0.3
Chicago	1.1	0.5	3.0	1.0

It may be inferred from the above table that the suburban location of Lincoln, Nebraska and Ann Arbor, Michigan have lead mass distribution differing slightly from Calumet Harbor samples or samples taken on Lake Michigan. Chicago and Lake Michigan samples show a relatively higher concentration of lead mass in small particles possibly due to a higher percentage of leaded combustion particles in the industrial areas of Chicago and sedimentation of large leaded particles over Lake Michigan.

B. Aging of Lead Aerosol

The study of aging of the lead aerosol in the observational program took advantage of Lake Michigan, over which aerosol traveled unaltered by local sources of lead. As mentioned, the travel time over the lake was considered to be the aging time. Lake Michigan furnished a large expanse, over which no sources of lead existed, and was of rather homogeneous surface flatness, humidity, and temperature. However it provided some difficulties especially due to thermal effects during the spring. There is evidence of a "cold dome" effect on the lake for two of the expeditions. In the "cold dome" wind velocities close to the surface were low and air was transported from such pollution sources as Chicago at a height greater than that sampled on the ship deck. The computed travel times were used as minimum aging times when the "cold dome" was detected.

Samples were divided into the three aging categories ennumerated in Section II, part A. In the following pages the three categories of lake aged lead aerosol are presented.

The first section of short term aging compares sets of three size vs. mass distribution samples taken simultaneously in Chicago and on two Lake Michigan locations downwind of Chicago. The three samples of any set vary only in aging since weather parameters and the source areas were virtually identical.

1. Short term aging

Short term lead aerosol samples were obtained on July 30, 31, 1968 and September 4, 5, 1968. Locations of samp-

lers were the Chicago Water Filtration Plant (Station I), Harrison-Dever Water Intake Crib (Station II), and the deck of R/V Inland Seas, about 10 miles east of the Harrison-Dever Crib, (Station III). The wind prevailed southwest to south during most of the situations.[1] A total of five 8-hour samples were taken.

An average of all samples taken at each station was computed and compared to the other stations. Estimated standard deviations for each stage were also plotted with the averages (Figure 8). No discernable difference was seen in the average mass distributions at the three stations. The lead spectra was quite similar from station to station and no rapid aging of the spectra seemed to have taken place.

Individual size distributions for each test and weather condition are presented in Appendix II.

---

[1] See Appendix II for details on wind and wind sensor locations.

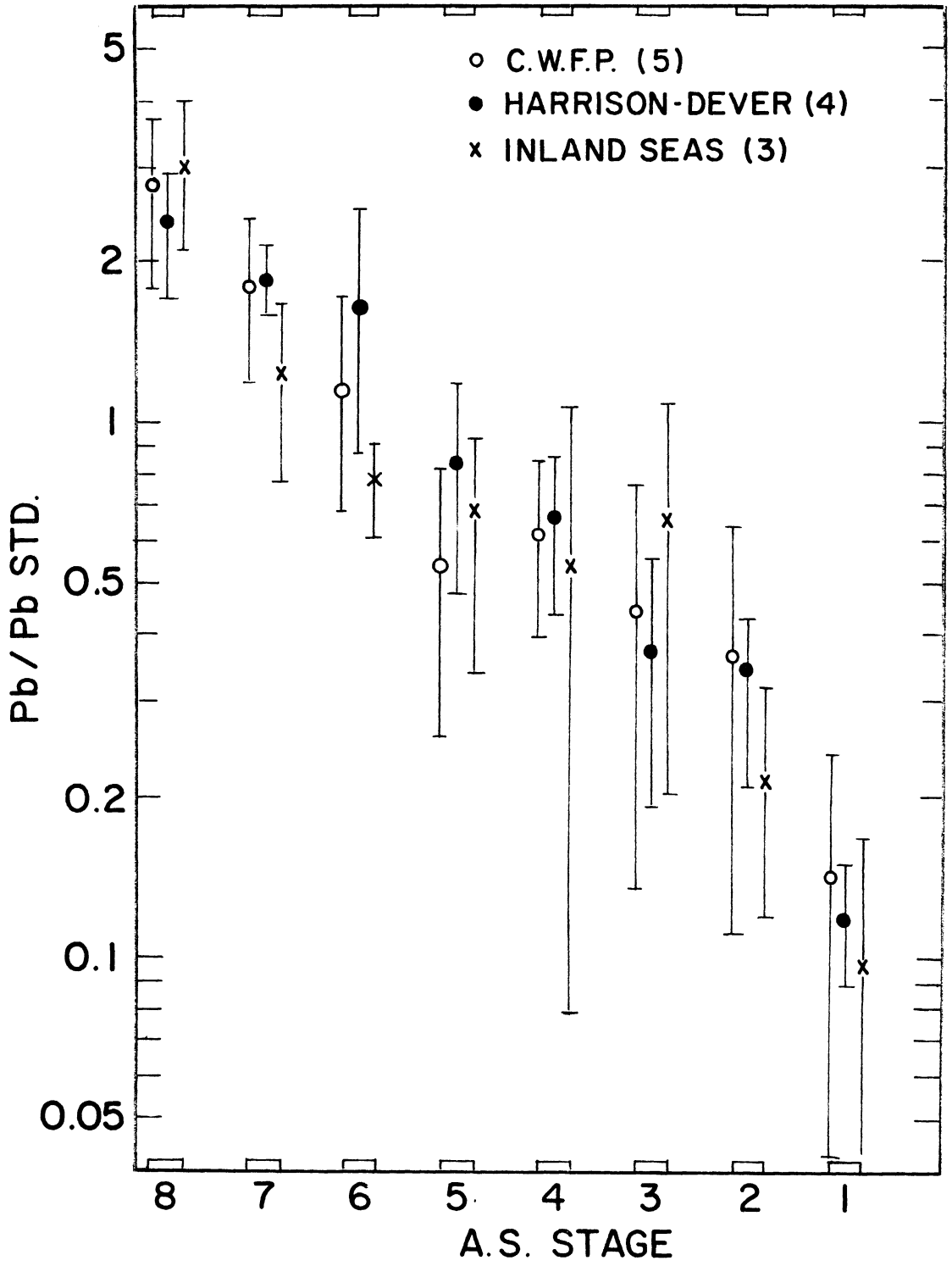

Fig. 8.--Ratio of lead mass percentage to mass percentage of the standard distribution for Andersen Sampler stage. Average short term aging distributions are shown.

2. Intermediate term aging

Sampling of intermediate term aged lead aerosol was accomplished on Lake Michigan although no comparative samples were taken at the shore of Lake Michigan, that region where the sampled air last passed before passing over Lake Michigan. The intermediate term aged lead aerosol should then be compared to source area aerosol for more distinct changes than in the short term aging case where the initial lead spectrum was known.

Intermediate term aged lead aerosols were obtained on two occasions. One occasion was July 9, 1968, aboard the R/V Inland Seas anchored in southern Lake Michigan. Meteorological data did not give a clear indication of a "cold dome" effect and trajectories from 0000 to 1200 EST implied aging of approximately one hour. Relative humidity recorded on the ship was quite constant during the day and was equal to or greater than 88 per cent. The land region last passed by the air was the area from the southern most tip of the lake to the Chicago region. Skies were partly cloudy (0.3 to 0.1) prior to frontal passage (about 1300 EST). Samples were taken every three hours for 9-hour periods. The size distributions remained quite stable during the duration of sampling, showing little diurnal effect.

Another size distribution sample was taken on the morning of May 23, 1968. According to meteorological data the "cold dome" effect, strong on 21 and 22 May, was missing. A very light rain commenced at 0300 EST preceded by a heavy fog. The sampled air appeared to be principally from the east shore of Lake Michigan, with an aging time of four to five hours. The temperature remained about 6.5° during the sampling period.

The average of the intermediate aged lead aerosol distribution was plotted, along with the average Chicago lead distribution (Figure 9). Consideration of standard deviations showed the distributions to be highly similar. A sedimentation effect (which is shown in Part II to be visible on stages 1 and 2) was perhaps visible in lower average values of the intermediate aged aerosol in comparison to the Chicago aerosol on stages 1 and 2.

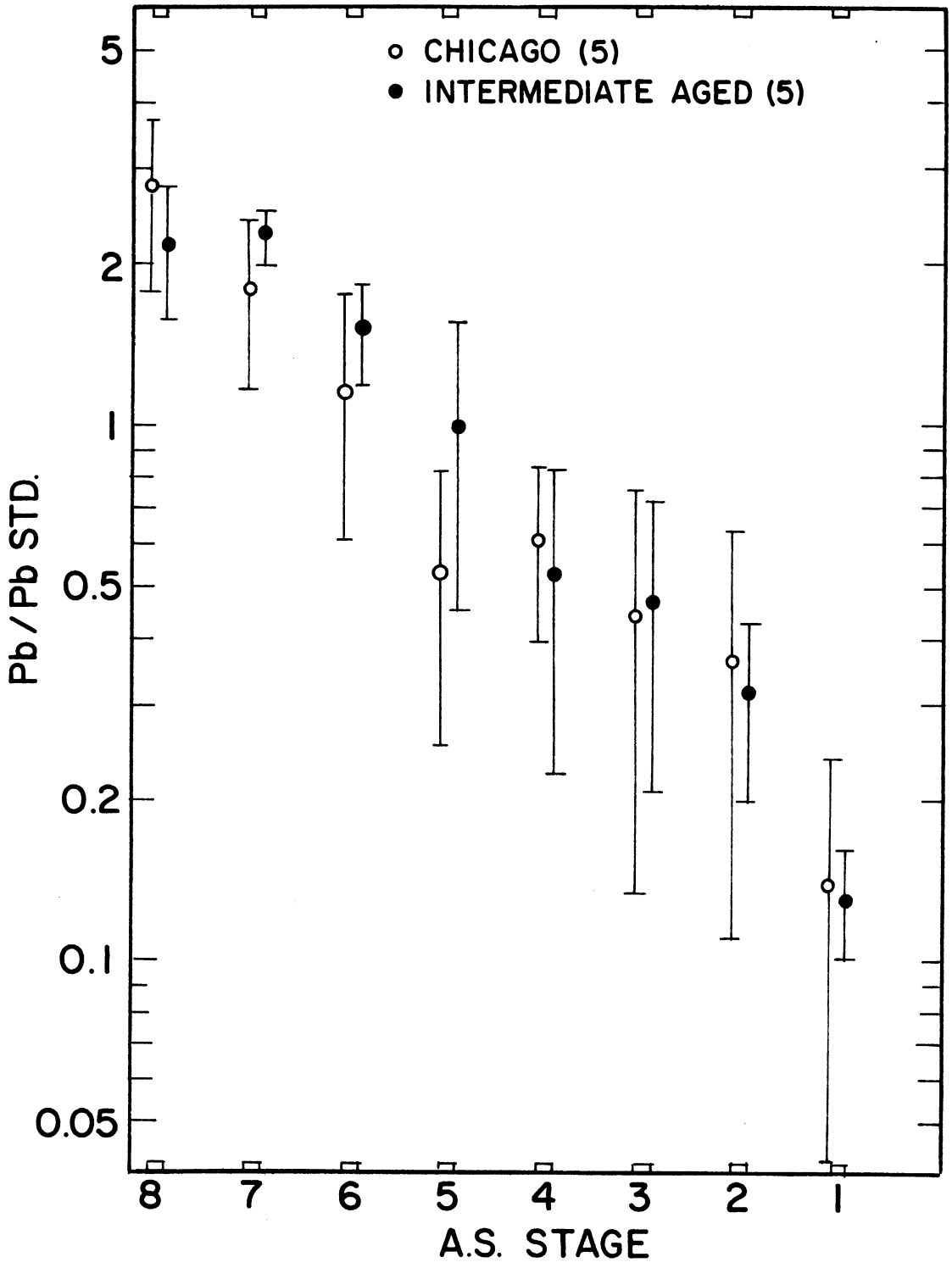

Fig. 9.--Ratio of lead mass percentage to mass percentage of the standard distribution for Andersen Sampler Stage. Averaged intermediate term aged and Chicago distributions are shown.

3. Long term aging

The final aging category, long term aged, represented aerosol samples far enough from the source region that one may characterize them as being "background" samples. Samples in this category, having been transported over the lake at least six hours, gave a long term change of size mass distribution when compared with source area size mass distributions. These samples were obtained on four days and a total of 18 were collected.

Nine samples, having nine hour overlapping sampling periods, were obtained on July 9 and 10, 1968. After a frontal passage (about 1300 EST) winds shifted to north-north east for the remainder of the expedition. Meteorological data gave no evidence of a "cold dome" effect and it was quite certain that normal transport was in effect. Trajectory analysis indicated, after frontal passage, that much of the air could have had its origin in the industrial regions of the southern Lake Michigan basin, and it was shown that the sample 1242-2100 EST was characterized by substantially higher total lead concentration than the subsequent samples. After 1500 EST air was principally transported from the eastern shore of Lake Michigan, an area having less industrial activity than the southern tip. Aging times of samples taken on July 9 after 1300 EST were from six to nine hours. Relative humidity during that time was very constant, as measured aboard the ship, ranging from 88 per cent to 93 per cent. Visibility was very good during the period with air temperature constant around 17°C. Weather conditions were quite constant over the sampling time and

differences of the lead spectra were probably due to changing sources and/or aging.

Two distributions (2126-2359 EST) had only 2 1/2 hours running time and therefore collected probably less than 20 nanograms of lead on Andersen stages other than the backup filter. Problems of blanks were quite pronounced and consequently only stage 7 (the backup filter) was reliable. The values for stage 7 agreed with the results preceeding and following the sampling period (2126-2359 EST).

On July 10, 1968, north-northeast winds predominated and again weather conditions were relatively constant. Relative humidity ranged from 84 per cent to 94 per cent, air temperature ranged from 14.1°C to 18.9°C, and visibility was practically unlimited. The position of the ship was inside the walls of Calumet Harbor up-wind of the industrial activity of south Chicago. Trajectory analysis indicated aging of from 7 to 12 hours. The land area over which the air had most recently passed was northern Michigan or perhaps Canada, regions having reduced lead inputs in comparison to southern Michigan, northern Illinois, and northern Indiana. The samples collected were remarkably free of diurnal changes in shape and were the smallest reliable samples collected. The total lead concentration was around 20 nanograms/meter^3. The total concentration, however, did decrease monotonically in station time as the age of each sample was increased.

Samples obtained on May 21, 1968 seem to have been inside the "cold dome". Trajectory analysis indicated low limits of aging for 10 hour (1513-1946 EST) duplicate samples.

Visibility was practically unlimited for the entire sampling period and air temperature varied between 8.0°C to 6.6°C. The samples were extremely slight in lead mass, a total lead mass of about 30 nanograms/m^3 being obtained.

The last set of highly aged lead aerosol samples was obtained on the R/V Inland Seas on May 22, 1968. The ship was anchored at a central position on Lake Michigan. Meteorological data indicated a "cold dome" so that trajectories gave lower limits for the aging time (about 5 hours). It is reasonble, however, to assume that these samples were "highly aged." Air temperature varied from 6.8°C to 12.7°C with clear air until 0200 EST when a heavy fog was observed. The first four samples of the May 22, 1968 set showed great similarity in shape. The fifth sample, however, showed a flattening out of the spectrum for Andersen stages smaller than 8. This was a possible effect of cloud scavenging (see page 70) since fog was observed during the time that this sample was taken.

Average samples of the Chicago source region, intermediate term aged, and high term aged aerosols are shown in Figure 10. The three averaged aerosols, considering the standard deviations, are highly similar. Increasingly aged aerosols suggested a sedimentation effect in the reduction in concentration of the lead mass at stages 1 and 2.

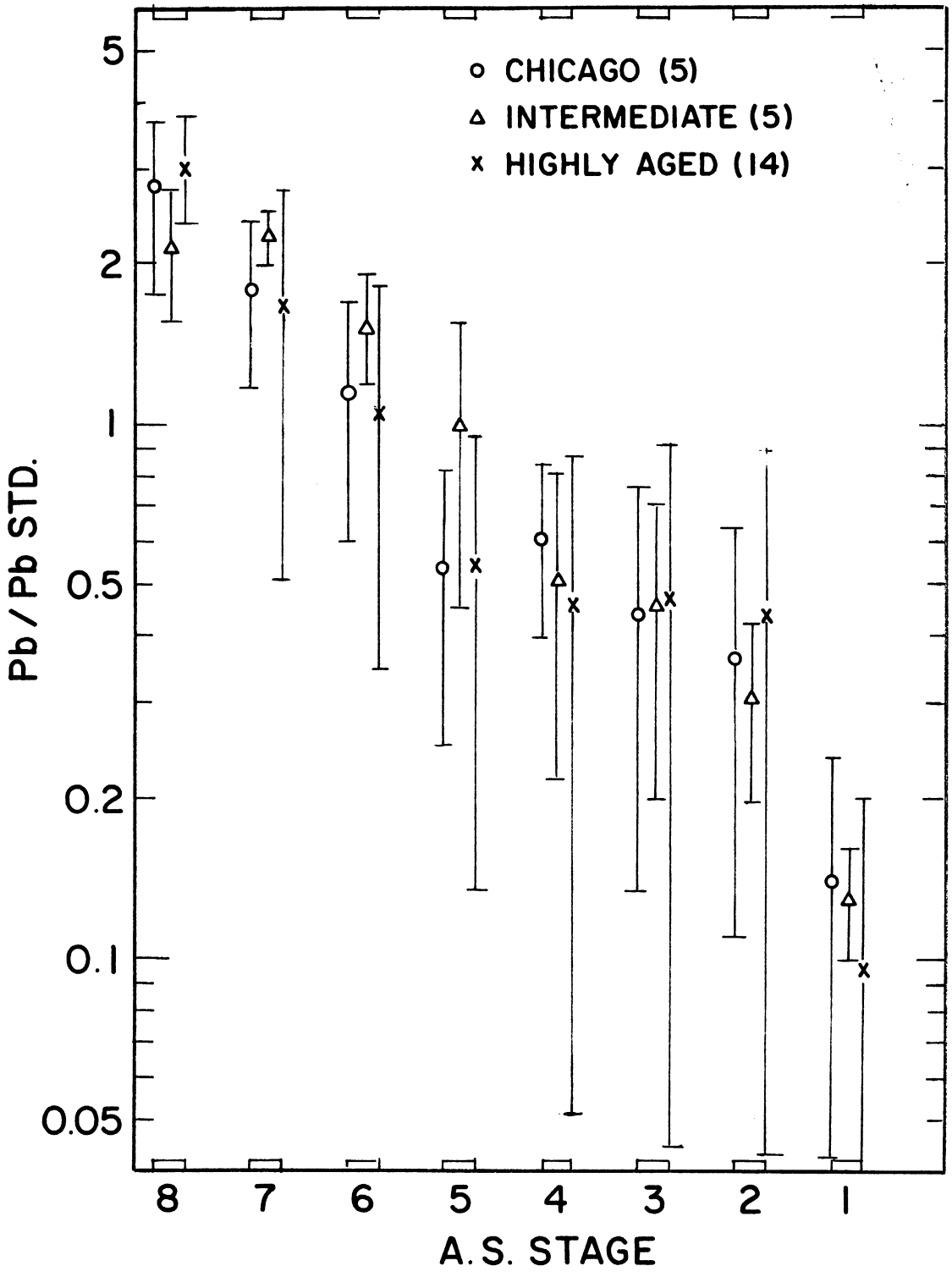

Fig. 10.--Ratio of lead mass percentage to mass percentage for Andersen Sampler Stage. Averaged Chicago, intermediate term aged, and highly aged distributions are shown.

A set of samples showing the aging effect was obtained on June 6, 1968 aboard the R/V Mysis moving east across the lake from Racine, Wisconsin, to Grand Haven, Michigan. A total of four samples were obtained as shown on the trajectory map, (Appendix II) the first sample dominated by local Racine air. The subsequent three samples were averaged since they were all "highly aged". These three samples were obtained in a "cold dome" of highly aged air as shown by the meteorological results. (See Appendix II). Haze was present during the entire crossing with visibility given as 2 miles until about 1200 EST when visibility increased to 4 miles. The aging effect could therefore be slightly masked by an agglomeration effect of water droplets. Temperature ranged from 9°C to 22°C.

Results (Figure 11) show a reduction of larger particles due to aging although the scatter, perhaps due to the presence of haze, does not make this a strong piece of evidence.

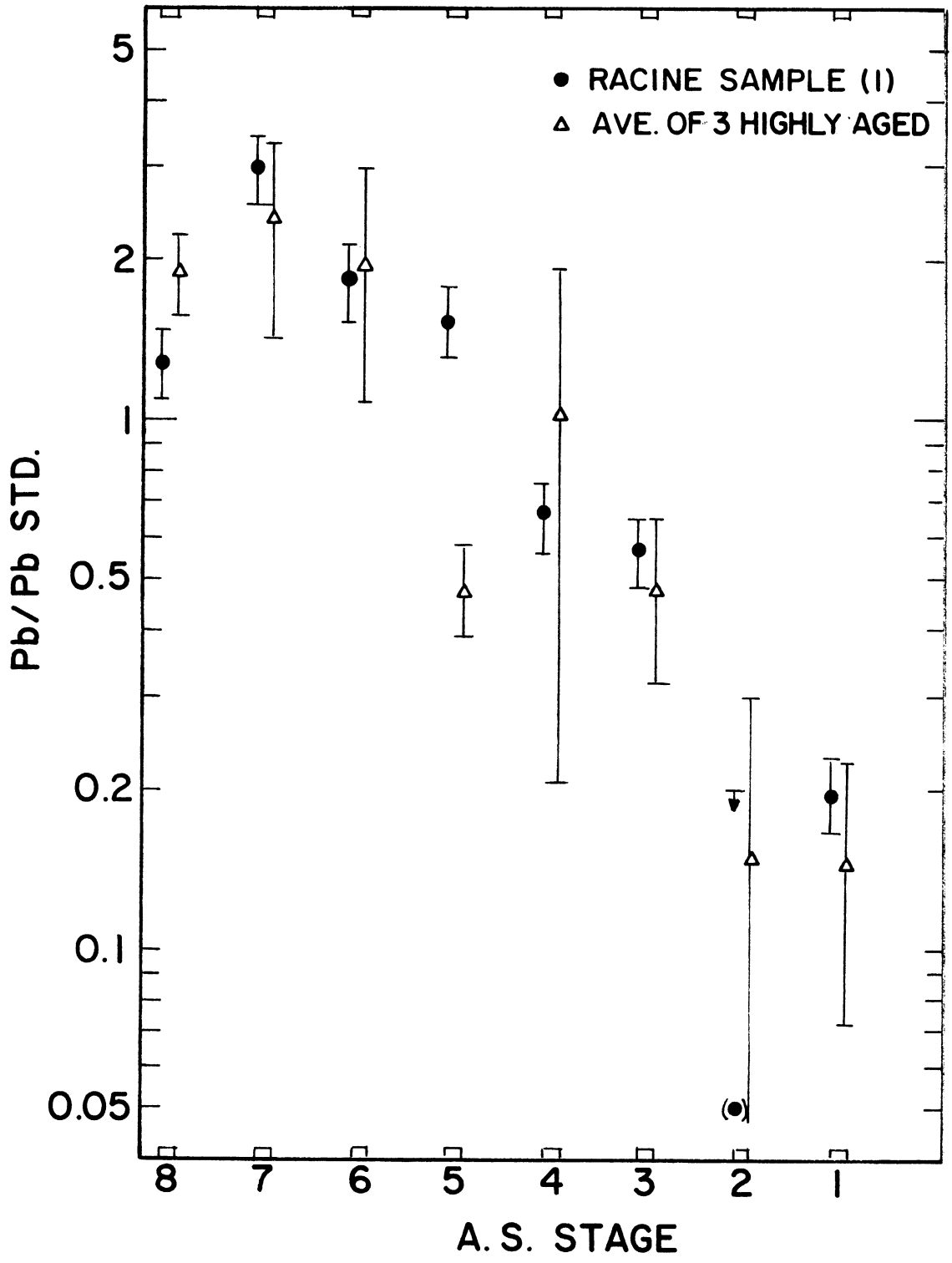

Fig. 11.--Ratio of lead mass percentage to mass percentage for Andersen Sampler stage. June 6, 1968 distributions are shown.

C. Variation of Lead Size Distributions with Weather Parameters

In the month of October, a number of mass vs. size distribution samples were obtained using 24-hour sampling times in an Ann Arbor, Michigan residential site in order to ascertain changes in the day to day lead size distribution. The lead mass vs. Andersen sampler stage was plotted by date (Figure 12).

The October 26 sample is within 20 per cent of the average value at each stage. Other samples not within the 20 per cent limit for all stages, but not forming a consistent trend, are October 16, 25, 28, and 29. Samples interpreted as favoring large particles, in comparison with the mean distribution are: 1) that of October 17, with stages 1, 2, and 3 having larger masses and stage 7 having a smaller mass than the average, and 2) that of October 18 with stages 2, 3, 4, and 5 having larger masses than average. Samples interpreted as favoring smaller particles, compared to the average distribution, are from October 14, 19, 27, and 30. The results of October 19, 1968 may be questioned, since lead mass on stage 1-7 is approximately the same as for the previous sampling day. The lead mass on the backup filter had nearly doubled in concentration due perhaps to contamination. The sample of October 27 was above average in mass on stage 7 and below average on stages 1, 2, and 3, as was the sample of October 30. The sample of October 14, was below average in mass on stages 1, 2, 3, and 4 and above average on stage 6.

The most obvious weather parameters, possibly correlating with the varying size distributions, are wind direction,

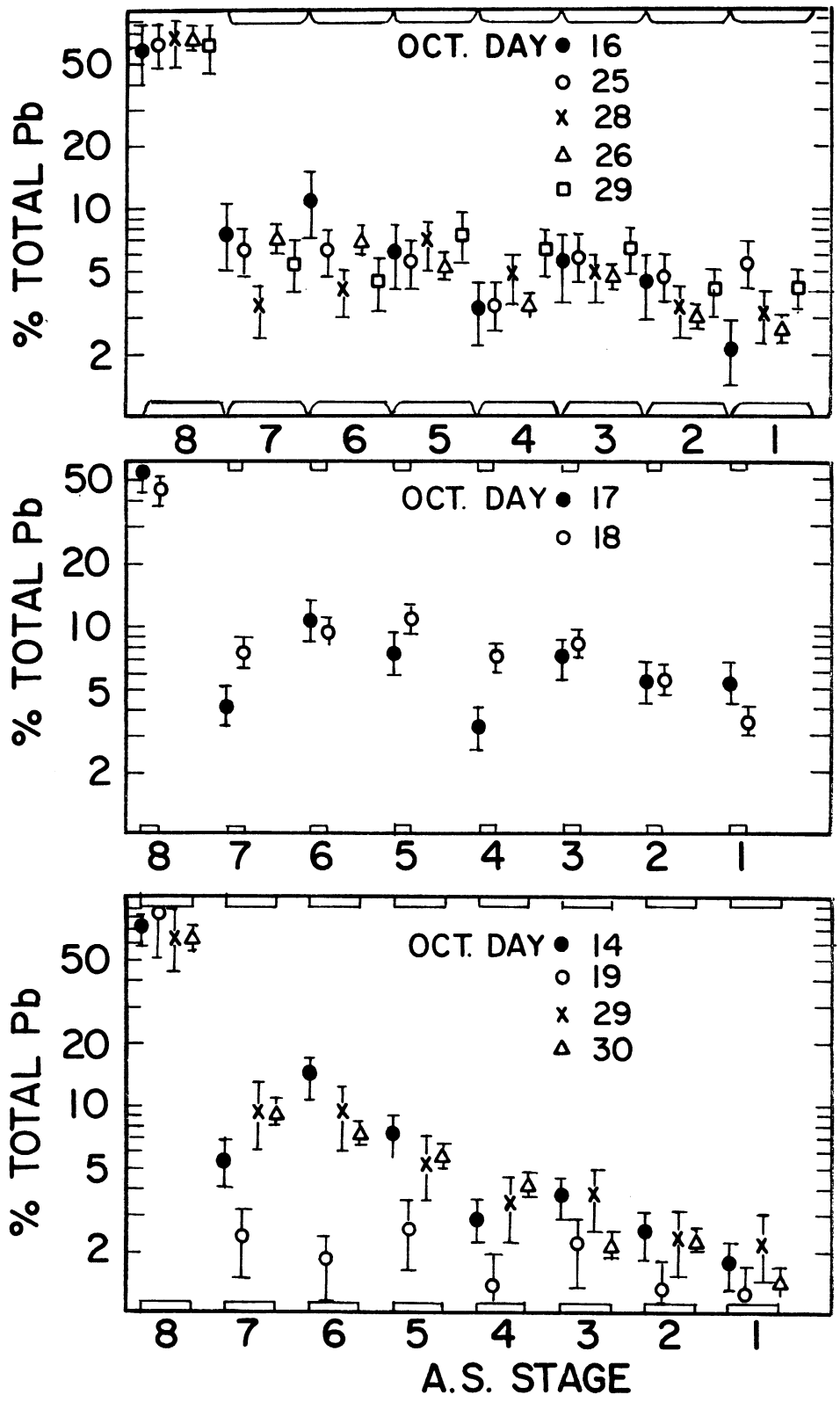

Fig. 12.--Lead mass percentage for Andersen Sampler stage for October, 1968 Ann Arbor samples.

rain, and fog or haze. Varying wind direction would bring in lead aerosol from differing sources. Rain would remove large particles selectively over small particles by impaction with larger lead aerosol particles. Fog and/or haze would seemingly cause a spectrum favoring large particles compared to the averaged distribution due to the scavenging action of the cloud droplets, the cloud droplets being part of the aerosol. Some weather parameters were given for the average, large, and small lead aerosol distribution subsets (Table 7).

TABLE 7

WEATHER STATISTICS FOR OCTOBER, 1968

Day (Oct.)	Wind Direction at 0700 EST	Max.,Min. Air Temp(°C)	Precip(cm)
Lead Mass Distributions Following the Average Distribution			
16	SE	27,14	0.0
25	NNE	9,4	0.18
26	SW	8,2	0.0
28	SW	10,3	0.15
29	W	5,1	Trace
Lead Mass Distributions Following the Large Distribution			
17	E	27,17	Trace
18	SE	26,12	0.87
Lead Mass Distributions Following The Small Distribution			
15	SW	28,16	0.0
19	SW	8,6	Haze,Fog 0.25
27	S	13,3	Fog 0.
30	WSW	10,0	Trace

No clear-cut cause and effect relationship emerged from these data. "Average" distributions had winds from all directions with or without rain. Distributions showing above average concentrations of large particles were noted even while rain was observed. Distributions showing above average concentration of small particles containing lead were found when fog and/or smoke were present. These distributions did have a wind direction predominantly from the south, however.

No correlation of weather parameters with lead size distribution shape was attempted, nor did it seem to be justified. Since weather parameters varied within the period of time being sampled, a correlation of individual weather effects did not seem possible with these samples. The shape of the lead mass distribution was of remarkable persistency in a wide range of meteorological conditions.

The samples taken in Lincoln, Nebraska all fell within 28 per cent of the average value for each stage (Figure 13). All three samples were taken in periods of no rain or fog although wind direction changed. Wind data from the Lincoln Airport is given in Table 8.

TABLE 8

WIND DATA FROM LINCOLN AIRPORT

Day (October)	Wind Direction
5	S until 2300, NW after 2300
6	NW until 1800, S after 1800
7	S
8	S until 2000, NW after 2000

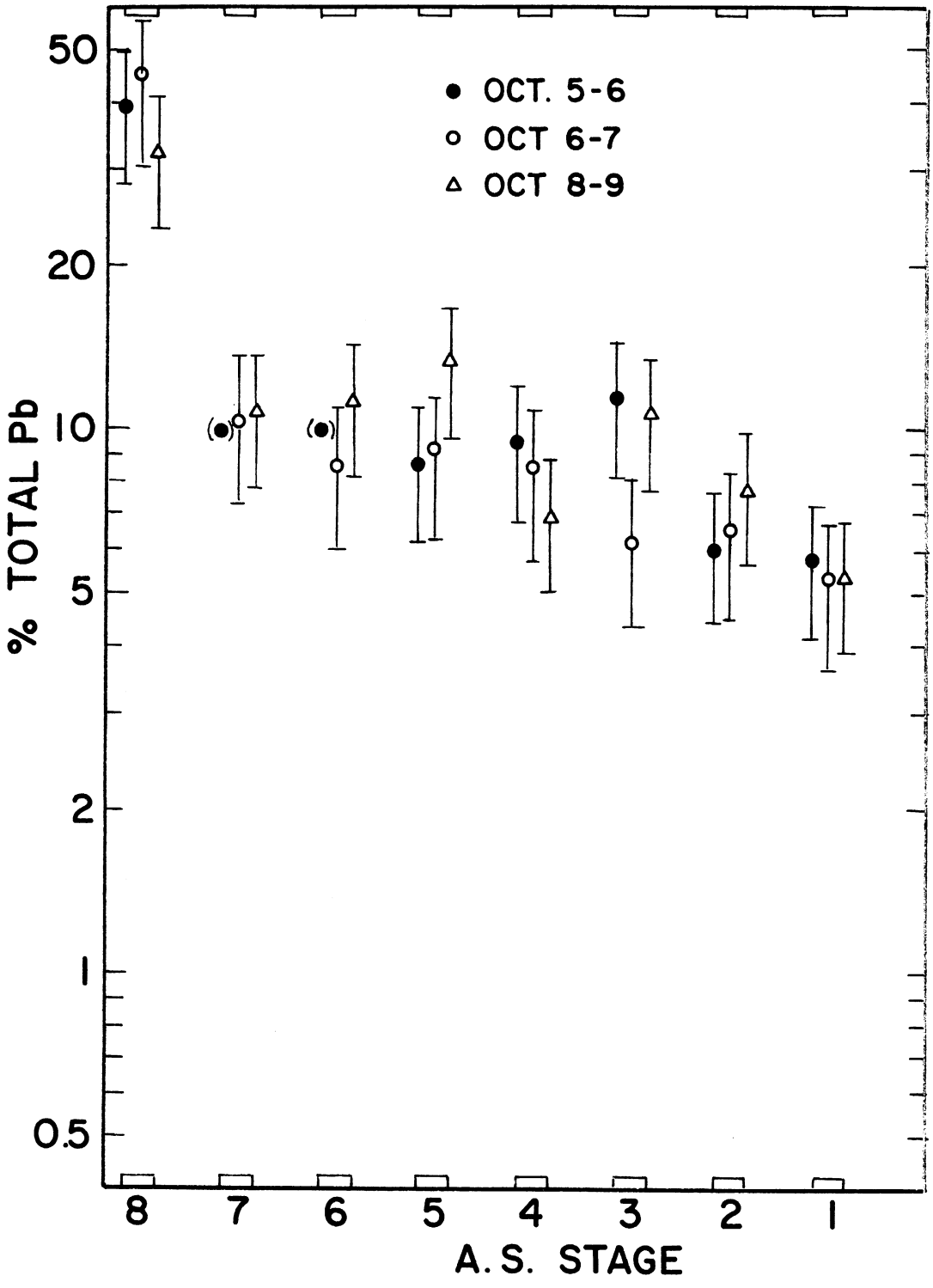

Fig. 13.--Lead mass percentage for Andersen Sampler stage for October, 1968 Lincoln samples.

In general, little change in lead size distribution was accompanied by little change of weather parameters in these samples.

Four samples (Figure 14) were taken in late February and early March to coincide with predominatly snowy or clear days. The samples, taken on the roof of the East Engineering Building follow: 1) February 22, 1969, 1100 EST- February 24, 1840, weather characterized as overcast but no precipitation, 2) February 24, 1969, 1905 EST- February 26, 1200 EST, weather characterized as light rain with ice pellets, occasional snow flakes, 3) February 26, 1300 EST- March 6, 1205 EST, weather characterized by clear skies, 4) March 6, 1250 EST- March 7, 1327, weather characterized by snow falling.

The samples beginning February 22 and March 6 seemed to show more mass in large particles while samples beginning February 24 and February 26 seemed to favor small particles. No relationship of spectrum shape with precipitation was found.

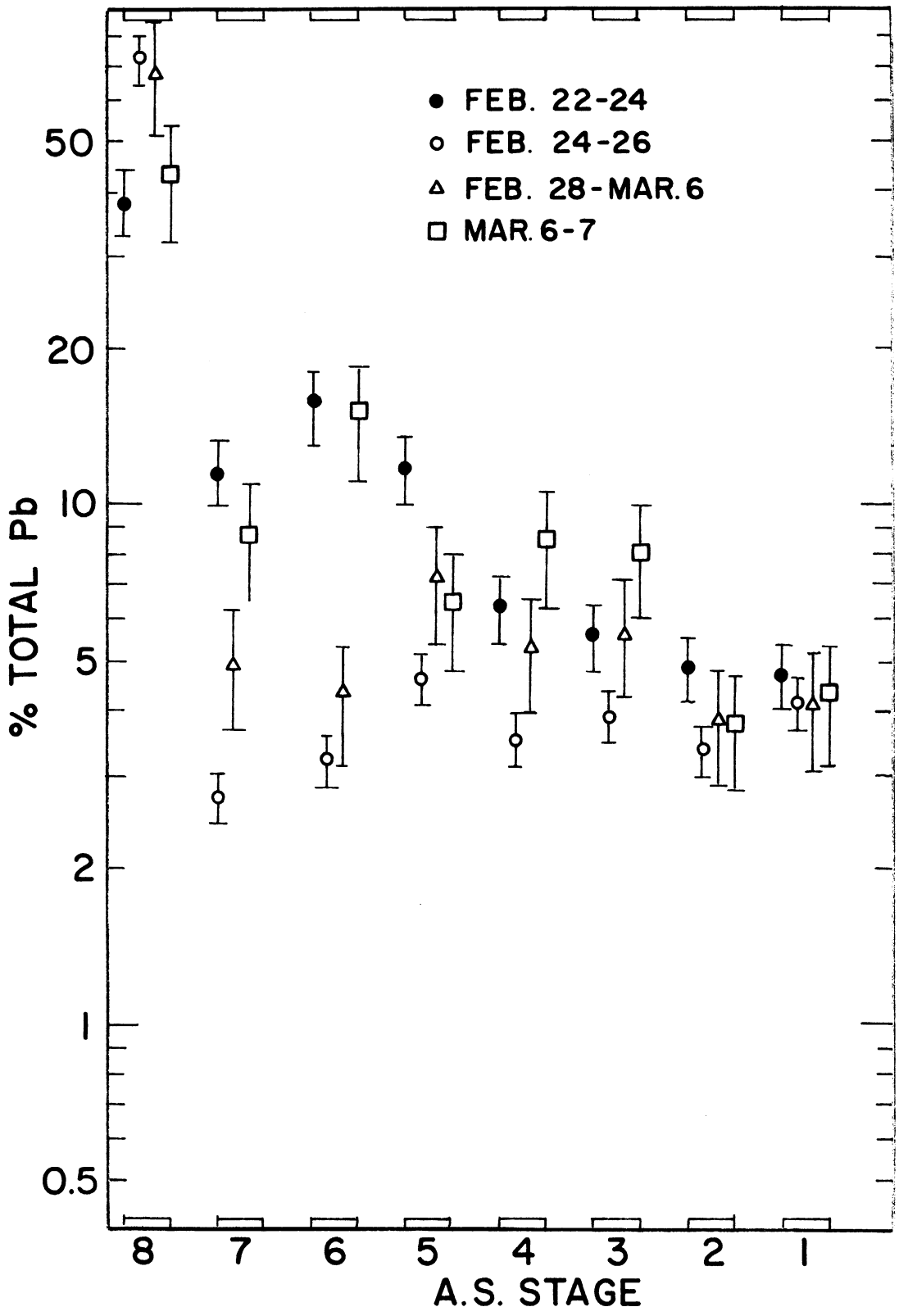

Fig. 14.--Lead mass percentage for Andersen Sampler stage for February, March, 1968 Ann Arbor samples.

IV. CONCLUSIONS

Four principal conclusions were reached from the observations taken.

First: The averages of the lead size distributions from source regions were characterized by mass distributions quite similar to the automobile exhaust lead size distributions of Mueller et al, (1962). Particles with a radius less than 1 μm contained 62-82 per cent of the lead mass. This result agreed with the work of Lee et al., (1968). The extrapolated mass median equivalent diameter (MMD) for the averaged Ann Arbor samples fell within the range of values given by Robinson and Ludwig (1964), who investigated lead size distributions in a number of urban areas in the United States. The MMD of the averaged Chicago samples ($\sim$ 0.4 μm) fell slightly outside the range of these values while the Lincoln, Nebraska value ($\sim$ 0.6 μm) was larger. The details of the distributions for $r > 0.2$ μm are somewhat different from those of Robinson and Ludwig. As stated, this difference may be due to the sampling instrumentation. Although in this study the differences of lead spectra with themselves and with other observed lead spectra were slightly greater than the experimental error, it was the lack of change over widely different source regions and weather conditions which was thought to be significant.

A summary of lead statistics is found in Table 9. In

TABLE 9

LEAD STATISTICS FOR ALL SAMPLES

		Andersen Sampler Stage (1-8)								No.
		1	2	3	4	5	6	7	8	
I. Source Region										
A. Ann Arbor, Michigan	$\bar{X}$	3.4	3.7	5.3	4.5	6.8	8.5	6.5	61.8	15
	S	1.5	1.2	2.0	1.9	2.2	6.5	2.7	12.2	
B. Lincoln, Nebraska	$\bar{X}$	5.6	6.8	9.6	8.3	10.5	9.9	10.4	39.1	3
	S	0.3	0.9	2.9	1.3	2.8	1.4	0.5	5.7	
C. Calumet Harbor, Chicago	$\bar{X}$	1.8	2.0	3.3	3.2	6.8	10.6	17.3	54.5	5
	S	1.3	1.2	2.3	3.2	2.2	5.1	5.9	5.1	
D. Central Water Filtr. Plant (Chicago)	$\bar{X}$	3.6	3.6	4.4	6.2	6.0	11.9	15.0	49.5	5
	S	2.6	2.6	3.1	2.3	3.2	5.5	5.9	16.0	
II. Rural Aged Samples										
A. Short term aged										
1. Harrison-Dever Water Intake	$\bar{X}$	3.0	3.5	3.7	6.6	9.2	16.3	15.5	42.6	4
	S	0.8	1.2	1.8	2.2	3.7	7.7	2.0	11.7	
2. R/V Inland Seas (Lake Michigan)	$\bar{X}$	2.5	2.2	7.1	5.3	8.1	8.4	10.5	55.6	3
	S	1.5	1.0	5.1	4.8	3.6	2.2	3.5	16.7	
B. Intermediate Aged	$\bar{X}$	3.4	3.2	4.8	5.3	11.1	15.3	19.6	38.1	5
	S	0.8	1.1	2.7	2.5	6.4	3.3	2.0	10.5	
C. Highly Aged	$\bar{X}$	2.4	4.3	4.7	4.5	6.0	10.3	14.2	53.4	14
	S	2.4	5.2	4.6	4.1	4.5	7.0	9.7	13.6	
III. Comparative "Junge" Distribution	$\bar{X}$	25.0	9.8	9.8	9.8	11.1	9.8	8.4	16.4	

this table x_i is the value of lead mass per stage i, $\bar{x}_i$ is the average of x_i over a group of samples, and s is the estimated standard deviation for that average. The estimated standard deviation was computed by

$$s^2 = \sum (x_i - \bar{x}_i)^2/(n-1).$$

In comparison with the "Junge" distribution (page 25) which is similar to the distribution for the total aerosol found over continents, the lead mass size distribution had a higher concentration of its total mass in small particles. A probable explanation for this is that the largest contribution of lead particles was from the combustion of leaded fuel in automobiles which provided a lead mass size distribution similar to that found in urban areas (Mueller et al., 1962; Robinson and Ludwig, 1964).

Second: Aging of the lead spectrum, without the effects associated with clouds, was a slow process. Inspection of Figure 10 revealed that the average amount of mass on each stage for all averaged samples fell within some interval whose limits approximated at least one of the estimated standard deviations for average mass per stage. Although a clear cut aging process was not observed, a consistent pattern in the highly aged samples revealed a small reduction of larger particles perhaps due to sedimentation. Small particles ($r < 0.3$ μm) were little affected, but it must be remembered that this broad and principal mass-containing range of the spectrum was given no resolution by the Andersen Sampler which collected it on a back-up filter.

Third: A remarkable constancy of the lead size distribution was observed in a variety of weather conditions.

The estimated standard deviation at each stage (excepting stage 6) was around 40 per cent of the mean value which, although somewhat larger than the estimated error of analysis, indicated that no large changes of the spectrum were observed. In addition, no consistent change of lead spectrum was observed for a given distinct change of meteorological condition, e.g., clear air or snow. The lack of observed lead size distribution response was consistent with the observations of Lee et al., (1968) for 6 metal particulate distributions including lead. This lack of response, however, contrasted with the study of Loucks (1969) for halogen aerosols.

The meteorological situations which were thought to produce the largest change were the presence of rain or fog. Since sampling occurred at ground level, rain processes would probably act only by impaction onto raindrops. Fog was not frequent nor particularly intense when samples were taken. Nonetheless it seemed reasonable to conclude that normal weather variations did not have a profound effect upon the lead size distribution in a source region of lead. The apparent immunity of the lead particulate from radical alteration during precipitation may be partially understood by reviewing the work of Greenfield (1957) on the scavenging of particulate by cloud and precipitation processes. It was found that the direct interaction of raindrops and particulate did not provide an efficient removal rate for particles $r \lesssim 5$ μm. Electrostatic effects were shown to be negligible (at least for radioactive particles) and thermal coagulation was shown to be an important removal process for particles smaller than $r \lesssim 0.05$ μm but

only within the cloud. McDonald (1964) reported that the region $0.05 \lesssim r \lesssim 5$ μm is "the least vulnerable to precipitation scavenging and hence tends, on the average, to exist in relatively high concentration."[1]

It was observed that the lead spectrum is located largely within this "gap". The lead distribution would be altered very little by rainfall, except for particles of radii larger than about 5 μm.

Soluble particles may act as nucleii for condensation for relative humidity less than 100 per cent (Dufour and Defay, 1963). However, for appreciable growth of the condensation droplets and consequent removal to occur, the air had to be supersaturated, a condition observed in fogs but practically absent in the above sampling. Likewise other scavenging processes associated with clouds could not be applied to ground level lead aerosol during rain since the cloud was not present at the ground.

Fourth: Small variations of the mass vs. size distributions of lead particulate larger than that collected by the backup filter for differing source regions were observed. The sampling sites of Lincoln, Nebraska and Ann Arbor, Michigan seemed to have a smaller mass concentration of lead in small particles than the other samples which were quite uniform in size distribution. Ann Arbor and Lincoln values of MMD_7 were ~ 2 μm and 1.8 ± 0.8 μm respectively. A region of heavy industrial pollution, Calumet Harbor, had $MMD_7 = 1.0 \pm 0.6$ μm and aged samples were characterized by

---

[1] J. E. McDonald, Cloud nucleation on insoluble particles, Journal of the Atmospheric Sciences, 21 (January, 1964).

MMD_7 = 1.0 $\pm$ 0.4 μm. Samples taken at the Central Water Filtration Plant had MMD_7 = 1.1 $\pm$ 0.5 μm. It shoud be mentioned, that MMD_7 was dependent upon the seven-stage Andersen Sampler and the calculated cutoff diameter of stage 7.

PART II. A NUMERICAL MODEL SIMULATING A LEADED AND SEDIMENTING AEROSOL IN THE PRESENCE OF AN UNLEADED BACKGROUND AEROSOL

I. INTRODUCTION

With a knowledge of the mechanics of aerosols, cloud physics, atmospheric electricity, the initial lead aerosol size distribution, and unleaded aerosol size distribution one may predict changes in lead aerosol size distribution in time. Predictions of change of the lead size distribution were made to explain and substantiate the results of the observations. The most provocative result was the apparent lack of change of the lead aerosol spectrum for short and long term aging. A second result which was considered was the difference of Ann Arbor and Lincoln sample distributions compared to the other sample distributions. Another result, lack of difference of the broad mass distribution with source area, was not considered but might be explained by a consideration of the source.

It has been shown that even in the industrial Chicago area the overwhelming source of lead particulates is in automobile exhaust (Winchester and Nifong, 1969). Major differences in the nature of initial lead spectra were not found in urban locations (Robinson and Ludwig, 1964), and although the nature of the mechanism producing larger leaded particles (coating and removal of lead deposits on the exhaust system) (Hirschler, 1957) is poorly understood and may produce small systematic variations of initial lead spectra as a function of location, little change should be expected on an areal average.

The mechanisms acting to change the lead size distribution are: gravitational sedimentation; impaction; diffusion; electrical effects; coagulation; and precipitation effects, both nucleation of cloud droplets and collisional collection by impaction and electrical attraction; as well as thermophoresis and diffusiophoreisis. Coagulation is due to Brownian motion, turbulence, and impaction due to the fallout of large particles. These mechanisms are discussed and developed in Appendix IV. The interaction of the above mechanisms on aerosol particles has been considered in theoretical models of aerosol aging. The models most relevant to lead aerosol aging are reviewed below.

A. A Survey of Theoretical Models of Aerosol Aging

1. The Smoluchowski coagulation equation

A description of Brownian coagulation, the mechanism which is considered most important in normal atmospheric aerosol aging, was formulated by Smoluchowski (1916). The result, which is derived in Appendix IV, is

$$\frac{dn_k}{dt}\, dr_k = 2 \sum_{i+j=k} KK(r_i, r_j) n_i n_j dr_i dr_j - 2n_k \sum_{j=1}^{\infty} KK(r_k, r_j) n_j dr_k dr_j .$$

where n is defined as on page 25.

The equation states that the rate of change of the number of particles in size class k (a size class taken as a set of particles $r_{min} \leq r_k < r_{max}$ whose properties are close to those of particles $r = r_k$) is dependent on two terms.

The first term expresses the increase of size class k particles by the collision of two smaller particles whose combined mass equals that of a k size class particle. The second term expresses the decrease of size class k particles by collision with other particles, thereby producing a particle larger than that of size class k. The number of collisions of particles between two size classes in a unit time interval is proportional to the number of particles in each size class times a coagulation coefficient KK, which is a function of temperature, particle size, and viscosity.

2. Friedlander's aerosol model

Junge and Friedlander, in constructing models of aging of aerosol size distributions, considered the total aerosol. Friedlander (1960) attempted to explain the shape of the subrange $r \gtrsim 0.1$ μm of the spectrum for the "continental aerosol" (see page 26) in terms of aerosol mechanics and not the initial size distribution. Coagulation and sedimentation were assumed to be the most important mechanisms for particles $r \gtrsim 0.1$ μm. The equation was

$$\frac{dn_k}{dt}\, dr_k = 2\sum_{i+j=k} KK(r_i, r_j) n_i n_j dr_i dr_j - 2n_k \sum_{j=1}^{\infty} KK(r_k, r_j) n_j dr_k dr_j$$

$$+ \frac{d}{dz}\, n_k VSED(k) dr_k .$$

The term VSED(k) is the Stokes sedimentation velocity, a function of particle size (derived in Appendix IV.)

The addition to the Smoluchowski coagulation formula above is that of gravitational sedimentation. That is, the third term to the right expresses change of concentration of size class k particles as the difference of particles leaving the volume concerned at the bottom from the particles entering at the top. The source of particles was assumed to be the coagulation of particles from the range $r < 0.1$ μm.

Three assumptions were made concerning the part of the spectrum consisting of particles with a radius larger than 0.1 μm.

ASSUMPTION 1. A state of dynamic equilibrium exists so that the rate of matter input from the process of coagulation, bringing matter in from particles smaller than $r = 0.1$ μm, is matched by removal of matter by sedimentation.

ASSUMPTION 2. Based on the similarity of the processes of aerosols to those of turbulence, where energy may originate at large wave length motions and be dissipated at small wave length motions, an analogy was made with the Kolmogoroff hypothesis of local similarity for quasi-stationary turbulence. That is, the upper end of the spectrum (particles larger than 0.1 μm) was completely determined by the parameters related to the coagulation rate, the gravitational settling rate, and the rate at which matter enters the upper end of the spectrum by the coagulation of smaller particles (which by assumption 1 is identically the sedimentation rate).

ASSUMPTION 3. There exist subranges of the upper end of the spectrum, one for which coagulational effects are negligible (assumed for particles larger than about 1 μm),

and another for which sedimentation is negligible (assumed for particles 0.1 μm ≤ r ≤ 0.5 μm).

Size distributions of these two subranges were solved by dimensional analysis and were given as

$$n(r) \propto r^{-5/2} \qquad \text{for } 0.1\ \mu m \leq r \leq 0.5\ \mu m$$
$$n(r) \propto r^{-19/4} \qquad \text{for } r > 1\ \mu m.$$

The subranges spectra were similar to

$$n(r) \propto r^{-4} \qquad \text{for } r \geq 0.1\ \mu m.$$

3. Junge's calculations

Junge (1964) worked with a numerical model of aerosol spectra that included mechanisms of coagulation and sedimentation. Other atmospheric mechanisms considered were turbulent coagulation, which was deemed unimportant for normal atmospheric conditions; photochemical oxidation of SO_2 particles; and processes in clouds.

Coagulation calculations were carried out on a Siemens S2002 computer. Constancy of the total volume of aerosol was used to check the accuracy of the calculations. Initial calculations were solved by using the uncorrected Smoluchowski formulation, later checked with a corrected version of the coagulation equations.

It was concluded that coagulation was the most important mechanism for reducing the concentration of small particles. Precipitative processes were important in the removal of large particles by rainout and attachment to cloud droplets.

Junge (1969) later made the statement that the quasi-stationary size distribution as proposed by Friedlander could have validity only at the upper and lower ends of the spectrum since only at those regions was there an adequate sink of particles, the sink being impaction and gravitational sedimentation for larger particles and thermal coagulation for small particles. In the middle regions, however, it was remarked that there was a lack of effective mechanisms for changing the distribution and a balance of mechanisms keeping an r^{-4} distribution could not exist. One explanation given for the observed continental distribution was that there existed a diversity of sources having input spectra which when mixed in specified proportions formed a broad log-normal distribution on a volume vs. log r plot.

B. Mechanisms Considered in the Lead Aerosol Aging Model

The assumption used in the numerical model was that the most important atmospheric processes were the interaction of leaded particles with non-leaded pollution particles, gravitational sedimentation, and turbulent diffusion. These processes were considered to be the most important during the time the samples were obtained. Turbulent diffusion acted mainly to dilute the aerosol and was discussed based on the original equations of coagulation without integration. In the experimental program, aging effects were observed over a body of water. Since, as was shown in Appendix IV, impaction was effective only for those small particles very near the surface it was neglected although

in cases presenting a greater impaction surface it could appreciably add to the removal of particles.

The charge carried on particles is uncertain. Fuchs (1964) studied the charge of 0.01 micron particles at equilibrium with the normal ionization of air at sea level. Ninety per cent of the particles were found to be uncharged while the other 10 per cent carried only a single charge. Since it was shown that a great deal of the total lead mass was contained by particles of radius $\sim$ 0.01 μm with about 60 per cent of the mass by particles of radius 1 μm, electrical effects were neglected. Likewise turbulent coagulation and impaction onto large particles were important only for large particles and were neglected.

This model differed from previous models in that a two component distribution was considered, having two different initial distributions. In order to simplify the problem the total mass distribution was established to be similar to the "Junge" distribution (page 25). According to Friedlander, this distribution would be expected to change very slowly in the subrange $r > 0.1$ μm and the total distribution was assumed constant.

To account for one of the two components of the spectrum, the model was operated to provide a simulation of lead aerosol aging and parameterically designed to investigate some of the features observed in different lead spectra.

II. CONSTRUCTION OF THE NUMERICAL MODEL

A. Form of the Differential Equation

The numerical model was constructed to have coagulation and sedimentation in a layer of varying depths of well mixed leaded particles and unleaded background particles. The equation describing the mechanisms considered but having only one component of the aerosol is that of Friedlander's model.

$$\frac{dn_k}{dt} dr_k =$$

$$2 \sum_{i+j=k} KK(r_i, r_j) n_i n_j dr_i dr_j - 2n_k \sum_{j=k-10}^{\infty} KK(r_k, r_j) n_j \, dr_k dr_j$$

$$+ \frac{d}{dz} \, n_k VSED(k) dr_k$$

The total range of particle size was $0.01\ \mu m \leq r \leq 10.0\ \mu m$. The total range was divided logarithmically into 91 size classes for which the characteristic radii were

$$r_i = 10^{-6} \times 10^{\frac{i-1}{30}}.$$

If N were the total number of particles contained of size $\leq r$ and $n = \frac{dN}{dr}$ then the number of particles contained in a given size class was ndr. The quantity dr was defined in

the program as $dr_i = r_{i+1} - r_i$ and $n(r) = n(r_i)$.

At the collision and adhesion of two particles the size class was changed if the sum of the volumes of the colliding particles was within the volume range of another particle class. Spherical particles were assumed to be produced by the collision process. Since a logarithmic scale was used particles many size classes smaller than a given particle would not produce a change of size, e.g. a particle of size class k would produce a particle of size class k + 1 when it collided with a particle of size class k - 10. The particle would not change its size class k, however, when it collided with a particle of size class k - 11. All particles were thus accounted for in the calculation.

The Smoluchowski coagulation formula was corrected for small particles by using the coagulation coefficient of Fuchs (1964) as derived in Appendix IV.

$$KK(r_i, r_j) = 8\Pi \frac{r_i + r_j}{2} \frac{D_i + D_j}{2} \beta$$

where $$\beta = \frac{1}{\frac{\bar{r}}{\bar{r} + \frac{\delta_r}{2}} + \frac{4\bar{D}}{G_r \bar{r}}}$$

where $\bar{r} = (r_i + r_j)/2$

$\bar{D} = (D_i + D_j)/2$

$\delta_r = \sqrt{\delta_i^2 + \delta_j^2}$

$G_r = \sqrt{G_i^2 + G_j^2}$

Lb(i) = the mean free path of particles of size class i.

$\bar{G} = (8k_{Boltzmann}T/(4/3\Pi^2 r^3))^{1/2}$.

$D_i = \bar{G}Lb\Pi/8$ is the diffusion coefficient.

In the calculations $\delta(i)$ was expressed in terms of Lb as given by Fuchs (1964) (Appendix IV) and the KK values were checked with his tabulated values.

VSED(i) is the corrected Stokes sedimentation velocity which is derived in Appendix IV.

$$VSED(i) = \frac{2gr^2}{9\eta}\left(1 + \frac{A\ell}{r_i} + \frac{Q\ell}{r_i}\exp(-B\, r_i/\ell)\right)$$

where g = gravitational acceleration
and η = the viscosity of the air.

A, Q, and B are constants given by Milliken (Appendix IV).

The equation which governed the total aerosol (including lead) in the model was solved by Friedlander and an equilibrium distribution similar to the "Junge" distribution was obtained. Indeed, measurements in a polluted atmosphere showed distributions similar to the "Junge" distribution (e.g. Petersen (1968)). The total spectrum was held constant while the lead portion was allowed to change. Thus, coagulation involved 1) coagulation of a leaded component with an unleaded component, 2) coagulation of the leaded component with itself and, 3) coagulation of the unleaded component with itself. The calculation showed the importance of the unleaded background aerosol level to the change of lead aerosol.

Beginning at time t = 0, the background particle distribution was already at equilibrium. At time t = 0 a frac-

tion, ld(i), of the particles in size class i of this distribution contained lead of mass ms(i). Since the particle distribution as a whole did not change and part of it was leaded, the leaded part changed while n(k) remained constant (i.e., n(k) remained constant, ld(k) was computed, and ms(k) was computed for each time step). The equations are

$$\frac{dn_k ld_k}{dt}\, dr_k = \sum_{i+j=k} KK(r_i, r_j) n_i n_j \Psi(i,j) dr_i dr_j$$

$$- \sum_{j=k-10}^{\infty} KK(r_k, r_j) n_k n_j \Psi(k,j) dr_k dr_j$$

$$+ VSED(k) \frac{d}{dz} n_k ld(k) dr_k$$

where $\Psi(i,j) = ld(i)(1 - ld(j)) + ld(j)(1 - ld(j)) + ld(i)ld(j)$

$$\frac{dn_k ld(k) ms(k)}{dt}\, dr_k = \sum_{i+j=k} KK(r_i, r_j) n_i n_j$$

$$- \sum_{j=k-10}^{\infty} KK(r_k, r_j) n_k nj \Phi(k,j) dr_k dr_j$$

$$+ VSED(k) \frac{d}{dz} n_k ld(k) ms(k) dr_k$$

where $\Phi(i,j) = ld(i)ms(i)(1-ld(j)) + ld(j)ms(j)(1-ld(j))$

$+(ms(i)+ms(j))(ld(i)ld(j))$.

The equation was integrated for 200-second time intervals and ld(k) and ms(k) were computed for each t ime step.

The size distribution of the background aerosol was expressed in a one parametric form. That is, for $r \geq 0.1$ μm,

$$n(r) = n(r_0)\left(\frac{r}{r_0}\right)^{-4}$$

for $r \leq 0.1$ $n(r) = n(r_1)$

$r_1 = 0.1$ μm

$r_{max} = 10.0$ μm

$r_{min} = 0.01$ μm (Figure 15)

The choice of the upper size limit of the total aerosol size distribution and the minimum radius at which the $n(r) \propto r^{-4}$ were not of great importance to the results of the calculation.

As will be shown the effect upon lead coagulation of the lower limit of the background distribution was negligible since in that region particles had a relatively large fallout velocity and coagulated mass was negligible in comparison with that of smaller particles. The radius at which the r^{-4} law started was shown to be the center of the region

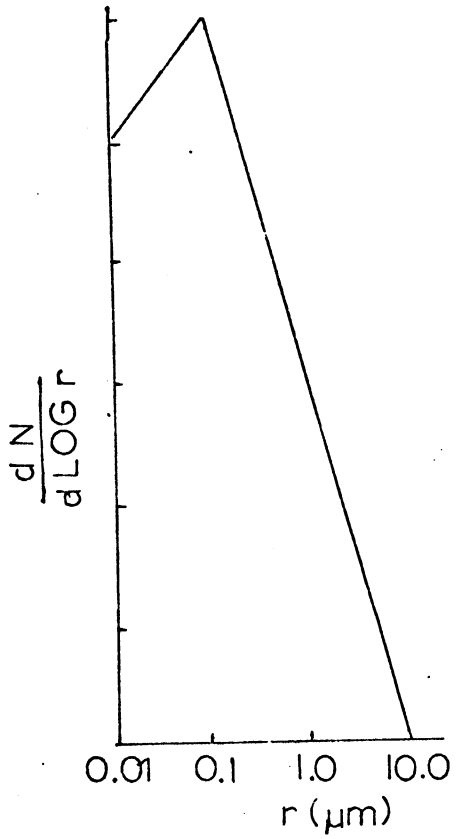

Fig. 15.--The total aerosol size distribution used in the numerical model.

of maximum gain of coagulated lead. The region $0.05 < r < 0.5$ μm was quite stable with respect to coagulation, however, so that the model's sensitivity for the choice of $r = 0.1$ μm as the minimum radius of the r^{-4} distribution was not great with respect to the change of lead mass in the spectrum as a whole.

The determining parameter of the background distribution was $n(r_0)$. For heavy pollution $n(r_0)$ was set at 10 (Kenline, 1968).

B. Method of Integration

The equations of lead spectrum growth were integrated using a standard fourth order Runge-Kutta scheme (Suzuki et al., 1969; Ralston and Wilf, 1960). A time interval of 200 seconds was used with a number of different total aerosol spectra and input leaded spectra. Nintey one size classes were used representing radii of from 0.01 micron to 10 microns.

C. Checks on Accuracy of the Model

As in Junge's calculations the total lead mass was checked at the end of each time-step integration. If the mass changed by as much as 10 per cent calculations were terminated. In practice total mass was reduced to a maximum of around 0.01 per cent in eight hours.

In addition, other tests were applied in the operation of varying initial conditions. The time step Δt was set at 50, 100, and 200 seconds for the same run. Differences in the results were observed only at the sixth decimal place at 1/2 hour for the three tests. One test used two different methods of integration; the Runge-Kutta method, used in the remainder of the calculations, and Hammings method. No significant difference was seen in the results.

Lastly, a test was applied in comparing the machine solution to removal of mass from the first size class to an analytic model of the same phenomenon (case 1). Analytical and numerical solutions agreed sufficiently. (Figure 16).

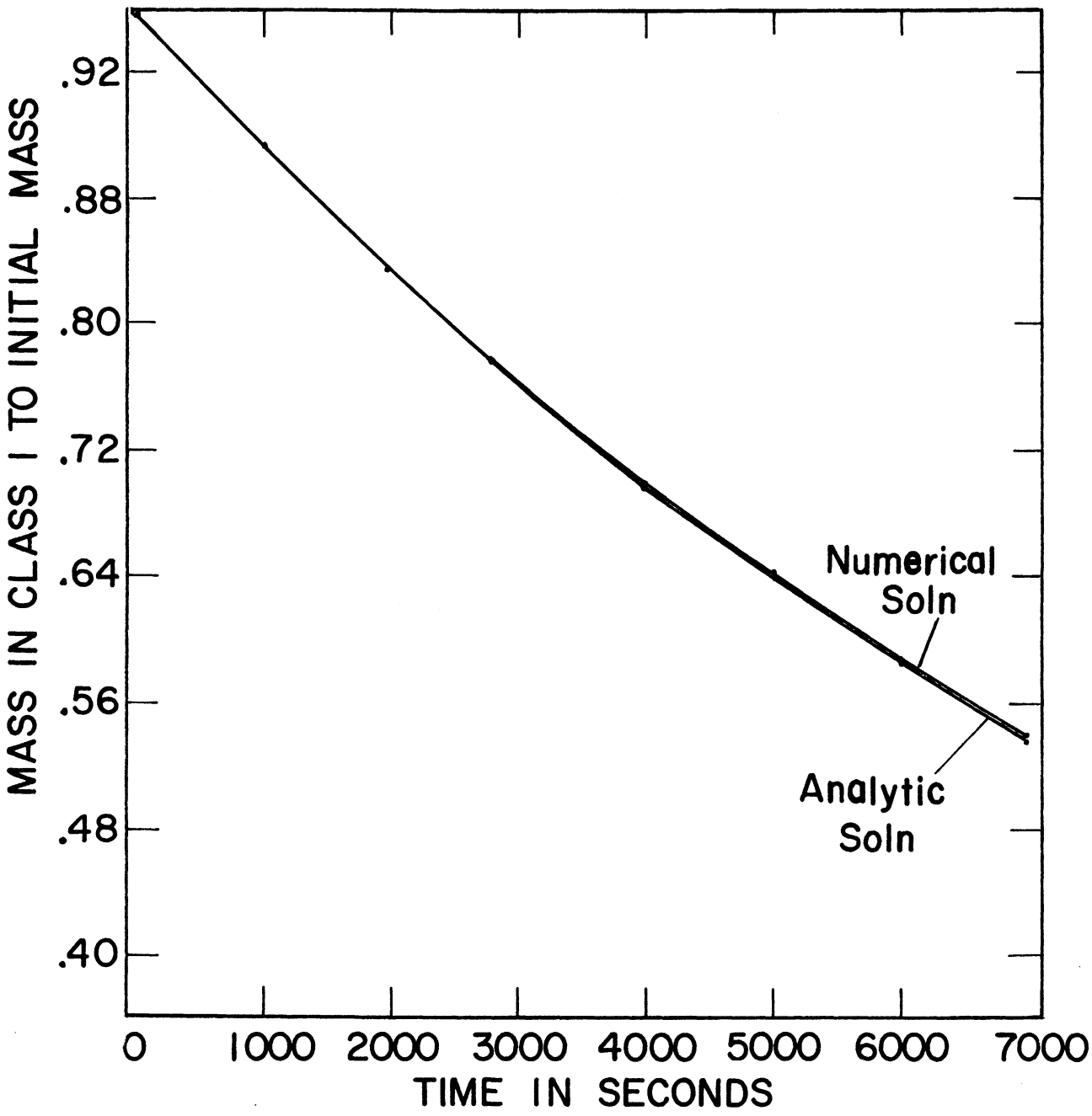

Fig. 16.--A comparison of the numerical solution and analytic solution of lead mass vs. time at r = 0.01 μm for Case 1

III. RESULTS AND DISCUSSION

In investigating the properties of the lead size distribution and its aging due to the mechanisms of coagulation and sedimentation, the most relevant questions in explaining the observed features were assumed to be those concerning the effect upon the aging distribution of variations of the initial lead input spectrum and the equilibrium of unleaded background spectrum. The input spectrum seemed to consist of 1) a spectrum directly due to combustion having a mean size from 0.01 to 0.05 microns and 2) a spectrum due to lead deposits "flaking off" the exhaust system surfaces, perhaps more poly-disperse and having particles greater than one micron. Two subranges of the initial lead spectrum ($0.01\ \mu m < r \leq 0.1\ \mu m$ and $0.1\ \mu m \leq r < 10\ \mu m$) were examined separately in the simulation experiments.

Aging of an input lead spectrum having the upper limit $r = 0.1\ \mu m$ was studied by varying the shape of the input lead spectrum in that region (Cases 1-4). Cases 1 through 3 considered an input lead spectrum where all lead was contained by particles of radius $0.01\ \mu m$ and where different total distributions were examined and the model mechanisms were isolated. The aging of an input lead spectrum having most lead mass in particles $r > 0.1\ \mu m$ was studied using an initial lead spectrum having little lead mass in particles $r < 0.1\ \mu m$ (Cases 5 and 6).

Relations seen in the two subregions of the initial lead spectrum (separated at r = 0.1 μm) were valid when the initial lead spectrum was treated as a whole. Of special interest was the effect of the total spectrum. An "urban model" (Case 8) total spectrum was set 10 times greater in mass than the "city of population 100,000-200,000" model (Case 7), both models having identical input lead spectra. The "urban" and "city of population 100,000-200,000" models were of benefit in interpreting two of the results of the observational section; 1) highly aged lead spectra were similar to source area lead spectra, implying a rather slow aging process and 2) more lead mass was found in stage 7 of the Andersen Sampler in "urban" compared to "city of population 100,000-200,000" locations. The primary purpose of this section was to investigate the aging of "urban" and "city of population100,000-200,000" model spectra by considering the subregions of the input spectra (Cases 1-6) and then the entire spectra (Cases 7-8).

The effect of vertical dilution due to vertical turbulent transport was indirectly studied by varying the depth of the effective layer containing the lead aerosol.

In summary, lead parameters studied are shown in Table 10.

A. Cases Concerning the Initial Lead Spectrum where all Lead Mass is in Particles of Radius 0.1 μm

CASE 1

The first case afforded an analytical treatment of removal from the input spectrum which, compared to the numerical solution, gave a quality check for the numerical integration. The background spectrum $n(r) \propto c(\frac{r}{r_0})^{-4}$ (r 0.1 μm)

TABLE 10

LEAD PARAMETERS USED IN THE NUMERICAL MODEL[1]

Case	Lead Input Spectrum	Background Spectrum	Layer Depth (m)
1	$n'(r)=\delta(r=0.01\mu m)$ corresponding to idealized combustion spectrum	$n(r)=c(r/r_0)^{-4}$ $(0.1\mu m \leq r \leq 10\mu m)$ $n(r)=0, (r < 0.1\mu m)$ $c=10=n(r_0)$	10
2,3	Same as for 1	$n(r)=c(r/r_0)^{-4}$ $(0.1\mu m \leq r \leq 10\mu m)$ $n(r)=const, r < 0.1\mu m$ $c=n(r_0)=10$	10,2
4	$n'(r)=const.$ $0.01\mu m \leq r \leq 0.1\mu m$	$n(r)=c(\frac{r}{r_0})^{-4}$ $(0.1\mu m \leq r \leq 10\mu m)$ $n(r)=const,$ $(0.01 \leq r \leq 0.1\mu m)$ $c=n(r_0)=10$	10
5,6	$n'(r)=r^{-4}$ $(0.1\mu m \leq r \leq 10\mu m)$ $n'(r)=const.$ $(0.01\mu m \; r \; 0.1\mu m)$	$n(r)=c(r/r_0)^{-4}$ $(0.1\mu m \leq r \leq 10\mu m)$ $n(r)=const.$ $(0.01\mu m \leq r \leq 0.1\mu m)$ $c=n(r_0)=10$	10,100
	$n'(r)=r^{-4}$ $(0.1\mu m \leq r \leq 10\mu m)$ $n'(r)=const.$ $(0.01\mu m \leq r \leq 0.1\mu m)$ $n'(r)=\delta(r=0.01\mu m)$	$n(r)=c(r/r_0)^{-4}$ $(0.1\mu m \leq r \leq 10\mu m)$ $n(r)=const,$ $(0.01\mu m \leq r \leq 0.1\mu m)$	100
7		c=1(City of 100,000-200,000 population Model)	
8		c=10(Urban Model)	

[1] In case 1 $\delta(r=0.01\mu m)$ means that all lead mass is

was allowed to coagulate with background particles. If the background concentration of size class j particles were $n_j dr_j$ and the concentration of lead particles of size r=0.01 μm were $n_i dr_i$, the rate of attachment of a lead particle of r=0.01 μm by a background particle of size class j (assuming no coagulation of lead particles r 0.01 μm and no sedimentation) was

$$\frac{d(\text{lead content of class j})}{dt} = \sum_i 4\Pi D(r_i, r_j) R_{ij} n_i n_j dr_i dr_j$$

where due to the initial condition

$$D(r_i, r_j) = D(r_i) + D(r_j) \sim D(r_i) \sim 10^{-4} \text{ cm}^2/\text{sec}.$$

and

$$R_{ij} = r_i + r_j \sim r_j$$

then

$$\frac{d(\text{lead content of class j})}{dt} = \frac{4\Pi(10^{-4})\, r_j^{-3}}{r_0^{-4}} dr_j\, n_i\, dr_i.$$

That is, lead was absorbed by j particles at a rate proportional to the number of particles in the r = 0.01 μm size of leaded particles divided by the volume of the j particle. Particles were accumulated in the 0.1 μm size range at a rate 10^6 more rapidly than in the 10 μm size range. On the other hand, a single 10 μm particle tended to collect lead particles 100 times more than a 0.1 μm

---

contained in particles of radius r = 0.01 μm. In cases 7 and 8 δ(r = 0.01 μm) means that a discontinuous high concentration of mass exists at particles of r = 0.01 μm.

particle. Initially, then, there was a growth of lead giving an r^{-3} volume spectrum.

If r_0 = 1 μm and c = 10 (corresponding roughly to 200 micrograms/m^3) integration of the above equation gives[1]

$$n_1 = n_1(t = 0)e^{-Kt}$$

where $K = 1/8.5X10^{-5}$ sec ~ 3 hours.

The time constant K varied inversely as c. A time of 30 hours was needed for an e^{-1} reduction of the initial lead spectrum in an atmosphere having 1/10 the particulate background concentration.[2]

The same model of the aerosol was integrated including a gravitational sedimentation mechanism and is shown in Figure 17.

---

[1] An estimate of Chicago particulate concentration is 185 micrograms/m^3 (Kenline, 1968).

[2] A similar treatment may be found by Greenfield (1957).

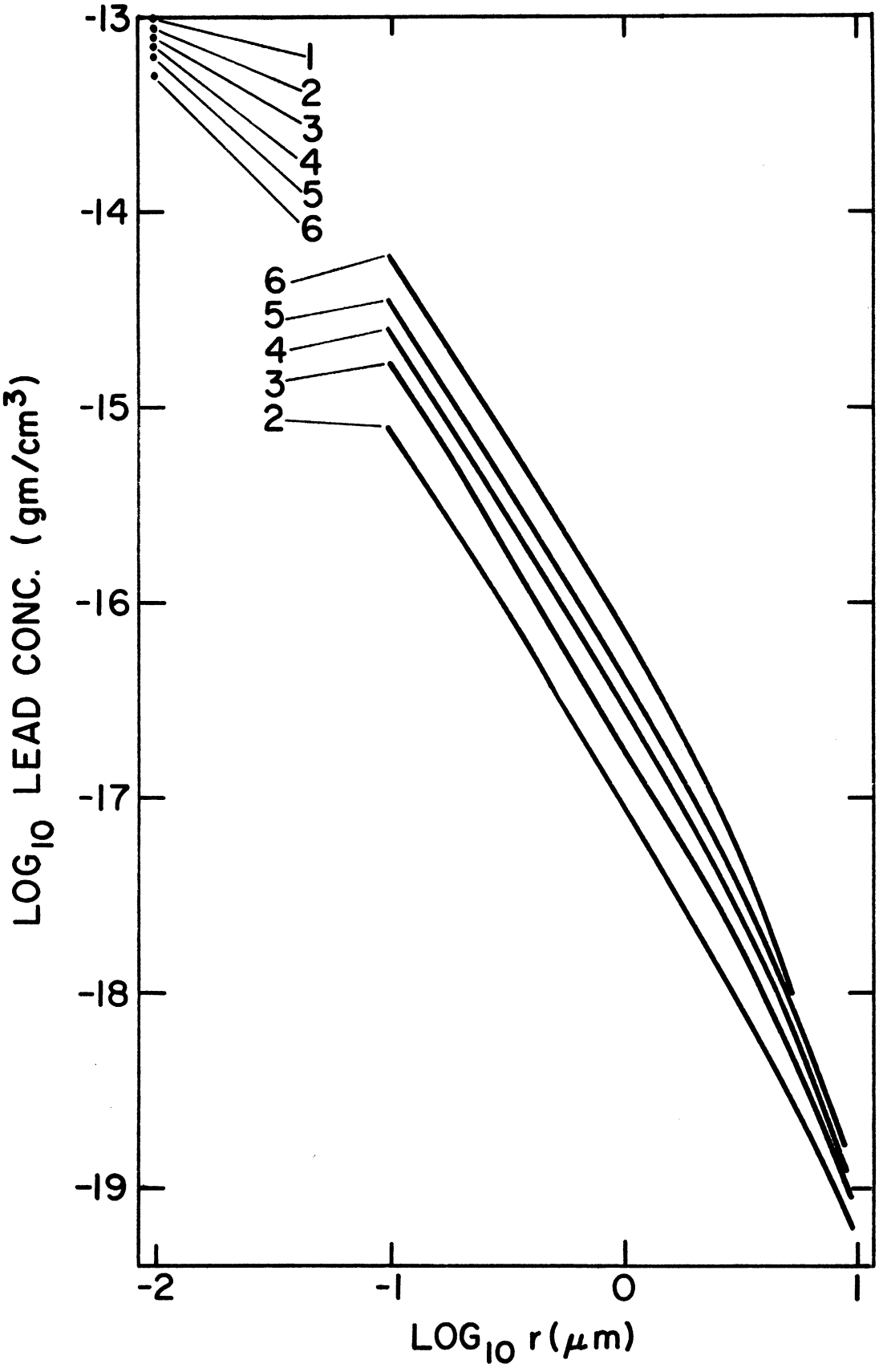

Fig. 17.--The numerical solution for Case 1. 1: 0 sec., 2: 800 sec., 3: 30 min., 4: 2800 sec., 5: 1 hr., 6: 2 hr.

In this model coagulation of the newly formed leaded particles and gravitational sedimentation were allowed. The similarity of the spectrum to $n(r) = cr^{-3}$ was noted although large particles affected by gravitational sedimentation deviated from it. Lead content of the largest particles reached a quasi-equilibrium after about a half hour. Smaller particles grew in lead concentration, matching the rate of decrease of the input spectrum.

CASE 2

In case two a more realistic background spectrum (one whose resulting lead distribution, when compared to the above results, may give some idea of the importance of the background distribution between 0.01 and 0.1 microns) was $n(r) = \text{constant}$ $(0.01\ \mu m \leq r \leq 0.1\ \mu m)$ with $n(r) = c(r/r_0)^{-4}$ $(0.1\ \mu m \leq r \leq 10\ \mu m)$. The equations were integrated for a total of seven hours with c set at 10. Results are shown in Figures 18 and 19.

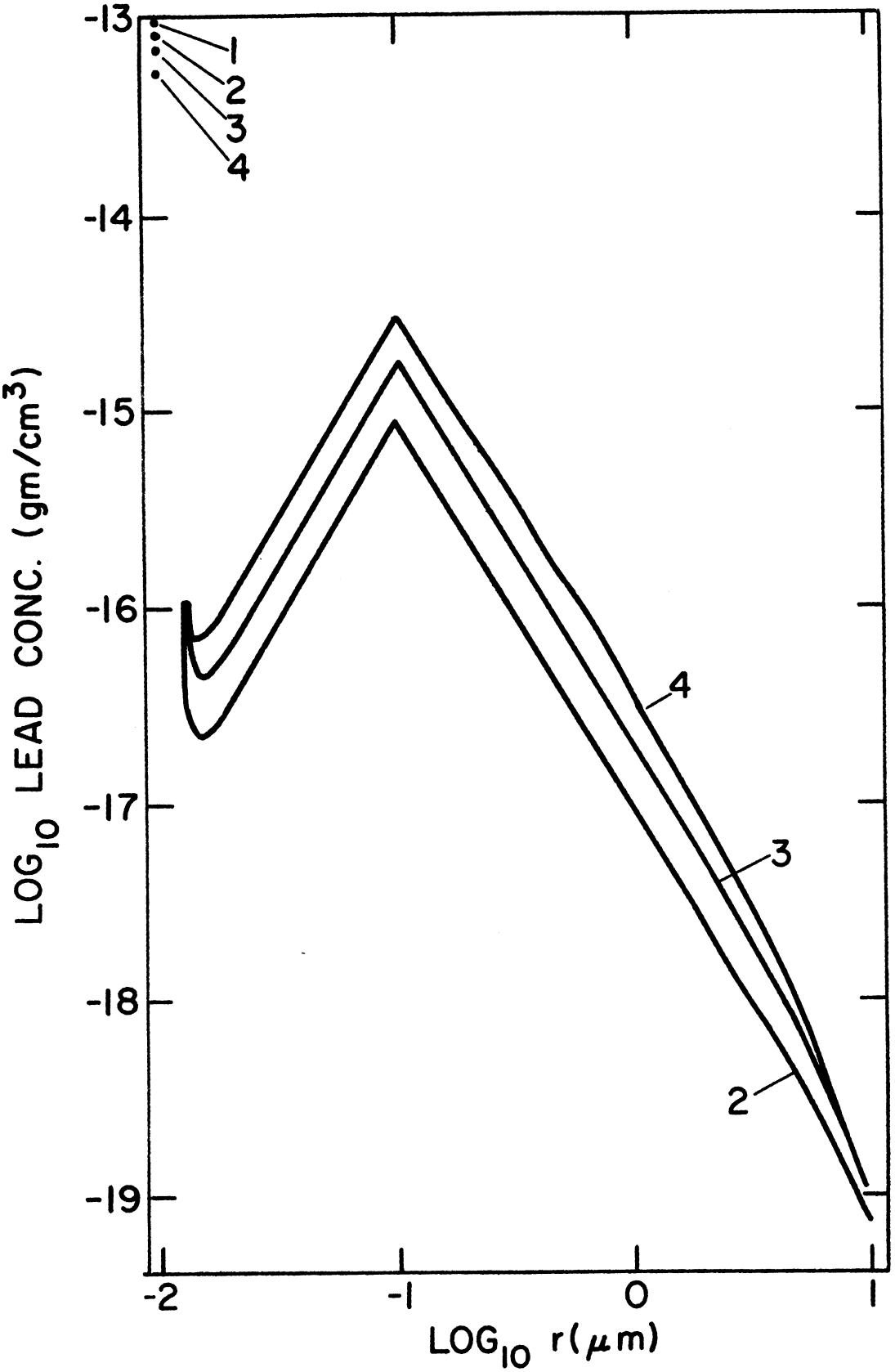

Fig. 18.--The numerical solution for case 2. 1: 0 sec., 2: 800 sec., 3: 30 min., 4: 1 hr.

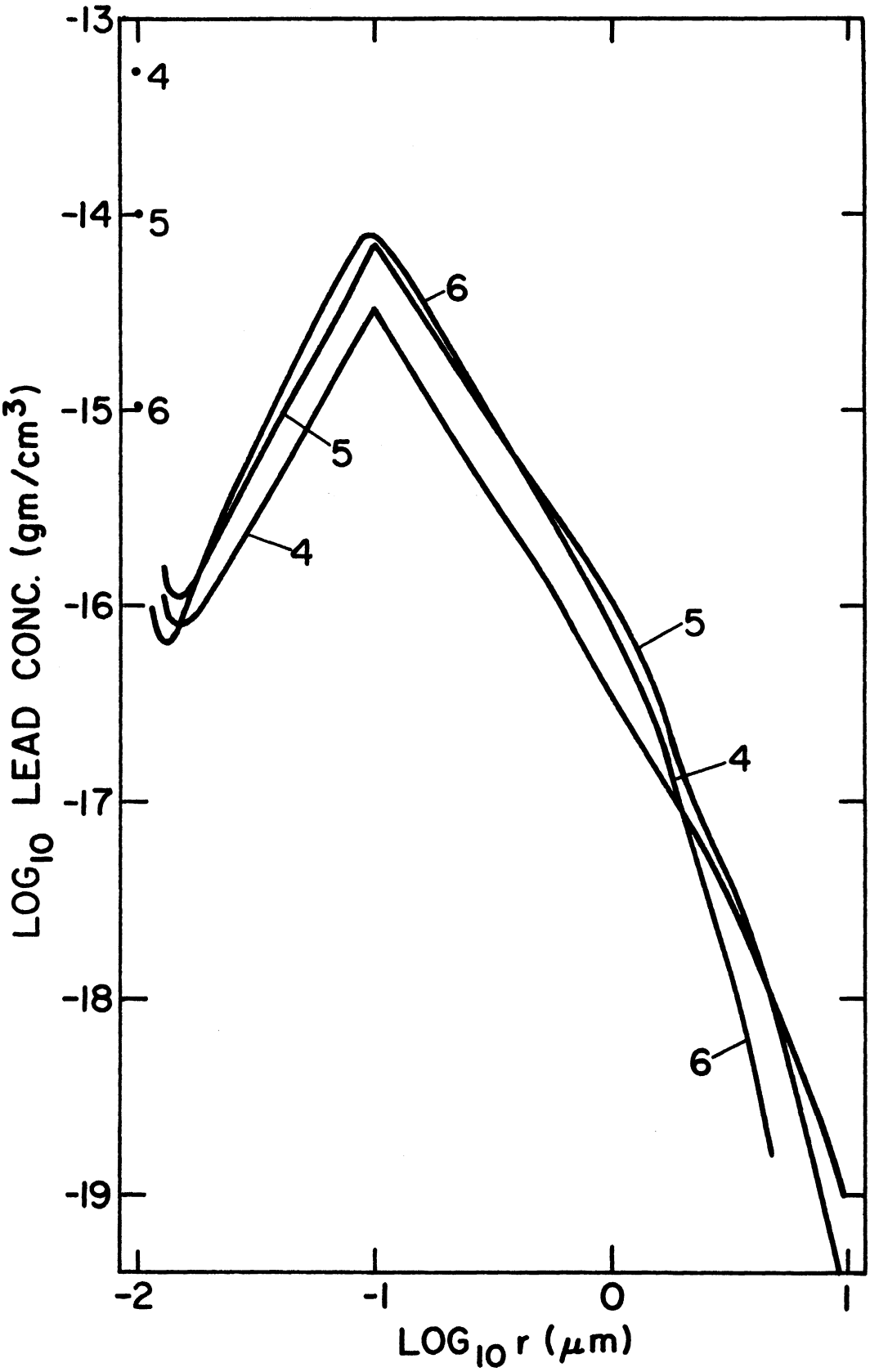

Fig.19 .--The numerical solution for Case 2. 4:1 hr, 5:4 hr., 6:7 hr.

In case 2 the removal rate of lead particles of radius 0.01 μm was practically doubled in comparison to case 1. The new lead spectrum was bimodal, having maxima at 0.01 μm and 0.1 μm (the maximum of the background particle concentration). As before, the rate of lead concentration deposition on small particles followed the decrease of the input spectrum particles. Almost as much lead mass was contained by the particles located in the region $0.01\ \mu m \leq r \leq 0.1\ \mu m$ as by the particles in the region $r > 0.1\ \mu m$. The plot did not indicate that the shape of the background spectrum in this region was of great importance in determining the mass of lead contained, since most of the deposited lead mass was contained by particles within a few size classes of the maximum concentration located at 0.1 μm. The shape of the lead size distribution for particles larger than $r = 0.1\ \mu m$ was very similar to the distributions found in the previous case, though slightly less in magnitude since the magnitude of the input spectrum was diminished at a greater rate. The rate of coagulation onto larger particles, proportional to this magnitude, was decreased. The particles at size 10 μm, in a quasi-equilibrium from 1/2 to 4 hours, were moved to a lower concentration level at 7 hours due to the decrease in coagulation input into these sizes from smaller sizes. In the interval 4 to 7 hours the leaded particle size distribution for $0.05\ \mu m \leq r \leq 0.5\ \mu m$ was changed little and represented a very stable part of the leaded particle spectrum for the mechanisms of coagulation and sedimentation.

CASE 3

The effects of the mechanisms may be seen by comparing the resulting size distributions for 4 differing models operated for two hours (Figure 20). The effect of both sedimentation and coagulation of leaded particles larger than 0.01 micron may be seen by comparing results of models having those mechanisms to the model having no coagulation except from the 0.01 μm particle size class and which had no sedimentation (Case 1). In the model where all lead mass was initially in particles r = 0.01 μm but which had no sedimentation, the distribution in the subrange $0.1\ \mu m \leq r \leq 10\ \mu m$ was, after two hours, similar to that of case 1. This similarity showed negligible lead contribution to larger particles from coagulation by intermediate particles which would have effectively added mass to larger particles.

When most of the lead was initially contained in the very small size classes and sedimentation was ignored lead growth in the larger particle size classes was practically linear, dominated by direct coagulation of small particles onto the larger particles, intermediate particles giving little or no contribution.

Case 1, having no background particles for $0.01\ \mu m \leq r \leq 0.1\ \mu m$ showed a slightly larger amount of mass at the range $0.1\ \mu m \leq r \leq 10\ \mu m$ than the model having $n(r) = \text{const.}$ $(0.01\ \mu m \leq r \leq 0.1\ \mu m)$ but the spectrum slope was identical. Thus the exact form of the spectral subrange $0.01\ \mu m \leq r \leq 0.1\ \mu m$ was not judged to be important in the growth of the spectral subrange $r \geq 0.1\ \mu m$ when all initial lead mass was contained by particles of radius r = 0.01 μm.

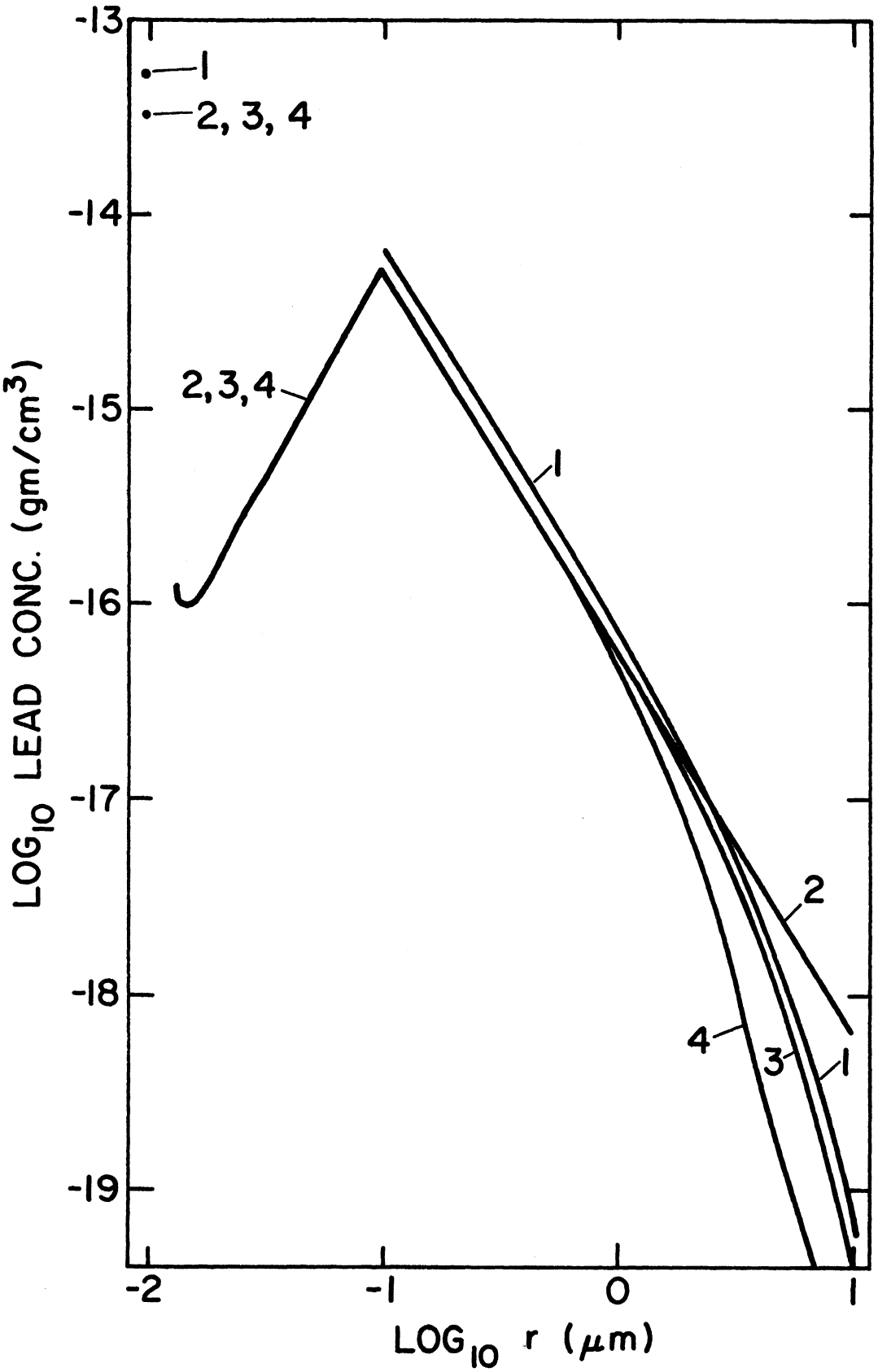

Fig. 20.--The numerical solutions for case 3 at 2 hours. 1: Casel, d=10m. 2: Case 2, coag., no sed. 3: Case 2, d=10m. 4: Case 2, coag. from r=0.01μm only d=2m.

The effect of vertical diffusion was studied indirectly. The effective layer depth was connected to the role of vertical turbulent transfer since the lead, having essentially a ground source, was diffused vertically by turbulence. If vertical turbulent transfer were weak, a small effective layer depth resulted. As shown by the two hour results for layers 2m and 10m, this effect was important primarily for particles $r > 1.0$ micron, smaller layer depths resulting in more removal of larger particles.

The effect of dilution on the rate of coagulation was not considered for this study. The rate of coagulation was proportional to the concentration squared. Hence, a reduction of concentration would be magnified in reduced coagulation as the square of the dilution.

CASE 4

The initial input spectrum was set at $n(r)$ = constant. ($0.01\ \mu m \leq r \leq 0.1\ \mu m$) each particle being pure lead. The equations were integrated for eight hours and results are shown in Figure 21.

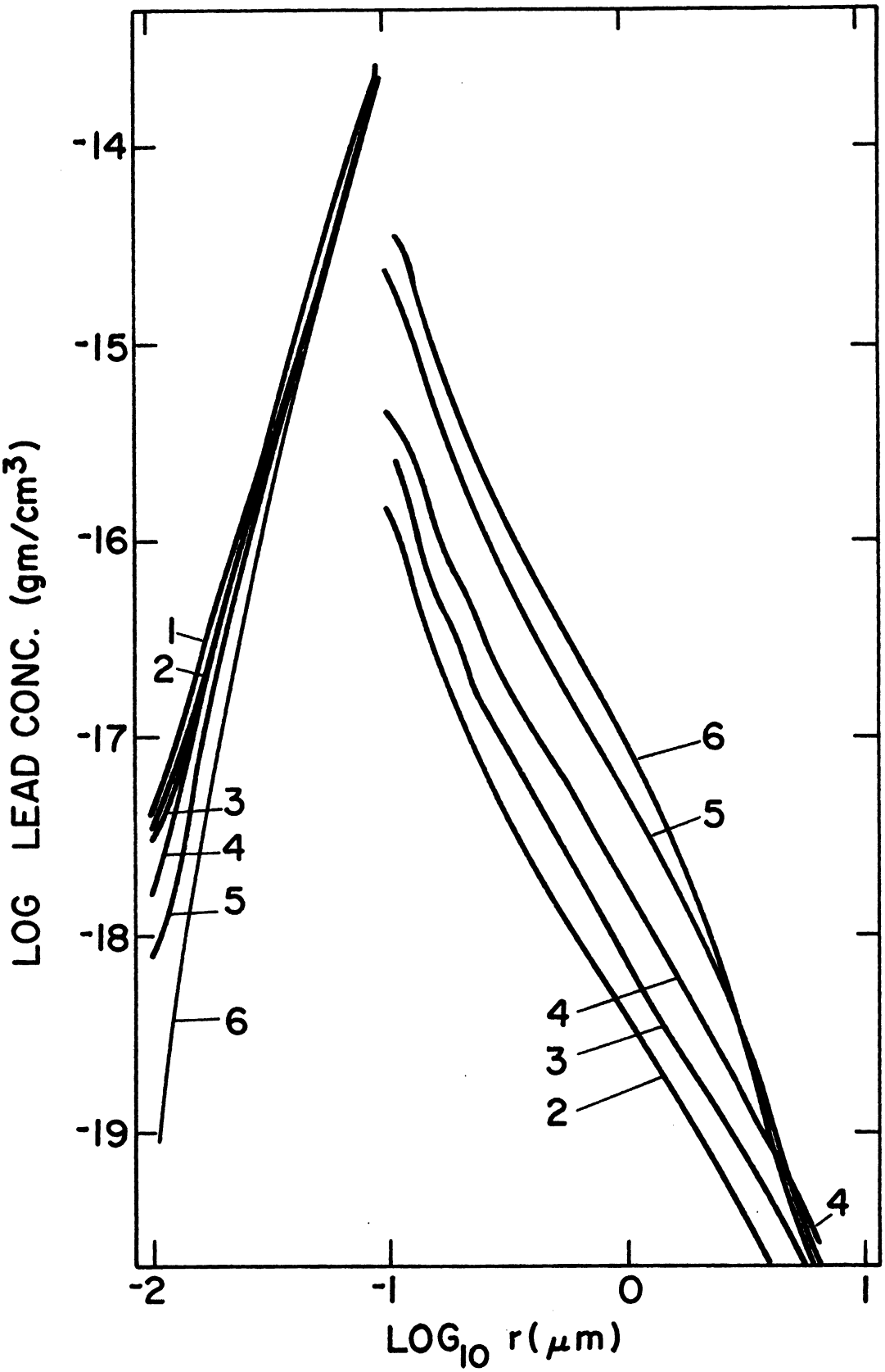

Fig. 21.--The numerical solution for Case 4. 1: 0 sec., 2: 800 sec., 3: 30 min., 4: 1 hr., 5: 4 hr., 6: 8 hr.

The most apparent result of such an initial distribution was reduced coagulation for the same total input as in Case 2. This was explained by the reduced coagulation of particles having radii more similar in magnitude. After eight hours a large reduction of r = 0.01 μm particles and an insignificant reduction of 0.1 μm radius particles was apparent. The r = 0.1 μm size class not only had a maximum deposition of particles coagulating from sizes smaller than itself, but in addition had a rather slow rate of removal from r = 0.01 μm particles. The slope of the size distribution for 0.1 μm $\leq$ r $\leq$ 10 μm was similar to those distributions having $n'(r)_0 = \delta$ (r = 0.01 μm) but was not affected as greatly in time due to gravitational sedimentation. This was probably due to an increased role of coagulation from particles intermediate in the size distribution.

B. Cases Concerning the Initial Lead Spectrum where most Lead Mass is in Particles of Radius $>$ 0.1 μm

CASE 5,6

An input spectrum including particles larger than 0.1 μm were of interest , especially when considering the lead particle spectra whose origins were the "flaking off" of lead deposits from surfaces of the automobile exhaust system. Such a distribution was assumed to be roughly parallel to the background distribution, i.e. n'(r) = const. (0.01 μm $\leq$ r $\leq$ 0.1 μm) and $n'(r) = c(r/r_0)^{-4}$ c = 10, r_0 = 1 μm. Layer depths of 10 meters and 100 meters were used (Figure 22.)

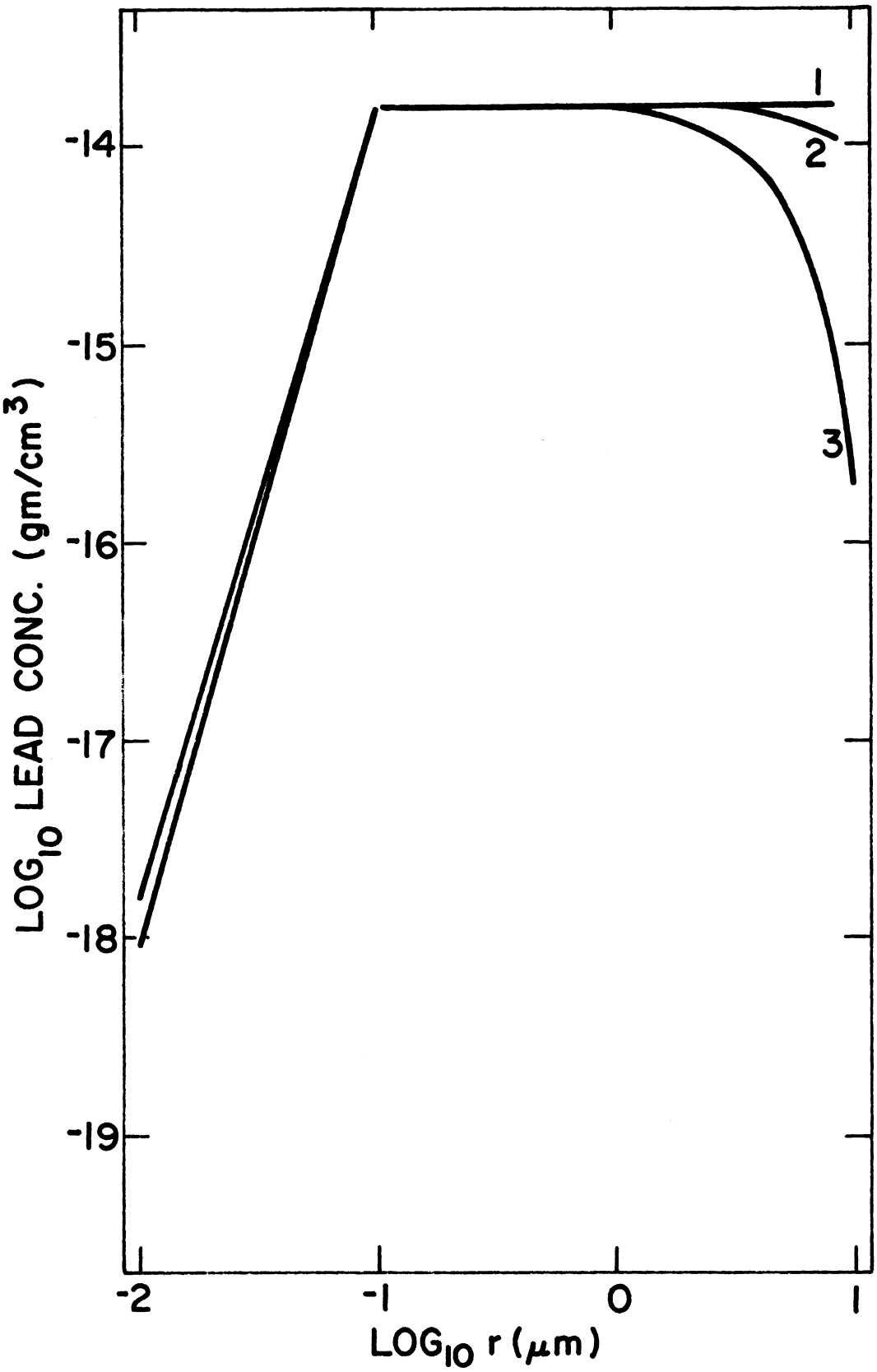

Fig. 22.--The numerical solutions for Cases 5 and 6. 1:0sec, 2:1 hr.(Case 6) 3: 1 hr. (Case 5).

The change in the spectrum subrange $r < 0.1$ μm is similar to that for Case 4. However, the subrange $0.1\ \mu m \leq r \leq 1\ \mu m$ was affected by a small addition of mass due to coagulation and the subrange $r > 1$ μm was decreased in concentration due to gravitational sedimentation. The change of the spectrum above one micron was especially great for small layer depths thus indicating that gravitational fallout and vertical turbulent transfer were important for this subrange.

C. "Urban" and "City of population 100,000-200,000" Lead Aerosol Aging Models

CASE 7,8

All the above features were combined in an input spectrum of lead where 95 per cent of the mass was distributed into an initial lead mass spectrum following the distribution of the background material
($n(r) = \text{const}$ $(0.01\ \mu m \leq r \leq 0.1\ \mu m)$ and
$n(r) = c\ (r/r_0)^{-4}$ $(0.1\ \mu m \leq r \leq 10\ \mu m)$ $r_0 = 1\ \mu m$) with 5 per cent of the initial lead mass at $n'(r) = (r = 0.01\ \mu m)$, a distribution perhaps similar to that actually injected into the atmosphere.[1] C was set at 1 to simulate the atmosphere

---

[1]This particular model does not correspond exactly to the observed distribution of Mueller et al., (1962) where 43-55% of the lead mass is found in particles of radius smaller than 0.3 microns as compared to 33 % for the present model. The exact form of the spectrum subrange r 0.3 μm is poorly known making a model of initial lead mass corresponding to reality impossibel at this time. However, the general properties of the above models (Case 7 and 8) along

of a "city of population 100,000-200,000" atmosphere, and at 10 to simulate an urban atmosphere. Layer depths were set at 100 m. Results are given in Figures 23-27.

---

with the knowledge of aging for various subranges of the spectrum (Cases 1-6) will substantiate the conclusions of Part 1, i.e. that lead aerosol size distribution changes rapidly only in the subranges $r < 0.05$ μm and 5 μm $< r$.

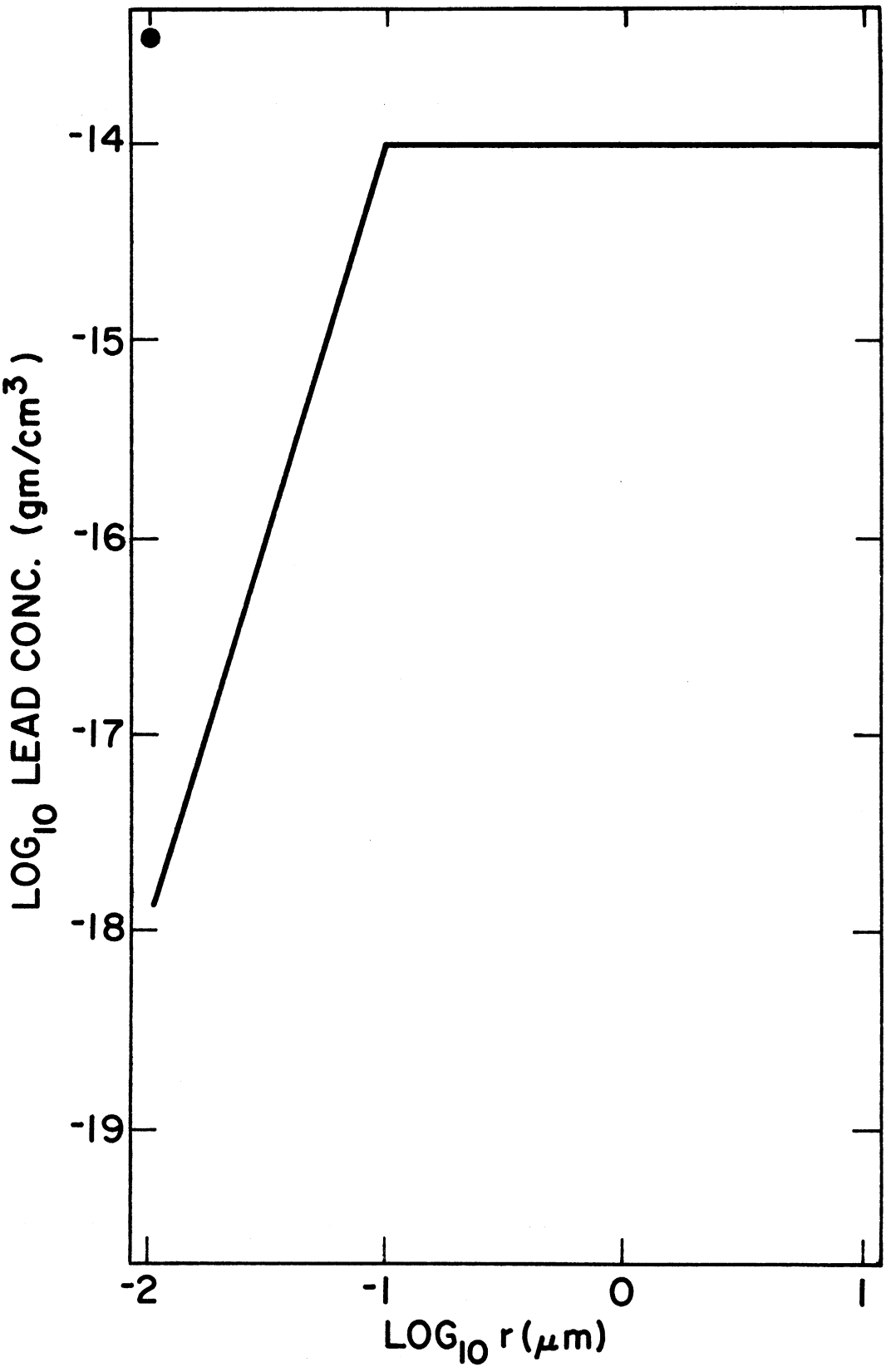

Fig. 23 .--The initial lead spectrum for cases 7 and 8.

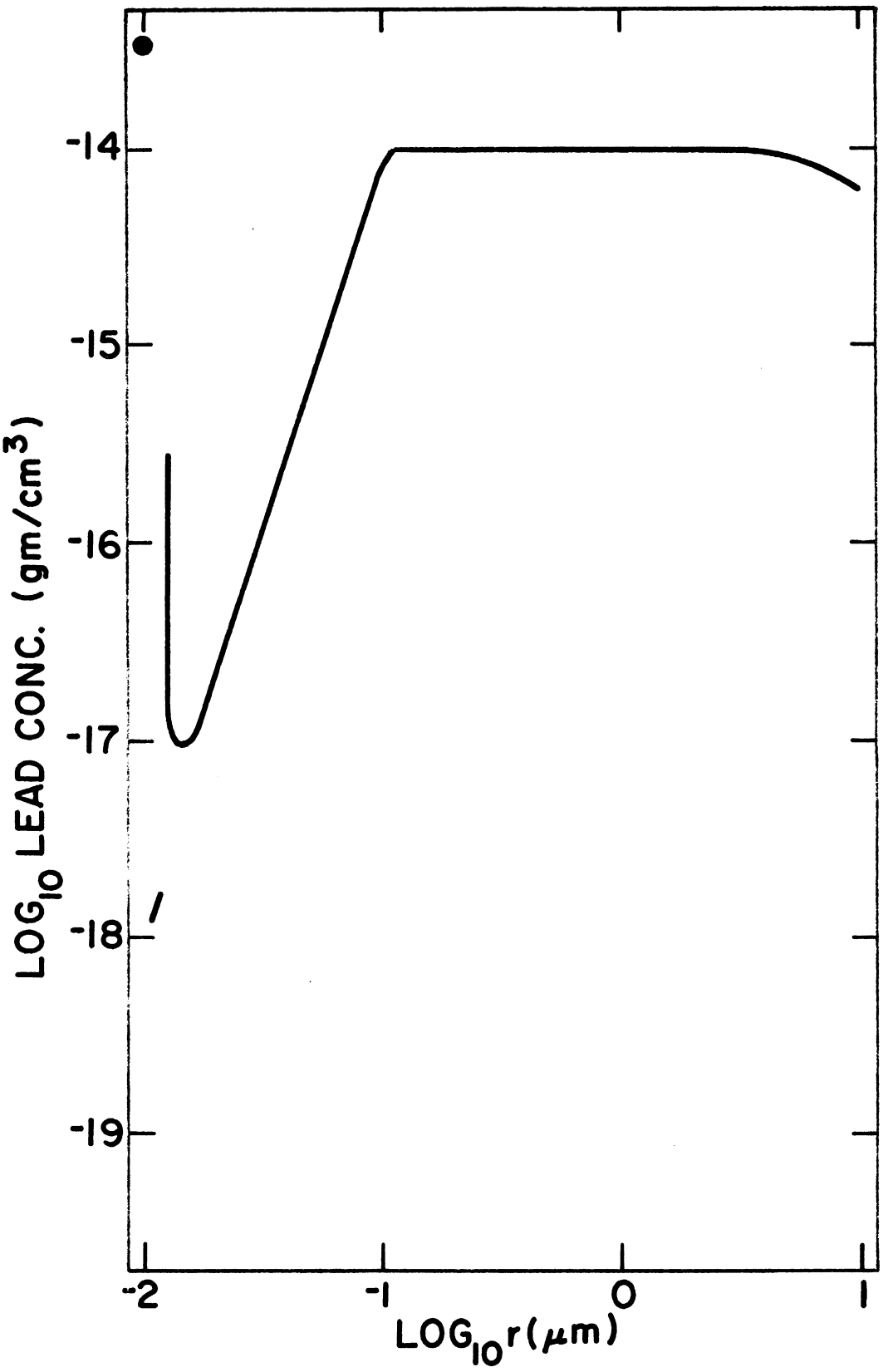

Fig.24 .--The numerical solution for Case 7 at one hour.

After one hour the spectrum of Case 7 showed little change except for $r < 0.05$ μm and $r > 5$ μm. In these two regions coagulation and sedimentation diminished the extremes of the spectrum.

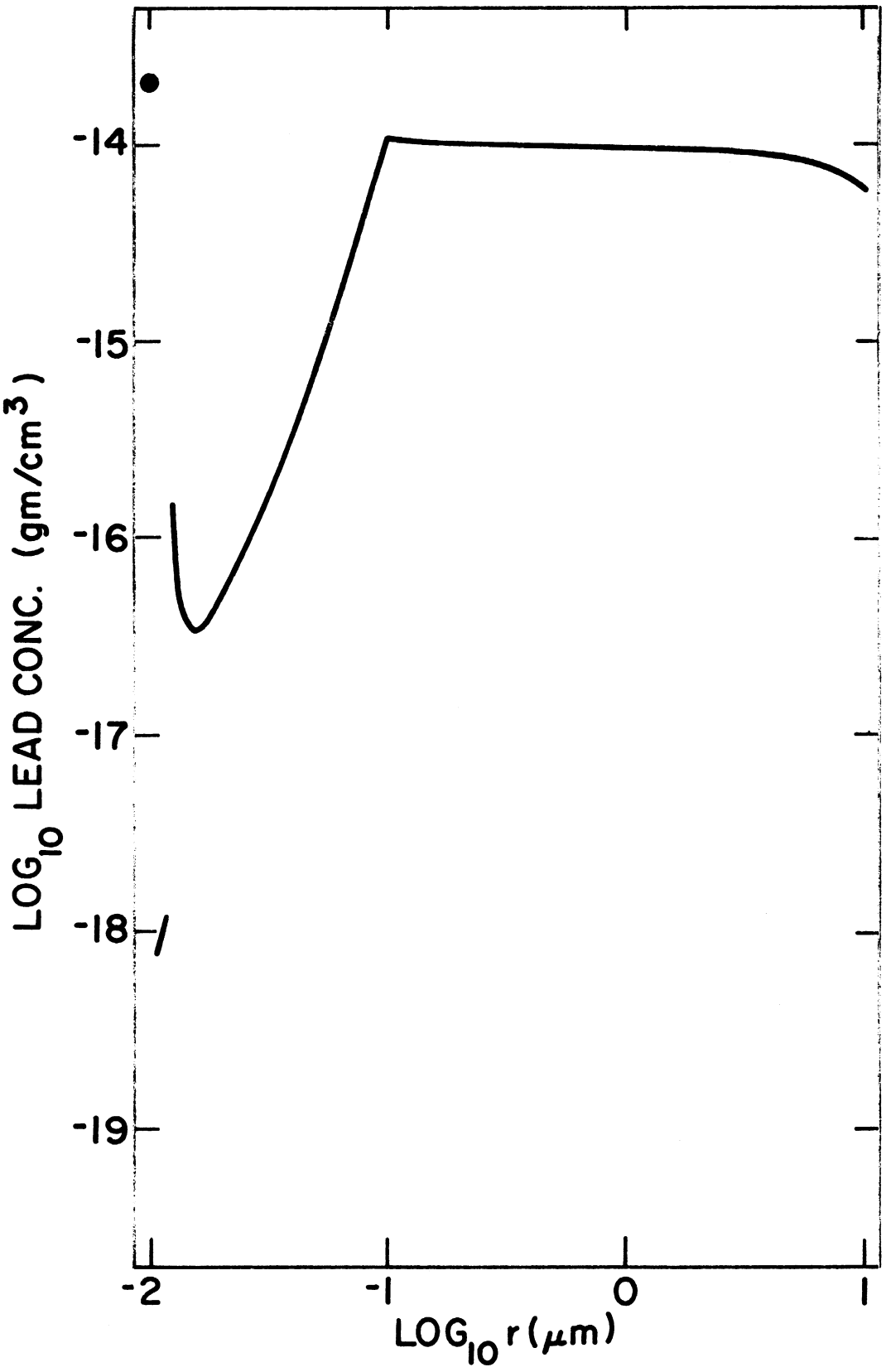

Fig. 25.--The numerical solution for Case 8 at one hour.

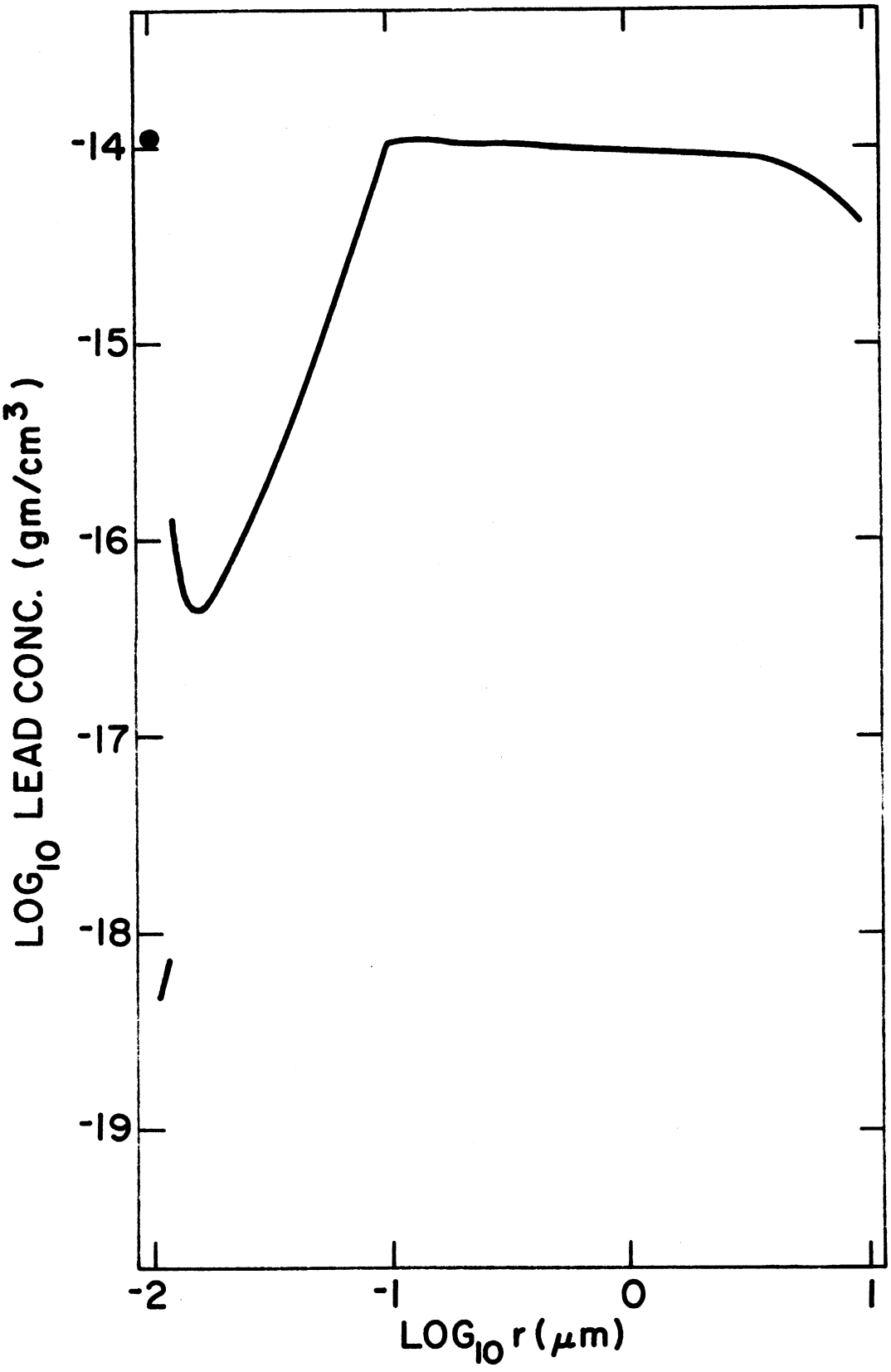

Fig.26 .--The numerical solution for Case 8 at two hours.

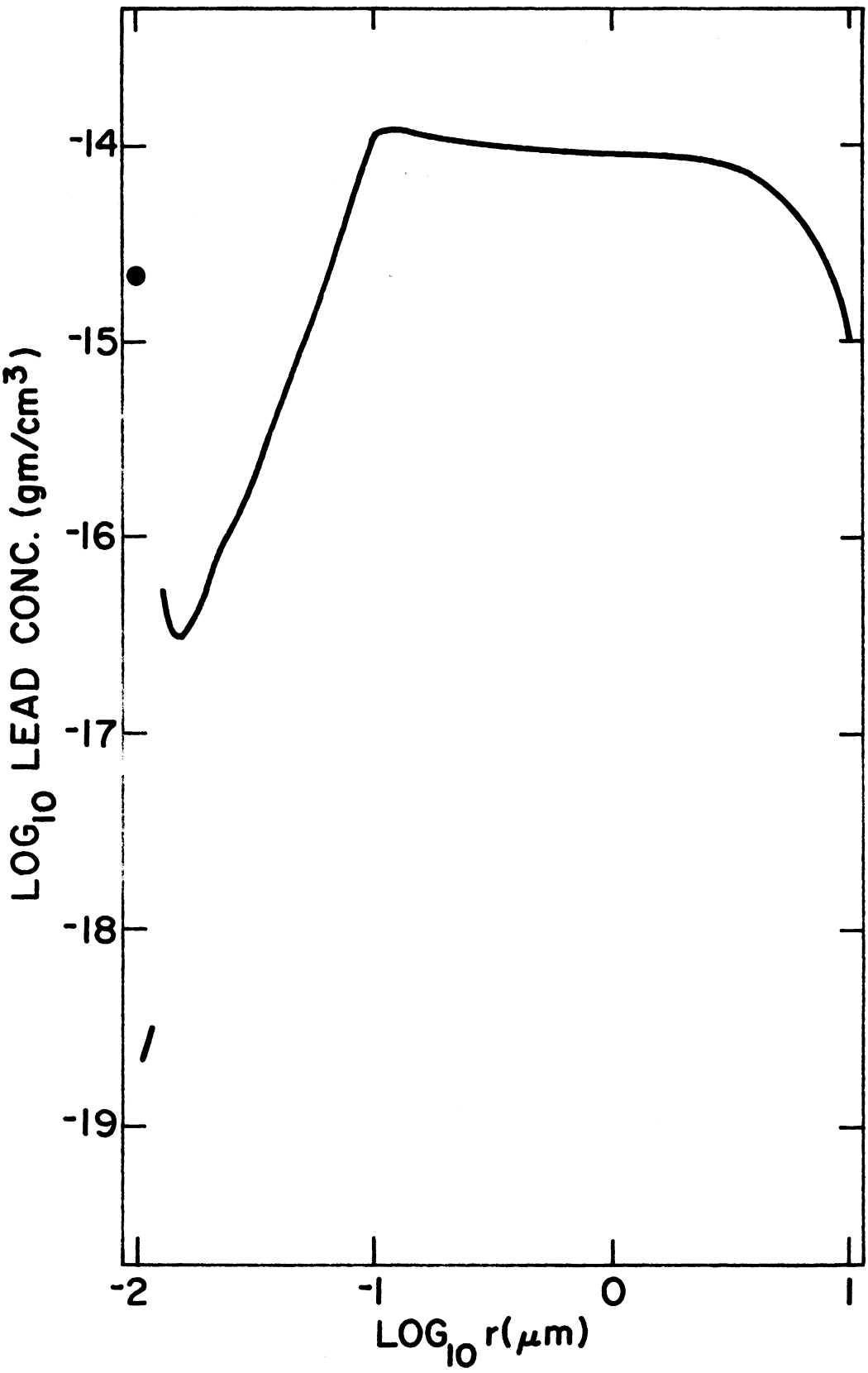

Fig.27 .--The numerical solution for Case 8 at five hours.

With the urban model a larger rate of coagulation from the smaller particle sizes was found. Nonetheless the spectrum 0.01 μm $\leq r \leq$ 1 μm was not radically changed, losses of these particles due to coagulation with larger particles being balanced with coagulation with the lead particles of 0.01 μm radius. Sedimentation again reduced the concentration of particles $r > 1$ μm. A build up of concentration was seen in the intermediate range (0.1 μm $\leq r \leq$ 1 μm), perhaps corresponding to the larger lead mass of Stage 7 in urban areas compared to "cities of population 100,000-200,000".

D. Fallout Rates

The amount of fallout from each of the models was computed in grams/sec.cm^2. The amount of fallout for the two models having only submicron inputs of lead reached a quasi-equilibrium values rather quickly. The models having lead initially at large sizes, (never establishing balance between coagulation and sedimentation) gave monotonically decreasing values of fallout. Sedimentation seemed to act as a significant sink of lead for distributions having a small effective layer depth, (i.e. situations where a vertical transfer mechanism was not effective would have gravitational sedimentation as a major sink of lead). (Figure 28.)

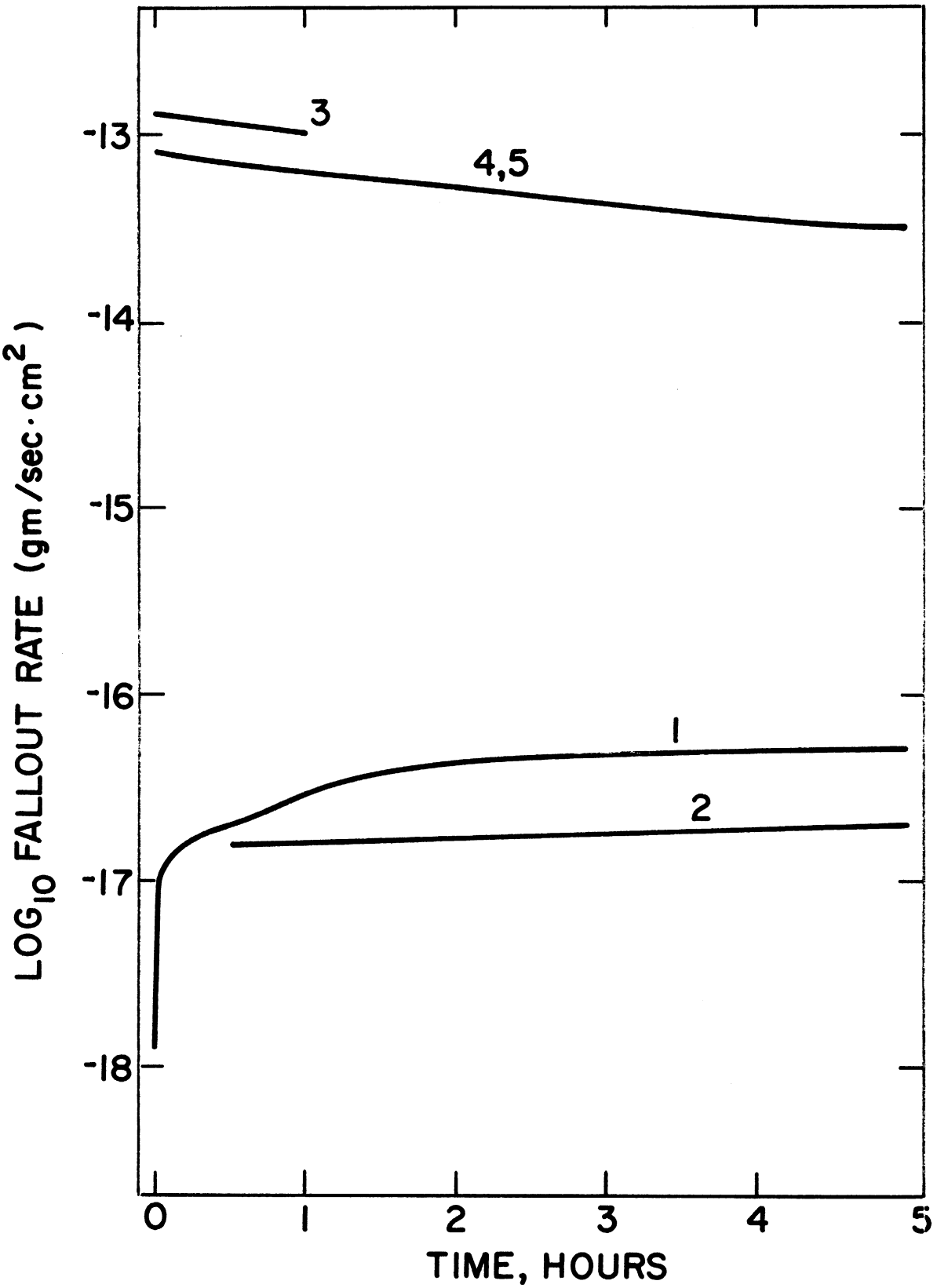

Fig. 28.--Fallout rates for Cases considered. 1: Case 2; 2: Case 4; 3: Cases 5, 6; 4: Case 7; 5: Case 8

E. Comparison of Model Aging and Observed Aging

Model aging and aging data were plotted in Figure 29. Trends in aging were highly similar for the model and for the data even though the initial size distribution did not correspond exactly to the Chicago size distribution.

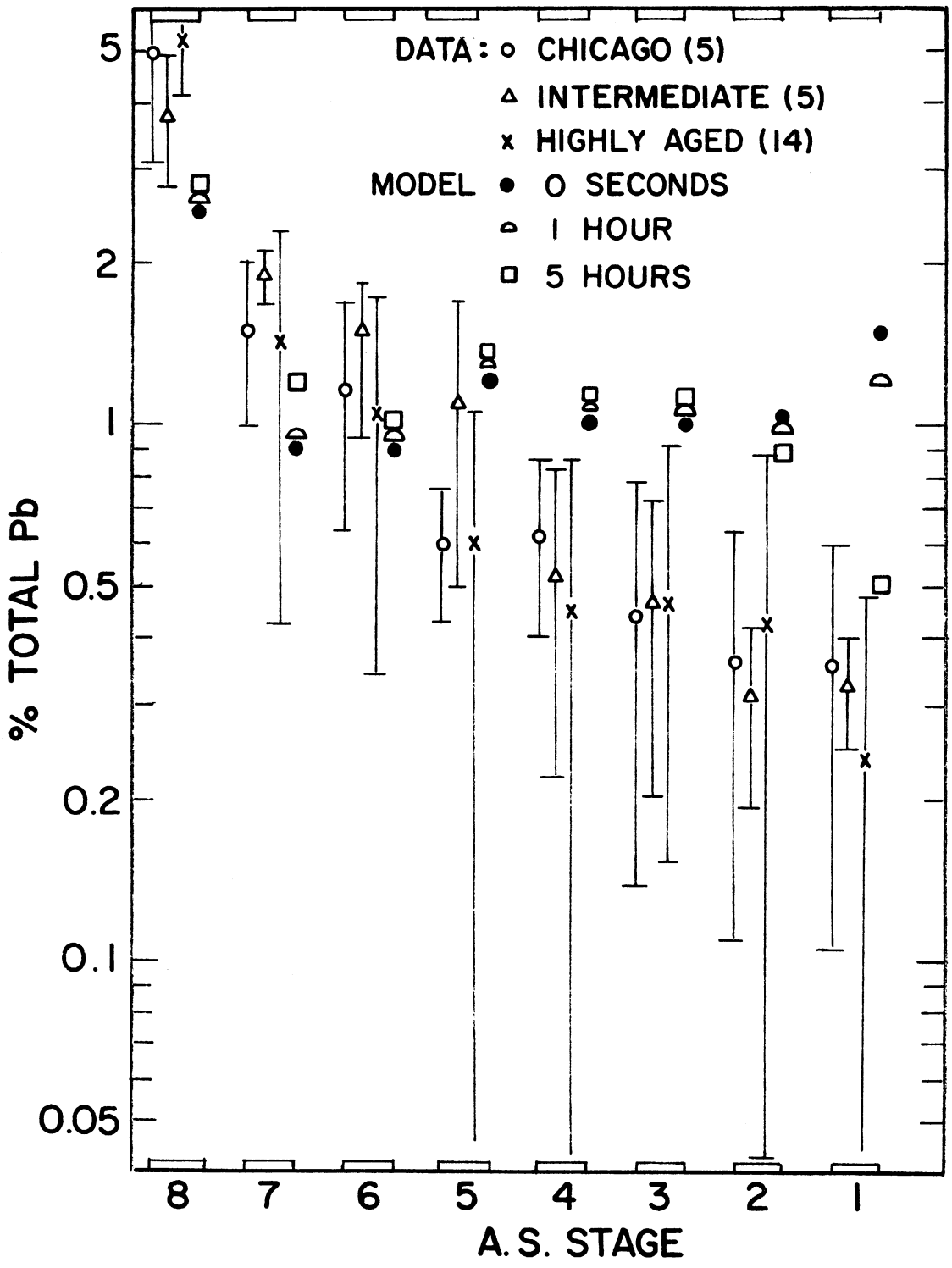

Fig. 29.--Comparison of aging from the model and data.

Results showed that, even though the observed lead mass distribution had more lead in the subrange of the spectrum $r < 0.2$ μm (Stage 8) than in the model, observed aging trends were highly similar to those of the model. Coagulational change of the spectrum was not observed since the coagulation occured largely from particles collected by Stage 8 to particles collected on Stage 8, (i.e., the active subrange for coagulation was collected on the backup filter). Only at Stage 1 was there a noticeable change due to gravitational sedimentation.

IV. CONCLUSIONS

First: Coagulation of leaded particles had the net effect of taking particles from the smallest sizes of the lead input spectrum and placing them mostly in the region $0.05\ \mu m \leq r \leq 0.5\ \mu m$ from which coagulational removal was slow. For a background distribution, assumed to be similar to that of Chicago, particles of 0.01 μm radius were reduced to 20 per cent of their original concentration in two hours. Significantly, even though a lead spectrum were initially unstable with respect to coagulation, the effect of coagulation with a background aerosol, having a high concentration at $r = 0.1\ \mu m$, would be to stabilize the lead spectrum with respect to coagulation and precipitation effects (see page 70).

The removal of particles from the smallest sizes (where much of the lead mass was contained) was expressed approximately in an exponential form exp(-kt) where k was inversely proportional to the total amount of mass in the aerosol. Since deposition of lead was largely on particles $0.05\ \mu m \leq r \leq 0.5\ \mu m$, it was expected that lead would be coagulated more quickly in urban locations compared to suburban locations onto those particles collected on stage seven of the Andersen Sampler.

Second: Gravitational fallout of leaded particles appeared to be most important near the source, its importance decreasing with aging. Sedimentation seemed to be

important only for particles larger than one micron.

The greater part of the coagulation was within the subrange collected by Stage 8 and Stage 7 of the Andersen Sampler. No rapid change of the lead spectrum was shown on Stages 1-6.

Third: Turbulent diffusion, having the effect of dilution, played a large role in the shape of the lead spectrum, both in determining an effective layer depth which in turn determined loss due to gravitational sedimentation and in determining the rate of coagulation which was proportional to the square of the concentration.

The model of lead aerosol aging confirmed observations that the lead aerosol size distribution did not change rapidly. Since calculations showed that particles $r < 0.05$ μm would rapidly coagulate onto $0.05\ \mu m \leq r \leq 0.5\ \mu m$ particles, the so called "gap" region for atmospheric removal (see p.70), the lead spectrum would be expected to have a minimum residence time of several hours. A simple calculation based on a mean concentration of 0.1 $\mu g/m^3$ in a 1000 meter layer over the United States and an infusion rate of 1.5X10"g Pb/year yielded a minimum residence time of approximately 4 days. A residence time of days would not be contradicted by this work.

LIST OF REFERENCES

LIST OF REFERENCES

Andersen, A. A. 1966. A sampler for respiratory health hazard assessement. J. Amer. Indus. Hyg. Assoc. 27: 160-165.

Barnard, A. J. 1953. The theory of condensation of super-saturated vapors in the absence of ions. Proc. Royal Soc. 220A: 132-141.

Bellaire, Frank R. 1965. The modification of warm air moving over cold water. Proc. 8th Conf. on Great Lakes Res. Univ. of Mich., Ann Arbor, Mich., 249-256.

Brief, R. S.; Jones A. R.; and Yoder J. D. 1960. Lead, carbon monoxide and traffic. J. Air Pol. Cntrl. Assoc. 10: No. 5, 384-388.

Burton, W. M., and Stewart, N. G. 1960. Use of long lived natural radioactivity as an atmospheric tracer. Nature. 186:No. 4725, 584-589.

Calingaert, G.; Lamb, F. W.; and Meyer, F. 1949. Studies in the lead chloride-lead bromide system. J. Am. Chem. Soc. 71: 3701-3720.

Chandrasekhar, S. 1943. Stochastic problems in physics and astronomy. Rev. of Mod. Phys. 15: No. 1, 1-89.

Cholak, J.; Schaver, L. J.; and Sterling, T. P. 1961. The lead content of the atmosphere. J. Air Pol. Cont. Assoc. 11: 281-288.

Collins, F. C. 1955. Time lag in spontaneous nucleation due to non-steady state effects. Proc. on the Conf. on Interfacial Phenomena and Nucleation. Edited by H. Reiss. 1: 165-180.

Courtney, W. 1961. Recent advances in condensation and evaporation. A.R.S. Jour. 31: 751-756.

Daniels F., and Alberty, R. A. 1966. Physical Chemistry. 3rd ed.; New York: Wiley and Sons.

Davies, C. N., and Aylward, M. 1951. The trajectories of heavy solid particles in a two dimensional jet of ideal fluid impinging normally upon a plate. Proc. of the Phys. Soc. 64: 889-911.

Dufour, L., and Defay, R. 1963. Thermodynamics of Clouds. New York: Academic Press.

Dunn, J. T., and Bloxam, H. C. L. 1933. The occurance of lead, copper, zinc and arsenic compounds in atmospheric dust and the sources of these impurities. J. Soc. Chem. Ind. (London). 52: 189-192.

Flesch, J. P.; Norris, C. H.; and Nugent, A. E., Jr. 1967. Calibrating particulate air samplers with monodisperse aerosols. J. Amer. Indus. Hyg. Assoc. 28: 507-516.

Fowler, R. H., and Guggenheim, E. A. 1939. Statistical Thermodynamics. Cambridge: University Press.

Friedlander, S. K. 1959. On the particle size spectrum of atmospheric aerosols. J. Meteor. 17: 373-374.

_____. 1960. Similarity considerations for the particle size spectrum of a coagulating, sedimenting aerosol. J. Meteor. 17: 479-483.

Fuchs, N. A. 1964. The Mechanics of Aerosols. New York: Pergammon.

Gatz, D. F. 1966. Deposition of atmospheric particulate by convective storms: The role of the convective updraft as an input mechanism. Ph.D. Dissertation, University of Michigan.

Gelman Instrument Co. 1968. Technical Specifications Manual. Ann Arbor, Michigan.

Goldschmidt, V. M. 1935. Rare elements in coal ashes. Ind. and Eng. Chem. 27: 1100-1101.

Green, H. L., and Lane, W. R. 1964. Particulate Clouds: Dusts, Smokes and Mists. New York: Van Nostrand.

Greenfield, S. M. 1957. Rain scavenging of radioactive particulate matter from the atmosphere. J. Meteor. 14: 115-125.

Hidy, G. M., and Brock, J. R. 1965. Some remarks about the coagulation of aerosol particles by Brownian motion. J. of Colloid Sci. 20: 477-491.

_____, and Lilly, D. K. 1965. Solutions to the equations for the kinetics of coagulation. J. of Colloid Sci. 20: 867-874.

Higuchi, W. I. 1959. The Agglomeration of Pb and PbO and its importance to Lead-alkyl Antiknock Effectiveness A Theoretical Study. Report to the Chevron Research Company, Richmond, Calif.

Hirschler, D. A.; Gilbert, L. F.; Lamb, F. W.; and Niebylski, L. M. 1957. Particulate lead compounds in automobile exhaust gas. Ind. and Eng. Chem. 49: 1131-1142.

_____, and Gilbert, L. F. 1964. Nature of lead in automobile gas. Archives of Environmental Health. 8: No. 2, 297-313.

Junge, C. E. 1955. The size distribution and aging of natural aerosols as determined from electrical and optical data on the atmosphere. J. Meteor. 12: 13-25.

_____. 1963. Air Chemistry and Radioactivity. New York: Academic Press.

_____. 1964. The Modification of Aerosol Size Distribution in the Atmosphere. Final Technical Report to Meteorologisch-Geophysikalisches Institut der Johannes Guttenberg, Universitat, Mainz.

_____. 1969. Comments on "Concentration and size distribution measurements of atmospheric aerosols and a test of the theory of self-preserving distributions." J. Atmos. Sci. 26: No. 3, 603-608.

Kenline, Paul A. 1968. Personal Communications.

Kruyt, H. R., ed. 1952. Coloid Science I. Amsterdam: Elsevier.

Lee, R. E., Jr.; Patterson, R. K.; and Wagman, Jack. 1968. Particle-size distribution of metal components in urban air. Environmental Sci. and Tech. 2: No. 4, 288-290.

Loucks, H. 1969. Particle size distributions of chlorine and bromine in mid-continent aerosols from the Great Lakes basin. Ph.D. Dissertation, University of Michigan.

McDonald, J. E. 1969. Cloud nucleation of insoluble particles. J. Atmos. Sci. 21: No.1, 109-116.

McKee, H. C. and McMahon, W. A., Jr. 1960. Automobile exhaust particulates - source and variation. J. Air Pol. Cntrl. Assoc. 12: No.11, 539-542.

Matson, W. R., and Roe, D. K. 1966. Trace metal analysis of natural media by anodic stripping voltammetry. Am. Chem. Soc., Anal. Inst. Div. Instrumental Analysis. 4: 19-22.

Millikan, R. A. 1923. The general law of fall of a small spherical body through a gas, and its bearing upon the nature of molecular reflection from surfaces. Physical Review. 22: No.1, 1-23.

Mueller, P. K.; Helweg, H. L.; Alcocer, A. E.; Gong, W. K.; and Jones, E. E. 1962. Concentration of fine particles and lead in car exhaust. ASTM Special Technical Publication. No. 352, 60-77.

Pasquill, F. 1962. Atmospheric Diffusion. London: D. VanNostrand Company Ltd.

Peterson, C. M. 1968. Measuring and relating atmospheric pollution to meteorological parameters. J. Air Pol. Cultrl. Assoc. 18: No. 10, 654-655.

Ralston, A., and Wilf, H. S. 1960. Mathematical Methods for Digital Computers. New York: Wiley.

Ranz, W. E., and Johnstone, H. F. 1952. Some aspects of the physical behavior of atmospheric aerosols. Proc. of the 2nd National Air Pol. Symp. Los Angeles.

Robinson E.; Ludwig, F. L.; DeVries, J. E.; and Hopkins, T. E. 1963. Variation of Atmospheric Lead Concentrations and Type with Particle Size. Final report to the Stanford Research Institute, Menlo Park.

_____, and Ludwig, F. L. 1964. Size Distributions of Atmospheric Lead Aerosols. Final report to the Stanford Research Institute, Menlo Park.

Savul, M., and Ababi, V. 1958. The copper, zinc, and lead content of several types of Romanian coal. Acad. rep populare Romine, Filiala Iasi, Studii cercetari stiint., Chim. 2., 251 as reported in U.S. Pub. Health Pub. No. 999-AP-12.

Strong, Alan E. 1968. The spring lake anticyclone: Its inducement on the atmosphere and water conditions. Ph.D. Dissertation, University of Michigan.

Suzuki, A.; Ho, N. F.; and Higuchi, W. I. 1969. Prediction of the particle size distribution changes in emulsions and suspensions by digital computation. J. Colloid and Interfacial Sci. 29: No. 3, 552-564.

Ter Haar, G. L.; Holtzman, R. B.; and Lucas, H. F., Jr. 1967. Lead and lead 210 in rain water. Nature. 216: 353-355.

Tufts, B. J. 1959. Determination of particulate lead content in air. Anal. Chem. 31: No. 2, 238-241.

U.S. Dept. Health, Education, and Welfare. 1955. Survey of Lead in the Atmosphere of three Urban Communities. Public Health Service Publication No. 999-AP-12.

Von Smoluchowski, M. 1916. Drei Vortrage uber diffusion Brownsche molekularbewegung, und Koagulation von Kolloid teilchen. Physik. Zeitschrift. 17: 557-571.

Wagman, J. 1966. Current problems in atmospheric aerosol research. Air and Water Pol. Int. J. 10: 777-782.

Weast, R. C. 1968. Handbook of Chemistry and Physics. The Chemical Rubber Company, Cleveland.

Winchester, J. W., and Nifong, G. D. 1969. Water pollution in Lake Michigan by trace elements from pollution aerosol fallout. Chemistry of the Great Lakes. Edited by Beeton, A. M., and Allen, H. E. Advances in Chemistry series, American Chemical Society.

Zimpel, C. F., Graiff, L. B. 1967. An electron microscopic study of tetraethyllead decomposition in an internal combustion engine. 11th Symposium (Int.) on Combustion. 1015-1025.

APPENDIX I

FURTHER DETAILS OF OBSERVATIONAL TECHNIQUES

A. Transfer of Sample from the Polyethylene Disk to the Sample Solution.

In transfering the sample from the collection slide to the sample solution, the polyethylene disk was subjected to ultrasonic vibration until all deposited material was visually removed. This procedure was tested by determining the lead content of a polyethylene disk whose sample had already been removed. A total of two successive tests were run after an initial sample was run. (Table I-1)

TABLE I-1

POLYETHYLENE DISK SAMPLE TRANSFER

Washing	Length of Sonic Treatment (min)	Response Cell 1	Cell 2	Cell 3	Cell 4
1	30	690	500	550	725
2	10	73	18	10	15
3	10	30	7	4	10
Reagent Blank	--	20	33	7	12
1	45	1250	286	540	290
2	10+scraping	72	4	12	24
3	10	19	18	5	4
Reagent Blank	--	19	5	2	9

Results showed that the sample, consisting of the disk, following the primary sample transfer yielded a total signal (including the blank) averaging 4.45 per cent of the first signal and that the following sample (3rd washing) yielded a signal practically equal to the signal of the reagent blank. The reagent blank (response of the apparatus to 10ml of pure 0.1 N NaCl solution) gave a background level

of lead due to laboratory procedures. The system blank gave a background level of lead due to the entire laboratory and field sampling program. It was determined by finding the response of the apparatus to a half section washing of a polyethylene disk which had undergone placement in the Andersen Sampler at the sampling site, but which did not collect sample. In general, the system blank lead signal was greater than the reagent blank lead signal.

Sample transfer of the backup filter consisted of treating a half filter sample immersed in 10 ml of 0.1 N NaCl solution to ultrasonic vibration. The filter portion was not removed for fear that a sizable loss of sample in the soaked filter would occur. Effectiveness of sample transfer was tested by retreatment with the ultrasonic cleaner and determination of the lead.

TABLE I-2

FILTER SAMPLE TRANSFER

Washing	Duration of Sonic Treatment (min)	Lead Signal			
		Cell 1	Cell 2	Cell 3	Cell 4
1	15	1440	3660	2780	--
2	10	1380	3430	2680	--
3	5	1410	3590	2590	--

The deviation was again small in this case.

B. Stability of Response

The sample was not changed while a series of eleven successive platings and strippings were performed. Results showed a slight decrease in signal. Due to this slight decrease it was concluded that lead standards, i.e., samples containing a measured amount of lead were run for each succeeding pair of samples (Figure I-1).

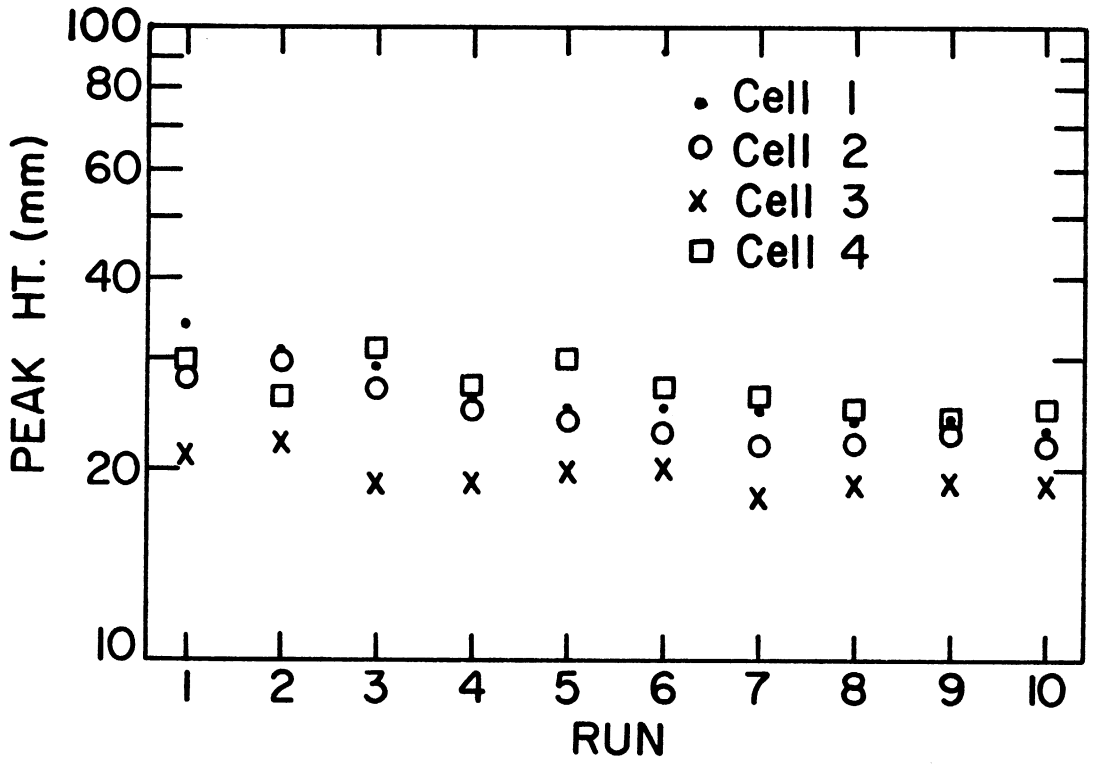

Fig. I-1.--Response of A.S.V. to a given lead sample.

C. Contamination of the Cells

In order to prevent an erroneously high signal due to lead carry-over or contamination, a system blank was run after every sample or standard. Thus, if the apparatus did become contaminated with lead it would have been readily seen. In general, the system blank tended to increase in its amount of lead during a days operation.

D. Linearity of Response

One set of data relating response vs. lead concentration was taken. Results showed a linearity of response to lead concentration (Figure I-2).

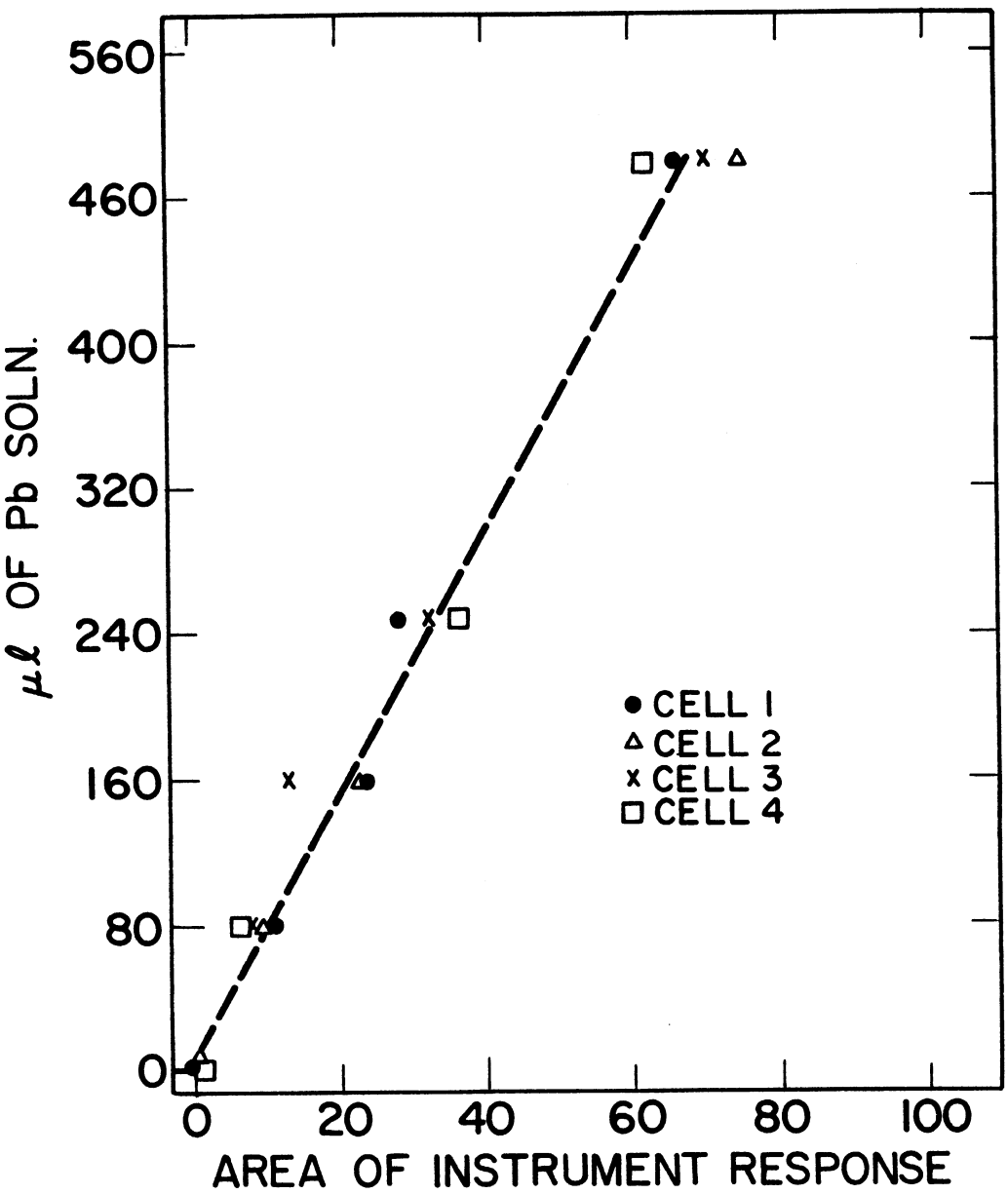

Fig. I-2.--Linearity of A.S.V. response to lead concentration.

E. Abstraction of Data

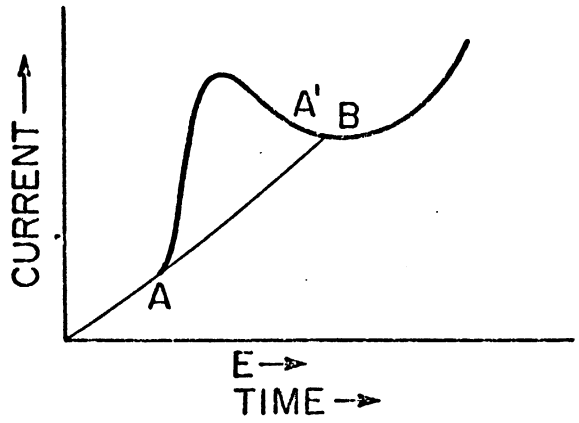

If a typical A.S.V. response to lead were characterized as curve A A' B then the straight line AB was drawn to close the curve of lead response. The area within this curve was then computed using a standard Keufell and Esser compensating polar planimeter (620,000). Three determinations of the area for more than 40 curves showed that any determination deviated less than 10 per cent from the mean. Subsequent areas were determined only once.

F. Estimation of Error

The total error of a series of lead measurements was estimated as the largest deviation from the mean value of lead standards minus the system blank. In general this error was considered a maximum value and averaged around 20 per cent for all series of lead determinations.

APPENDIX II

PRESENTATION OF
INDIVIDUAL LEAD SIZE DISTRIBUTIONS
AND
WEATHER DATA

TABLE II-1

MASS CONCENTRATION OF LEAD IN NANOGRAMS/CUBIC METER

LOCATION	DATE	TIMES						
ANDERSEN SAMPLER STAGE								% ERROR
1	2	3	4	5	6	7	8	
CWFP	JULY 30,1968				0800-1600			
11.	17.	26.	32.	32.	28.	49.	390.	39.
H-D	JULY 30,1968				0800-1600			
50.	56.	33.	120.	82.	110.	155.	610.	16.5
INLAND SEAS	JULY 30,1968				0800-1600			
14.2	10.75	29.7	37.8	41.9	28.5	49.3	137.	20.
CWFP	JULY 31,1968				0800-1600			
49.9	36.6	6.4	62.	32.	149.	172.5	277.	27.
H-D	JULY 31,1968				0800-1600			
21.2	24.6	24.6	46.0	51.0	103.5	135.5	478.	27.5
INLAND SEAS	JULY 31,1968				0800-1600			
12.3	12.3	59.3	18.3	38.	54.	38.	295.	43.
CWFP	SEPTEMBER 4,1968				0800-1600			
80.	41.6	79.	94.	64.5	139.	119.	694.	28.
H-D	SEPTEMBER 4,1968				0800-1600			
34.7	25.	34.7	62.	120.	311.	188.	400.	50.
INLAND SEAS	SEPTEMBER 4,1968				0800-1600			
9.45	9.1	10.8	13.4	39.6	46.2	88.0	575.	29.5
CWFP	SEPTEMBER 4,1968				1600-2400			
13.35	22.6	52.0	63.	99.	243.	455.	1550.	38.2
H-D	SEPTEMBER 4,1968				1600-2400			
17.7	28.5	41.7	40.1	90.9	116.	117.	198.	37.8
INLAND SEAS	SEPTEMBER 4,1968				1600-2400			
34.8	9.85	25.8	12.2	8.7	3.5	39.4	53.2	81.6
CWFP	SEPTEMBER 5,1968				0000-0800			
9.2	20.7	27.7	25.2	36.3	48.3	53.5	98.	13.4
H-D	SEPTEMBER 5,1968				0000-0800			
15.4	12.0	22.8	29.8	53.7	44.9	48.8	60.0	23.7
INLAND SEAS	JULY 9,1968				0000-0900			
8.6	9.2	7.8	12.7	28.2	33.8	56.5	95.0	62.2
INLAND SEAS	JULY 9,1968				0600-1500			
9.6	8.7	14.5	18.4	37.6	49.0	58.0	56.5(P)	17.5
INLAND SEAS	JULY 9,1968				0920-1800			
7.15	9.55	12.3	9.1	16.0	22.7	39.8	87.0	46.5

TABLE II-1--Continued

MASS CONCENTRATION OF LEAD IN NANOGRAMS/CUBIC METER

LOCATION	DATE	TIMES						
		ANDERSEN SAMPLER STAGE						% ERROR
1	2	3	4	5	6	7	8	
INLAND SEAS	MAY 22,1968				0830-1230			
3.8	20.	70.	73.	173.	161.	140.	210.	11.8
INLAND SEAS	MAY 23,1968				0107-0507			
20.	17.	15.	15.	27.	140.	170.	460.	10.
INLAND SEAS	JULY 9,1968				1242-2100			
3.42	2.72	4.42	4.17	8.3	6.0	.286	21.0	20.7
INLAND SEAS	JULY 9,1968				1510-2359			
.267	.60	.60	.625	-	-	.117	3.42	11.7
INLAND SEAS	JULY 10,1968				0305-1200			
-	.194	.10	.12	.56	.18	.71	5.95	15.6
INLAND SEAS	JULY 10,1968				0601-1501			
.08	.08	0	.43	.40	1.39	2.03	5.75	60.
INLAND SEAS	JULY 10,1968				0902-1800			
.21	.21	.95	.90	.50	1.01	.72	3.6	44.
INLAND SEAS	JULY 10,1968				1236 2100			
.11	.03	0	0	.48	.48	1.74	3.44	50.
INLAND SEAS	JULY 10,1968				1500-2400			
	.08	.11	.08	.05	3.26	4.15	3.75	46.
INLAND SEAS	MAY 21,1968				1513-1946			
1.6	7.5	.8	-	-	3.2	5.8	21.	80.
INLAND SEAS	MAY 21,1968				1513-1946			
.17	.83	3.6	.37	-	1.7	3.9	35.	80.
INLAND SEAS	MAY 22,1968				1045-1446			
1.8	1.8	2.5	3.7	9.1	13.	21.	40.	30.
INLAND SEAS	MAY 22,1968				1038-1710			
2.4	-	9.1	2.2	10.3	36.	38.	86.	30.
INLAND SEAS	MAY 22,1968				1254-1644			
4.0	4.0	3.5	6.5	49.	7.5	125.	400	19.7
INLAND SEAS	MAY 22,1968				2058-0058			
12.0	9.0	17.5	36.	51.	87.	48.	340.	36.4
INLAND SEAS	MAY 22,1968				2314-0316			
20.	21.	13.	23.	23.	36.	22.	132.	07.6
MYSIS	JUNE 6,1968				0510-0713			
29.	0.	34.	40.	100.	105.	150.	135.	14.3

TABLE II-1--Continued

MASS CONCENTRATION OF LEAD IN NANOGRAMS/CUBIC METER

LOCATION	DATE	TIMES						
		ANDERSEN SAMPLER STAGE						% ERROR
1	2	3	4	5	6	7	8	
MYSIS	JUNE 6,1968				0723-0904			
17.	4.2	17.	0.	25.	110.	84.	120.	26.
MYSIS	JUNE 6,1968				0946-1104			
80.	0.	12.	64.	18.	64.	40.	150.	18.1
MYSIS	JUNE 6,1968				1142-1419			
10.	9.2	17.0	36.0	12.7	31.	70.	80.	05.5
ANN ARBOR	OCTOBER 14-15,1968				0100-0130			
53.5	74.3	115.0	85.6	217.	452.	158.	1770.	25.
ANN ARBOR	OCTOBER 16-17,1968				0030-0030			
9.4	20.6	25.9	14.7	27.4	51.7	33.4	264.	34.
ANN ARBOR	OCTOBER 17-18,1968				0110-0100			
14.0	14.4	18.8	8.9	19.8	28.3	10.7	149.	20.
ANN ARBOR	OCTOBER 18-19,1968				0100-0010			
21.0	31.3	53.	42.9	61.5	56.2	46.6	286.	11.
ANN ARBOR	OCTOBER 19-20,1968				0010-0220			
29.6	34.4	55.6	31.7	68.0	27.4	61.5	2210.	37.
ANN ARBOR	OCTOBER 25-26,1968				1748-1730			
27.4	24.5	30.0	17.7	28.2	31.5	32.2	310.	24.4
ANN ARBOR	OCTOBER 26-27,1968				1745-1745			
11.8	12.8	19.9	14.9	22.0	30.0	31.1	278.	10.
ANN ARBOR	OCTOBER 27-28,1968				1745-1750			
4.0	4.5	7.0	6.4	10.	18.0	18.0	120.	32.2
ANN ARBOR	OCTOBER 28-29,1968				1750-1825			
8.3	9.0	13.0	13.0	19.0	10.5	8.9	180.	28.8
ANN ARBOR	OCTOBER 29-30,1968				1825-1818			
21.	20.	32.	32.	38.	21.	26.5	300.	28.
ANN ARBOR	OCTOBER 30-31,1968				1818-2325			
25.8	43.2	37.8	73.	104.	132.	166.	1170.	10.
ANN ARBOR	FEBRUARY 22-24,1968				2300-1840			
20.2	20.7	23.9	27.0	50.6	69.5	48.8	163.	14.
ANN ARBOR	FEBRUARY 24-26,1968				1805-1200			
24.4	19.8	22.7	20.5	27.4	18.9	15.8	432.	10.
ANN ARBOR	FEBRUARY 26-MARCH 6,1968				1300-1205			
25.2	24.1	35.5	33.2	44.8	27.3	30.9	432.	24.4

TABLE II-1--Continued

MASS CONCENTRATION OF LEAD IN NANOGRAMS/CUBIC METER

LOCATION	DATE	TIMES						
		ANDERSEN SAMPLER STAGE						% ERROR
1	2	3	4	5	6	7	8	
ANN ARBOR	MARCH 6-7, 1968				1250-1337			
14.	12.1	26.	27.8	20.9	50.3	28.3	140.	24.9
CALUMET H.	MAY 20, 1968				1733-2359			
18.	30.	80.	170.	220.	215.	500.	2000.	
CALUMET H.	MAY 21, 1968				0001-0159			
185.	210.	360.	400.	550.	210.	450.	2900.	
CALUMET H.	MAY 21, 1968				0206-0555			
100.	60.	20.	20.	200.	640.	970.	2000.	10.
CALUMET H.	MAY 21, 1968				0635-1032			
1.	3.9	9.7	10.	14.5	31.0	49.0	150.0	10.
CALUMET H.	MAY 21, 1968				0635-1032			
5.2	4.7	7.2	6.3	15.0	35.0	49.0	120.0	10.
SIDNEY, N.Y.	OCTOBER 19-20, 1968				1300-1300			
1.92	1.1	3.48	5.32	3.61	9.6	14.9	90.36	17.2
LINCOLN, NEBR.	OCTOBER 5-6, 1968				2009-2009			
9.9	10.1	19.4	15.9	14.6	(17)	(17)	64.1	26.8
LINCOLN, NEBR.	OCTOBER 6-7, 1968				0057-0107			
5.85	7.25	6.8	9.35	10.0	9.3	11.2	49.6	29.5
LINCOLN, NEBR.	OCTOBER 8-9, 1968				0200-1400			
8.25	11.9	16.6	10.6	20.8	17.0	16.7	50.0	26.2

TABLE II-2

MASS CONCENTRATION OF LEAD IN NANOGRAMS/CUBIC METER

LOCATION	DATE	TIMES					
ANDERSEN SAMPLER STAGE							
1	2	3	4	5	6	7	8
INLAND SEAS	MAY 20,1968				0756-1005		
40.	40.	20.	20.	20.	40.	50.	40.
INLAND SEAS	MAY 20,1968				1404-1543		
4.2	1.9	-	3.6	15.	13.2	14.2	NOT ANAL
INLAND SEAS	MAY 21,1968				1055-1455		
-	10.	-	-	-	12.5	5.3	33.
INLAND SEAS	MAY 21,1968				1055-1455		
20.	30.	3.	6.	6.	15.	39.5	40.
INLAND SEAS	MAY 22,1968				0630-1030		
46.	74.	25.	35.	60.	230.	170.	4.3
INLAND SEAS	MAY 22,1968				0756-1077		
-	2.8	-	-	15.	10.2	2.9	5.8
INLAND SEAS	MAY 22,1968				1454-1854		
15.	15.	34.	18.	42.	30.	35.	26.
INLAND SEAS	MAY 22,1968				1651-2051		
6.	6.8	7.3	8.8	15.	18.	21.	11.
INLAND SEAS	MAY 22,1968				1904-2304		
.1	.4	1.3	.7	2.3	-	-	5.5
INLAND SEAS	JULY 9,1968				0255-1202		
.08	22.	5.1	1.8	9.4	16.2	210.	180.
INLAND SEAS	JULY 9,1968				2126-2359		
(10.7)	.03	(18.)	-	.16	.06	.16	12.
INLAND SEAS	JULY 9,1968				2126-2359		
2.8	-	(9.3)	4.8	1.15	-	-	8.9

In this Table the lead size distributions are all highly aged. A serious blank problem arose prohibiting good definition of the entire lead spectrum. The distributions may be of use in an estimation of total lead content in rural air.

TABLE II-3

LEAD STATISTICS OF MASS DISTRIBUTIONS				
LOCATION	DATE	TIMES	MOD OF STAGES MICRONS	STAGE 8/ IMPACT STAGE 8 ("JUMGE")
CWFP	JULY 30,1968	0800-1600	1.2	4.0
H-D	JULY 30,1968	0800-1600	1.1	3.0
INLAND SEAS	JULY 30,1968	0800-1600	1.5	2.4
CWFP	JULY 31,1968	0800-1600	0.8	2.1
H-D	JULY 31,1968	0800-1600	0.8	3.3
INLAND SEAS	JULY 31,1968	0800-1600	3.3	3.4
CWFP	SEPTEMBER 4,1968	0800-1600	2.0	3.2
H-D	SEPTEMBER 4,1968	0800-1600	0.8	2.1
INLAND SEAS	SEPTEMBER 4,1968	0800-1600	0.95	4.4
CWFP	SEPTEMBER 4,1968	1600-2400	0.6	3.8
H-D	SEPTEMBER 4,1968	1600-2400	0.97	1.9
INLAND SEAS	SEPTEMBER 4,1968	1600-2400	3.3	1.7
CWFP	SEPTEMBER 5,1968	0000-0800	1.1	1.9
H-D	SEPTEMBER 5,1968	0000-0800	1.2	1.3
INLAND SEAS	JULY 9,1968	0000-0900	0.85	2.3
INLAND SEAS	JULY 9,1968	0600-1500	0.95	1.9
INLAND SEAS	JULY 9,1968	0920-1800	0.88	2.6
INLAND SEAS	MAY 22,1968	0830-1230	1.02	1.5
INLAND SEAS	MAY 23,1968	0107-0507	0.65	3.3
INLAND SEAS	JULY 9,1968	1242-2100	2.0	2.5
INLAND SEAS	JULY 9,1968	1510-2359	0.85	3.6
INLAND SEAS	JULY 10,1968	0305-1200	1.03	4.7
INLAND SEAS	JULY 10,1968	0601-1501	0.71	3.4
INLAND SEAS	JULY 10,1968	0902-1800	2.0	2.7
INLAND SEAS	JULY 10,1968	1236 2100	0.59	3.3

TABLE II-3 Continued

LEAD STATISTICS OF MASS DISTRIBUTIONS

LOCATION	DATE	TIMES	MED OF STAGE 8/ IMPACT'N STAGES MICRONS	STAGE 8 ("JUDGE")
INLAND SEAS	JULY 10,1968	1500-2400	0.74	1.6
INLAND SEAS	MAY 21,1968	1513-1946	1.03	3.2
INLAND SEAS	MAY 21,1968	1513-1946	0.94	4.7
INLAND SEAS	MAY 22,1968	1045-1446	0.79	2.6
INLAND SEAS	MAY 22,1968	1038-1710	0.71	2.8
INLAND SEAS	MAY 22,1968	1254-1644	0.59	4.1
INLAND SEAS	MAY 22,1968	2058-0058	1.03	3.4
INLAND SEAS	MAY 22,1968	2314-0316	2.0	2.8
MYSIS	JUNE 6,1968	0510-0713	0.88	1.4
MYSIS	JUNE 6,1968	0723-0904	0.74	1.9
MYSIS	JUNE 6,1968	0946-1104	1.00	2.6
MYSIS	JUNE 6,1968	1142-1419	0.91	1.8
ANN ARBOR	OCTOBER 14-15,1968	0100-0130	0.97	3.7
ANN ARBOR	OCTOBER 16-17,1968	0030-0030	1.05	3.6
ANN ARBOR	OCTOBER 17-18,1968	0110-0100	2.0	3.4
ANN ARBOR	OCTOBER 18-19,1968	0100-0010	2.0	3.0
ANN ARBOR	OCTOBER 19-20,1968	0010-0220	2.0	5.4
ANN ARBOR	OCTOBER 25-26,1968	1748-1730	3.5	3.8
ANN ARBOR	OCTOBER 26-27,1968	1745-1745	1.1	4.0
ANN ARBOR	OCTOBER 27-28,1968	1745-1750	2.0	3.9
ANN ARBOR	OCTOBER 28-29,1968	1750-1825	2.0	4.2
ANN ARBOR	OCTOBER 29-30,1968	1825-1818	2.1	3.8
ANN ARBOR	OCTOBER 30-31,1968	1818-2325	0.97	4.1
ANN ARBOR	FEBRUARY 22-24,1968	2300-1840	1.06	2.3
ANN ARBOR	FEBRUARY 24-26,1968	1805-1200	3.3	4.5
ANN ARBOR	FEBRUARY 26-MARCH 6,1968	1300-1205	1.9	4.3

TABLE II-3--Continued

LEAD STATISTICS OF MASS DISTRIBUTIONS

LOCATION	DATE	TIMES	MED DF IMPACT STAGES MICRONS	STAGE 8/ STAGE 6 ("JUNGE")
ANN ARBOR	MARCH 6-7,1968	1250-1337	1.1	2.7
CALUMET H.	MAY 20,1968	1733-2359	0.82	3.8
CALUMET H.	MAY 21,1968	0001-0159	2.0	3.3
CALUMET H.	MAY 21,1968	0206-0555	0.62	3.0
CALUMET H.	MAY 21,1968	0635-1032	0.77	3.4
CALUMET H.	MAY 21,1968	0635-1032	0.71	3.1
SIDNEY,N.Y.	OCTOBER 19-20,1968	1300-1300	0.59	4.2
LINCOLN,NEBR.	OCTOBER 5-6,1968	2009-2009	.	2.4
LINCOLN,NEBR.	OCTOBER 6-7,1968	0057-0107	2.0	2.8
LINCOLN,NEBR.	OCTOBER 8-9,1968	0200-1400	2.0	2.0

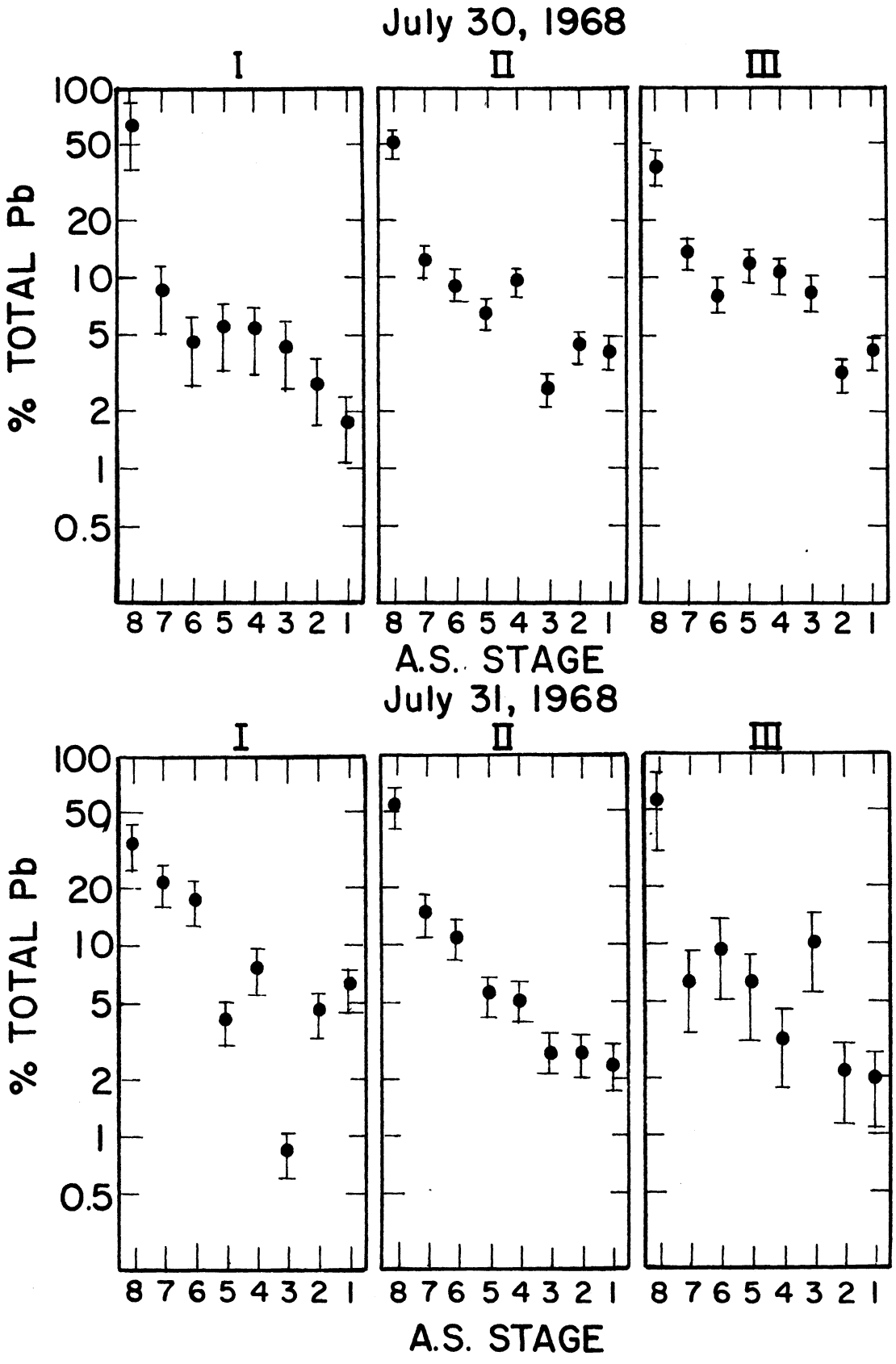

Fig. II-1.--Lead mass percentage for Andersen Sampler stage for short term aged samples. I=CWFP, II=H.D., III=Inland Seas.

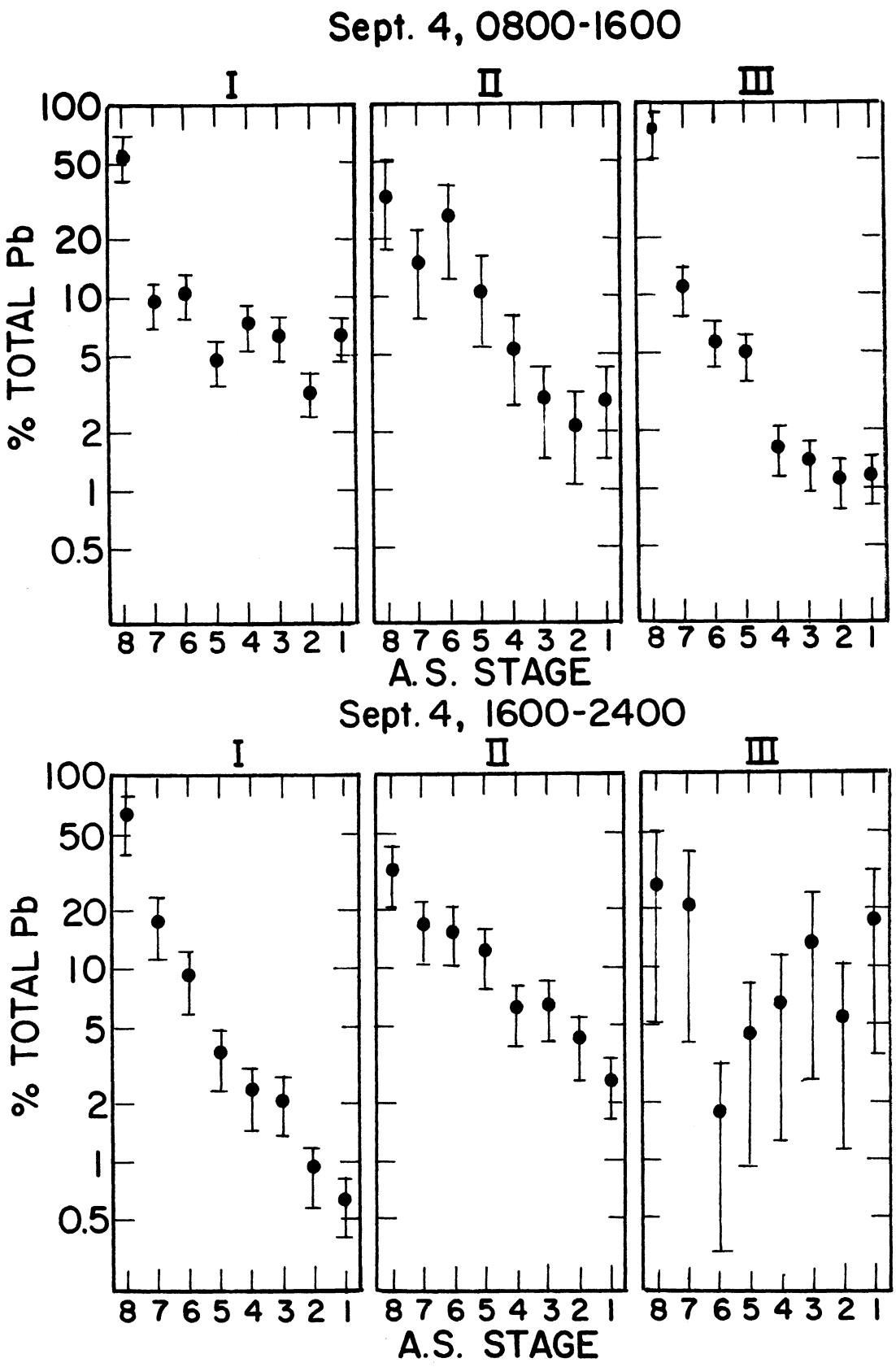

Fig. II-1--Continued

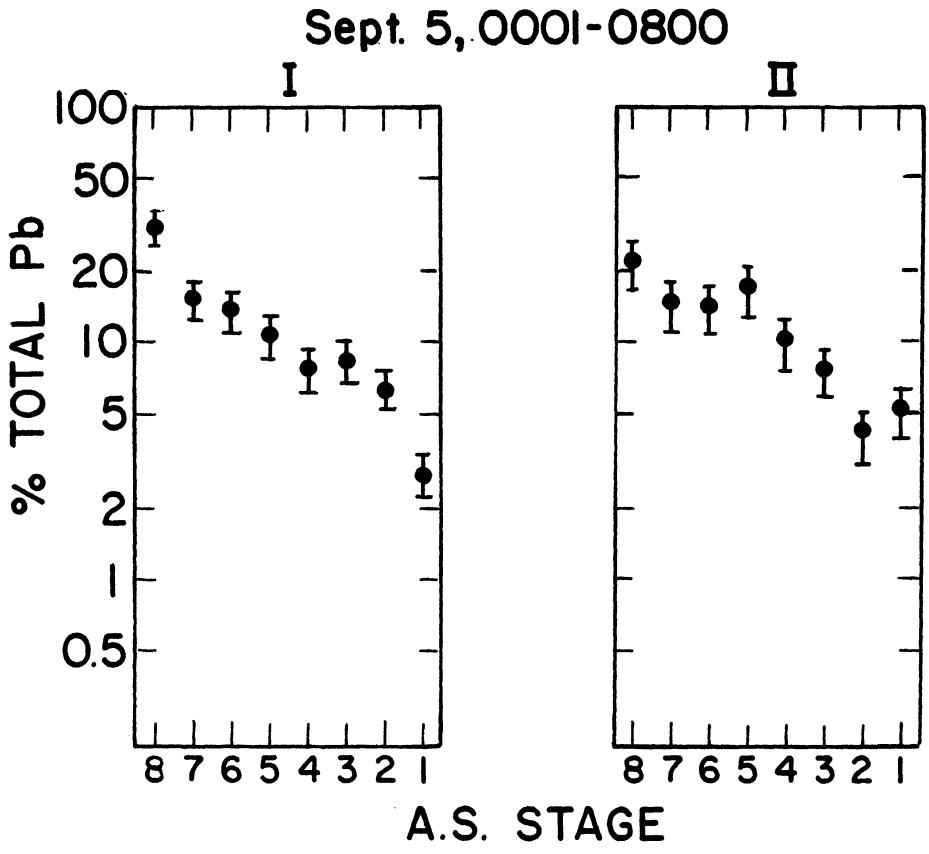

Fig. II-1.--Continued.

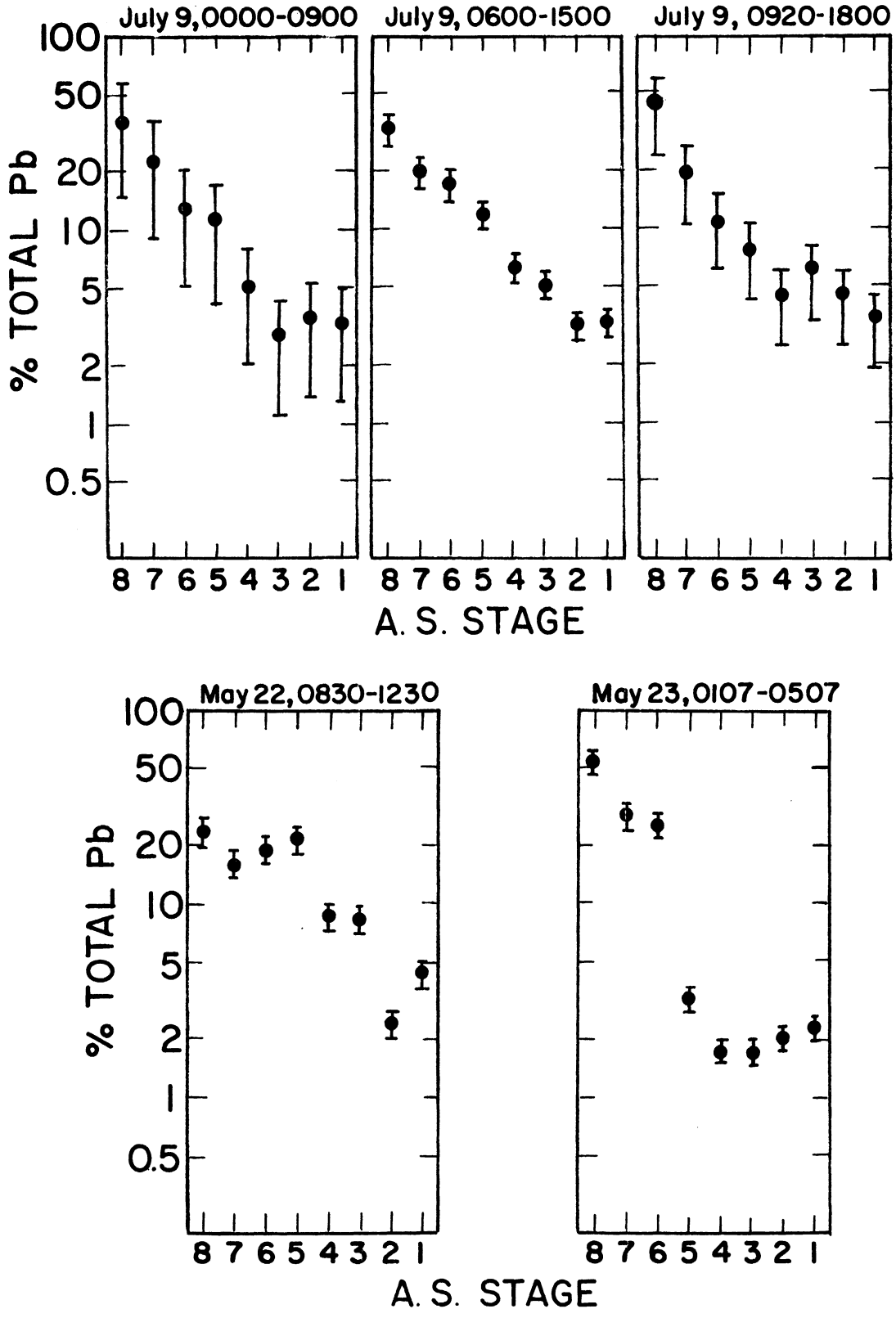

Fig. II-2.--Lead mass percentage for Andersen Sampler stage for intermediate term aged samples.

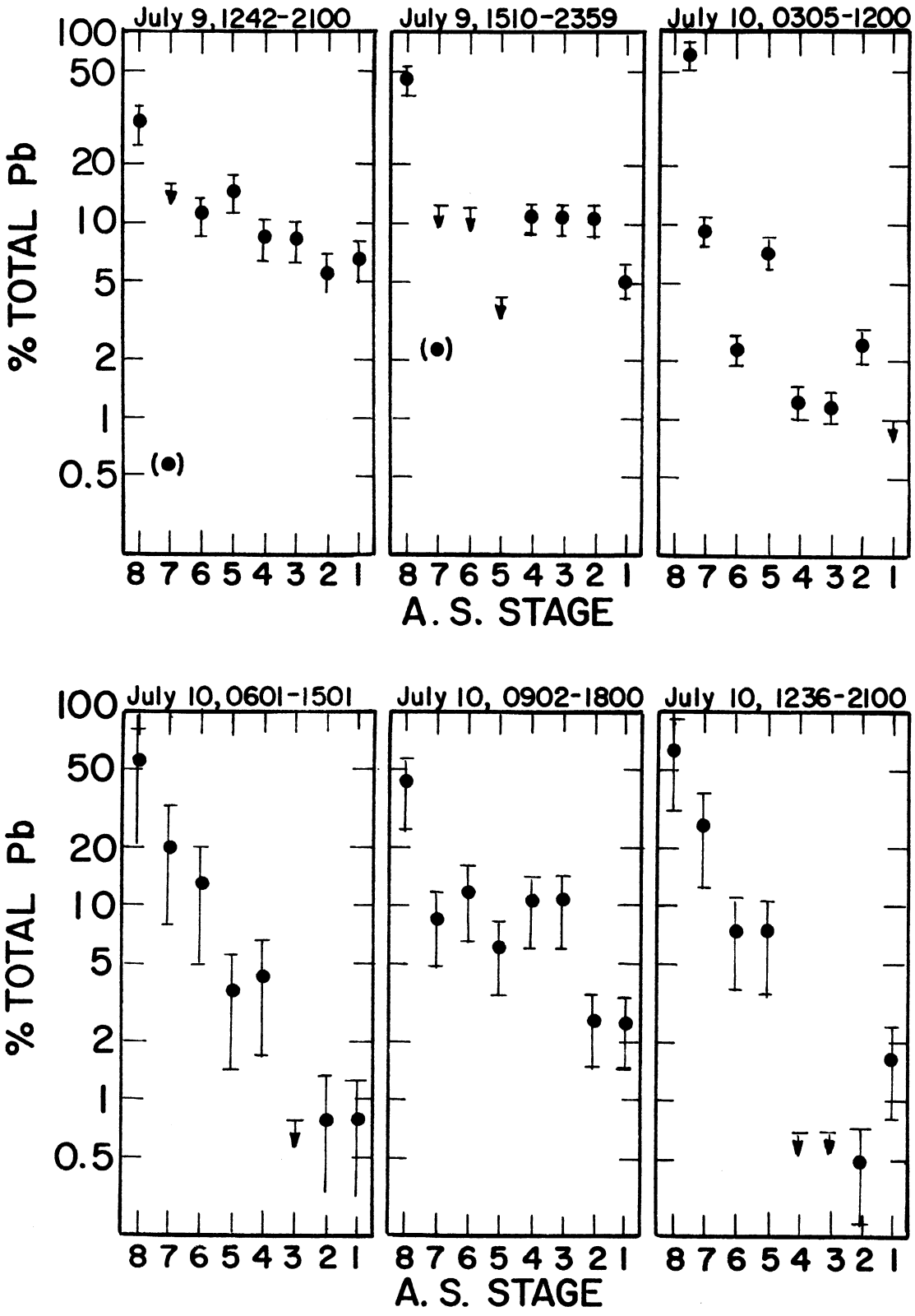

Fig. II-3.--Lead mass percentage for Andersen Sampler stage for highly aged samples.

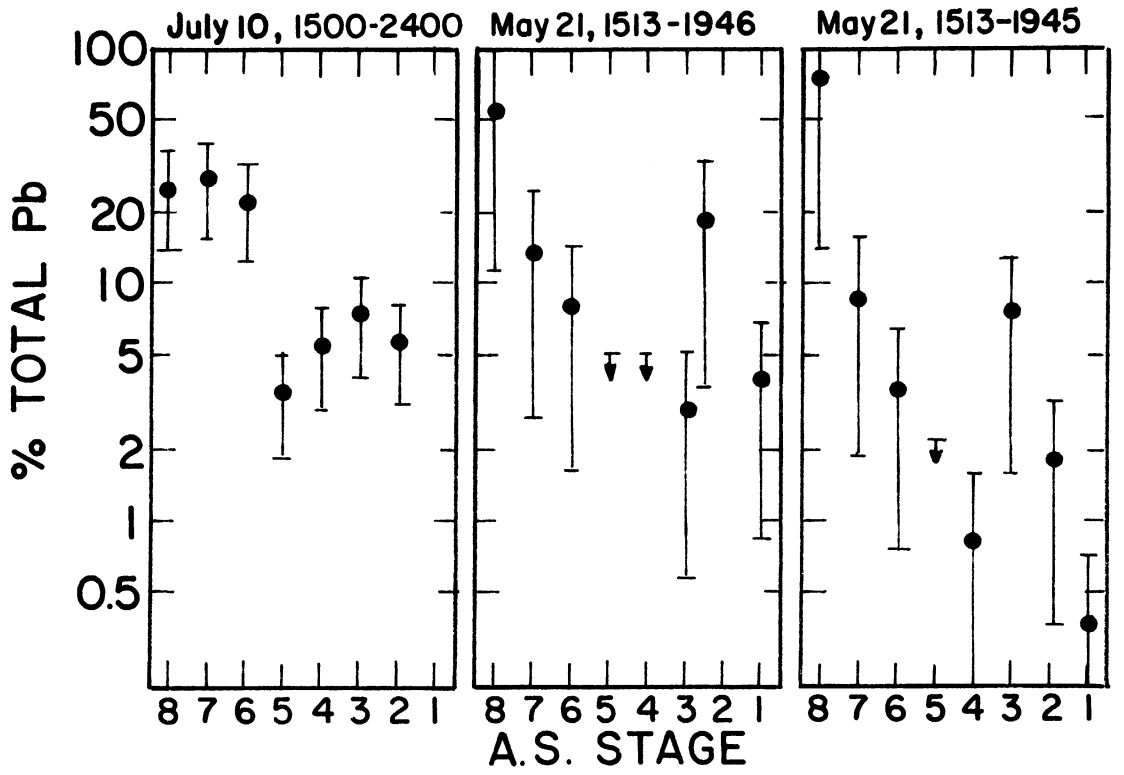

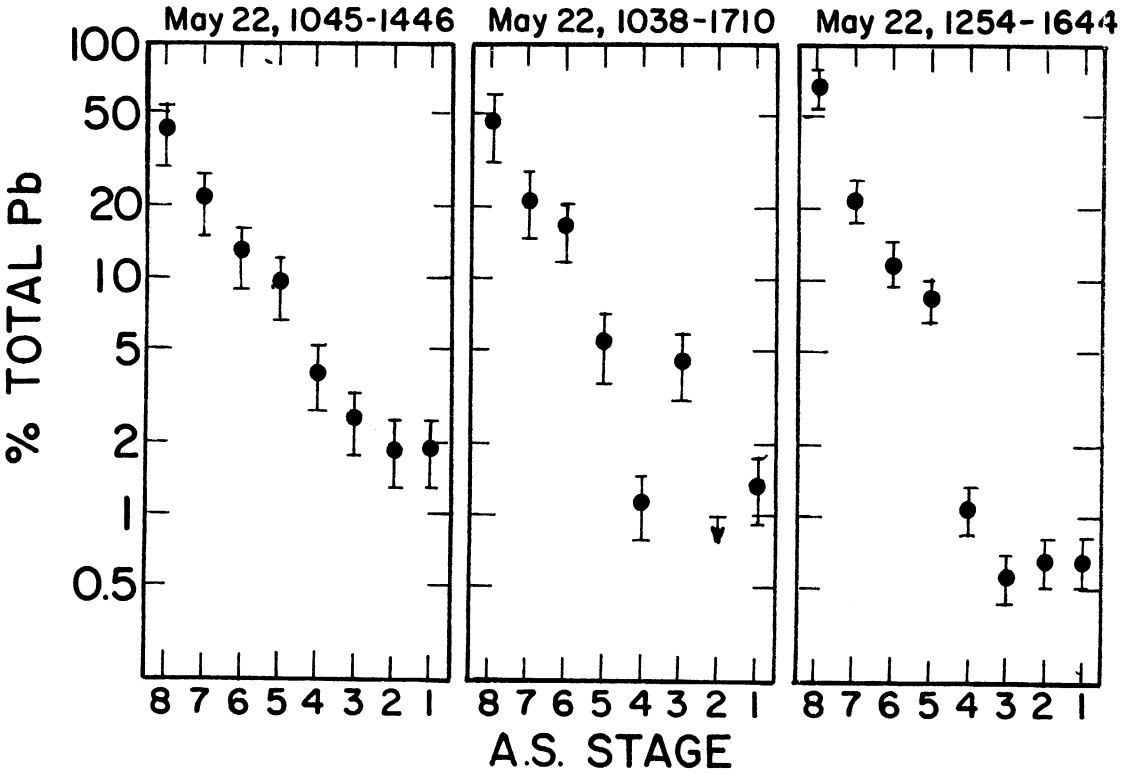

Fig. II-3--Continued.

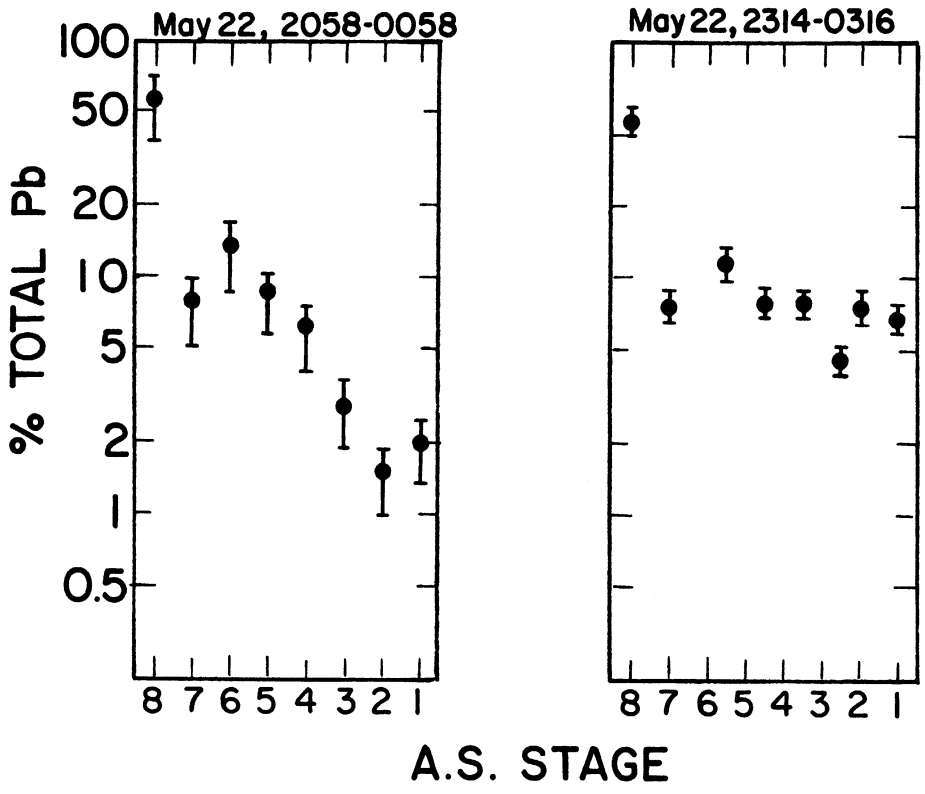

Fig II-3--Continued.

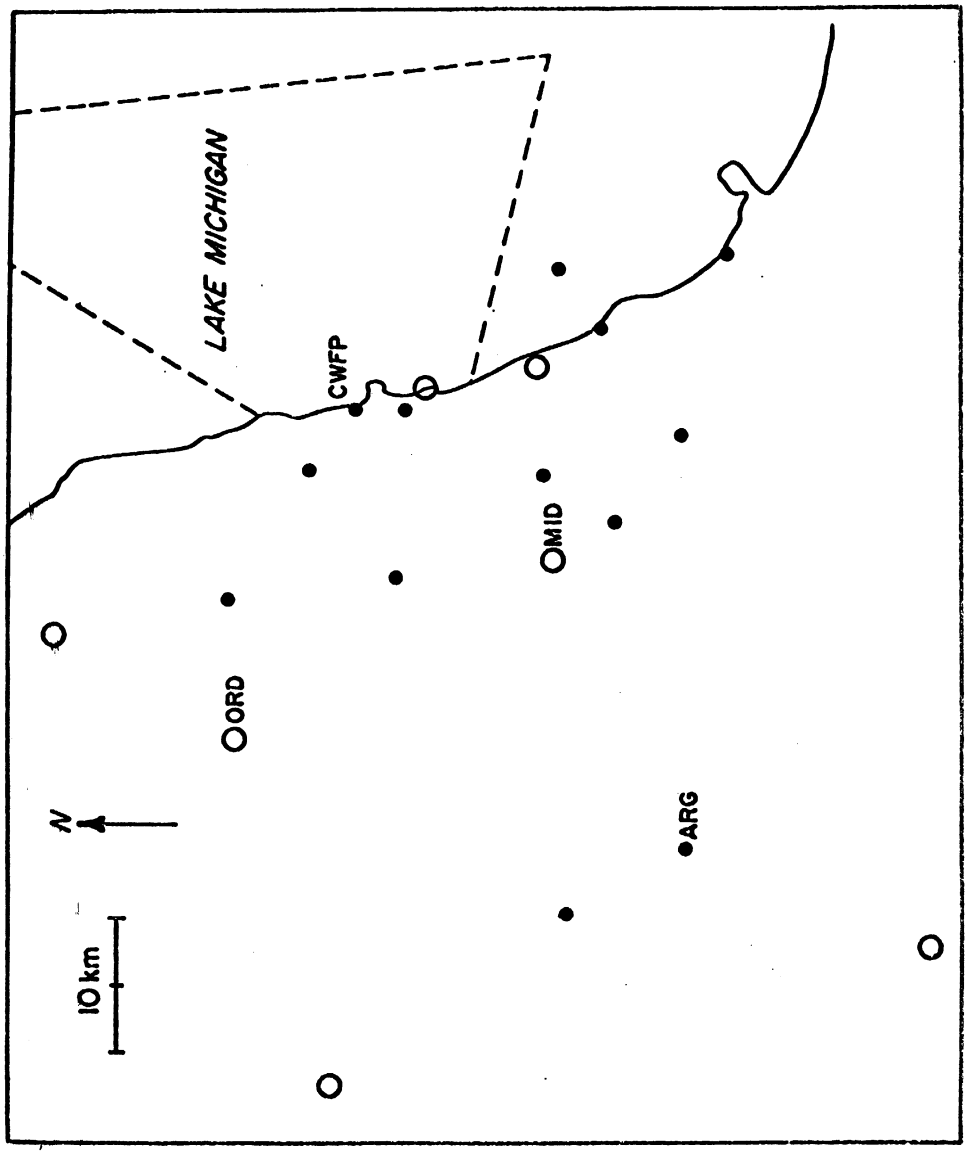

Fig. II-4.--Wind recording stations in the Chicago Area. The dotted line is the perimeter of the area covered by the R/V Inland Seas.

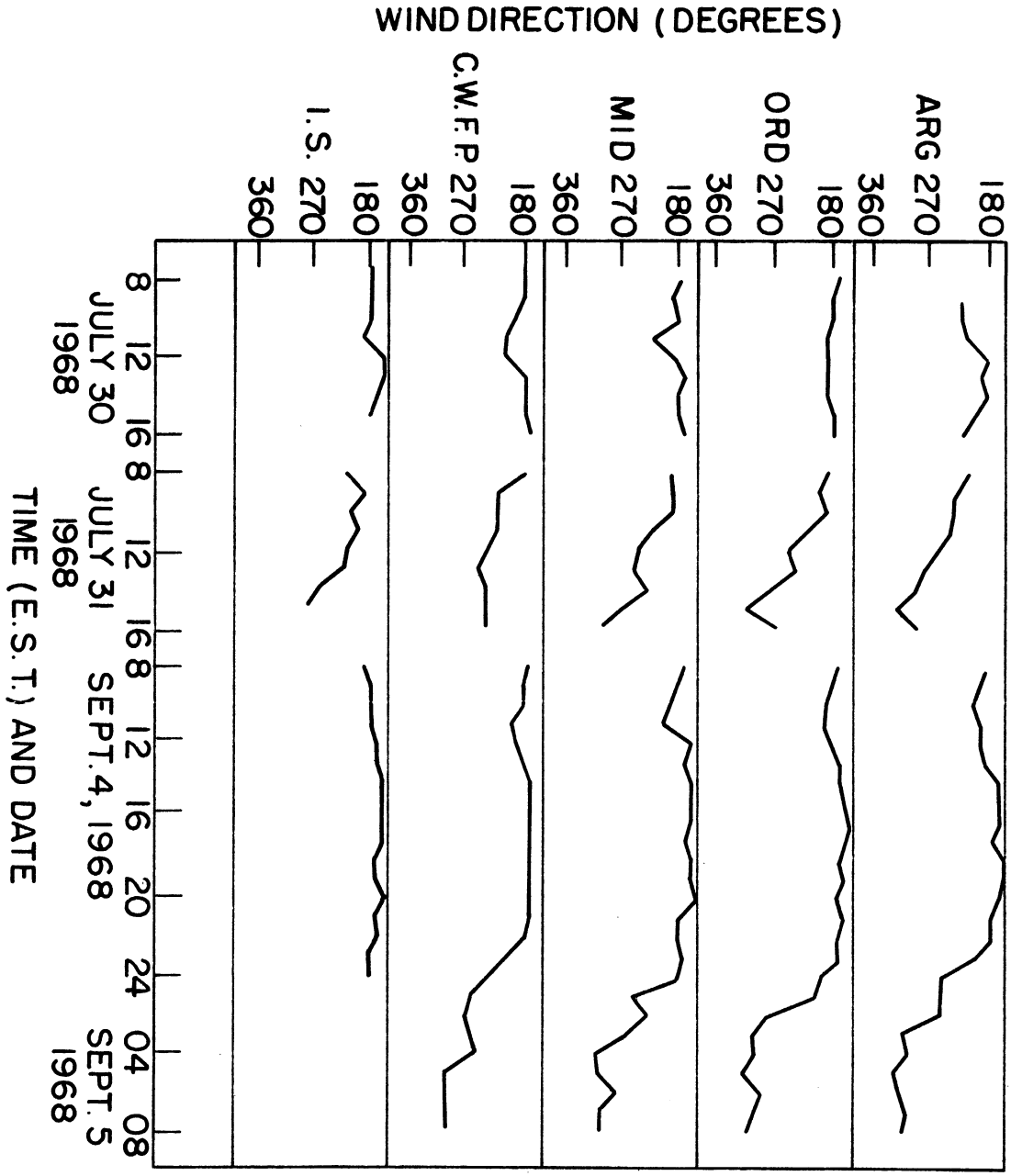

Fig.II-5.--Wind direction in the Chicago area July 30, 31 and Sept. 4-5.

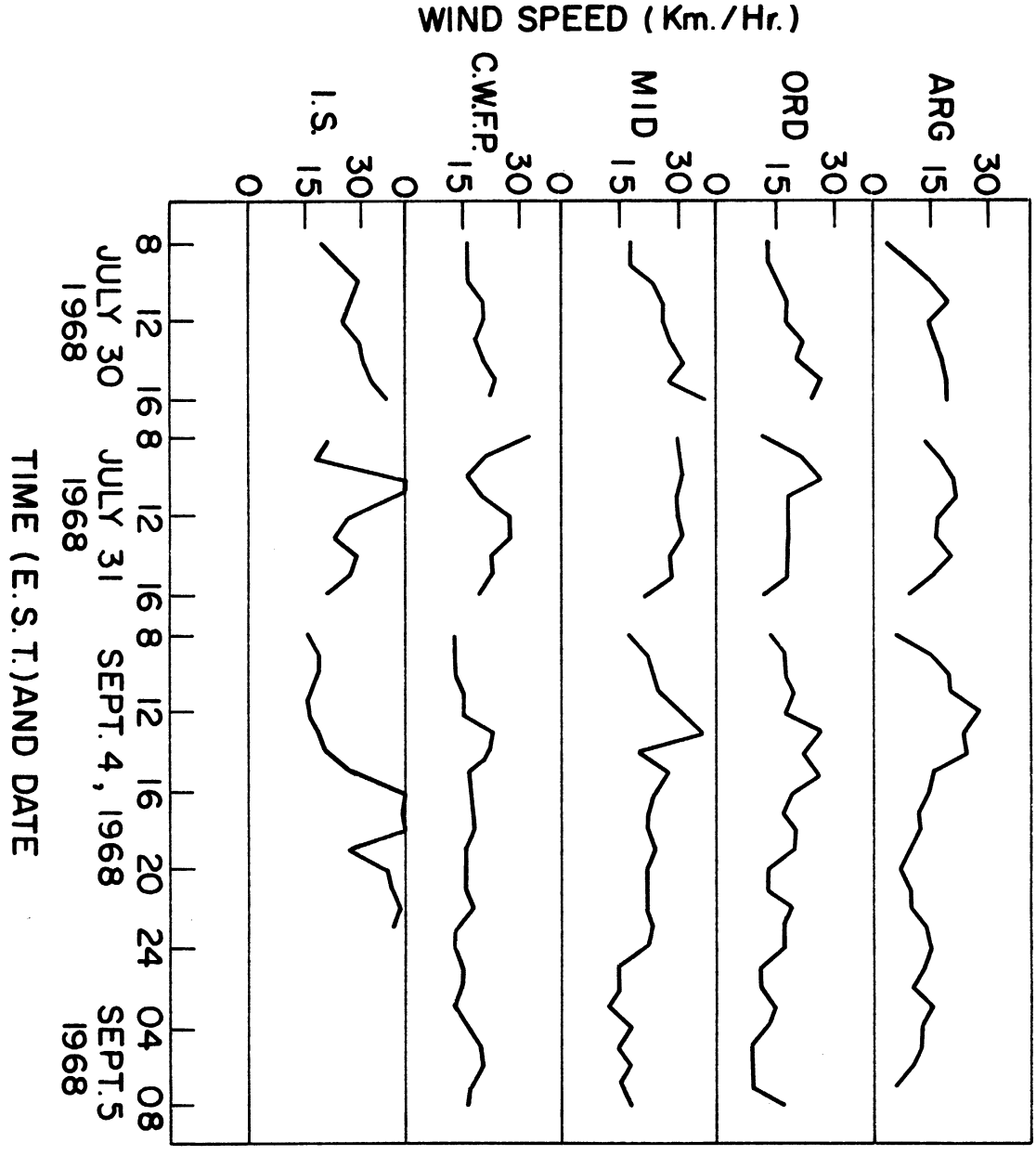

Fig.II-6.--Wind speed in the Chicago Area July 31 and Sept. 4-5.

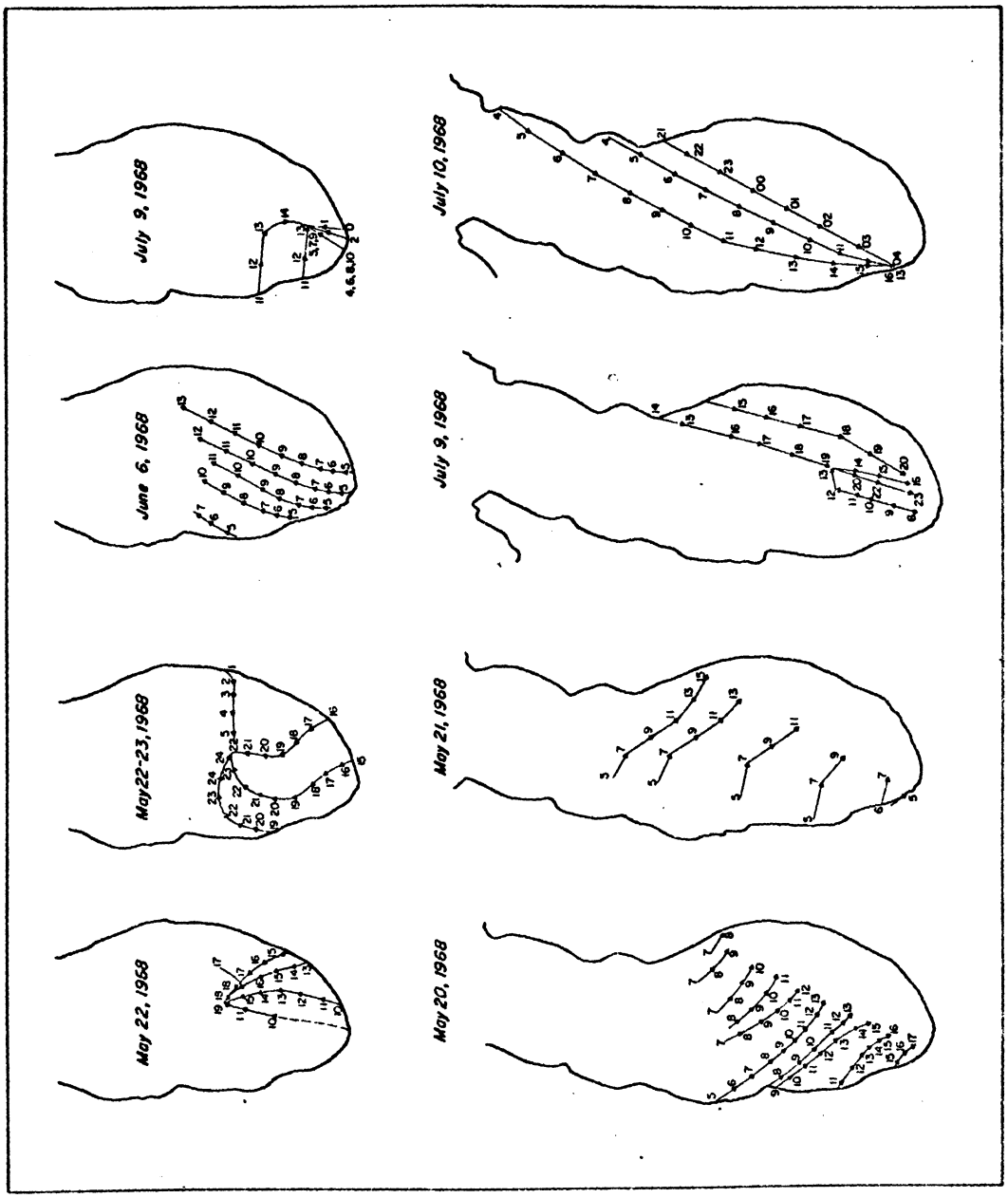

Fig. II-7.--Trajectory maps of Lake Michigan. Numbers indicate hour (EST) of day.

TABLE II-4

WEATHER STATISTICS FOR MAY 21, 1968

Time	Wind Speed at Mast (m/sec)	Wind Speed at 100m (m/sec)	Wave ht. (m)	Comment
645	——	6.4	0.0	Swell
700	3.7	7.3	0.0	Swell
800	2.6	4.0	0.0	Swell
900	2.1	1.6	0.0	Swell
1000	2.1	7.0	0.0	Swell
1100	3.2	0.2	0.0	Swell
1200	2.1	1.9	0.0	Swell
1300	2.6	0.9	0.0	Swell
1400	2.6	0.8	0.0	Swell
1500	4.7	4.3	0.0	Swell

TABLE II-5

WEATHER STATISTICS FOR MAY 22, 1968

Time (EST)	Wind Speed at Mast (m/sec)	Wind Speed at 100m (m/sec)	Wave ht. (m)	Comment
0613	——	8.5	——	
0700	3.2	9.7	.2	
0800	3.7	11.7	.2	
0900	3.7	10.7	.2	
0955	2.6	10.1	.2	
1045	3.2	9.9	.2	
1200	3.7	8.7	.4	
1250	4.2	13.2	.4	
1355	3.2	12.5	.2	
1455	4.2	9.5	.2	
1555	4.2	9.8	.2	
1655	4.2	10.3	.2	
1800	3.7	9.9	.2	
1900	3.2	9.4	.2	
2000	4.2	11.2	.2	
2100	3.2	——	.0	
2200	3.7	——	.0	
2300	4.2	——	.0	
2400	4.2	——	0.0	

TABLE II-6

WEATHER STATISTICS FOR MAY 23, 1968

Time (EST)	Wind Speed at Mast (m/sec)	Wind Speed at 100m (m/sec)	Wave ht. (m)	Comment
0100	2.1	——	0.0	2m Swell, Fog
0200	.5	——	0.0	2m Swell, Fog
0300	3.7	——	0.0	1m Swell, Fog/ Rain
0400	3.2	——	.2	1m Swell
0500	3.7	——	.3	
0600	4.7	15.0	.3	
0700	3.9	15.5	.3	
0800	3.7	13.9	.3	
0900	4.2	9.8	.3	
1000	4.2	9.3	0.3	

TABLE II-7

WEATHER STATISTICS FOR JUNE 6, 1968

Time (EST)	Wind Speed at Mast (m/sec)	Wind Speed at 100m (m/sec)	Wave ht. (m)	Comment
0500	6.4	——	0.3	Haze
0700	7.9	12.5	.0	Haze
0900	8.5	10.9	.0	Haze
1100	10.0	8.4	.0	Haze
1300	9.0	9.1	.0	Haze
1500	8.5	5.8	0.0	Haze

TABLE II-8

WEATHER STATISTICS FOR JULY 9, 1968

Time (EST)	Wind Speed at Mast (m/sec)	Wind Speed at 100m (m/sec)	Wave ht. (m)	Comment
0000	5.3	——	0.6	
0200	8.4	——	.6	
0400	5.8	——	.6	
0600	5.3	13.1	.6	
0800	5.3	11.5	.6	
1000	4.2	11.1	.3	
1200	2.1	5.4	.0	
1400	5.8	10.9	.3	Frontal Passage
1600	6.4	9.6	1.0+	
1800	7.9	13.1	1.0+	
2000	7.4	——	1.0+	
2200	6.4	——	1.0+	

Relative Humidity = 88%
Air Temperature = 14.2°C
17.9°C decreasing to 14.2°C
Visibility unlimited

T = 0500 EST
(000<T<0500)

TABLE II-9

WEATHER STATISTICS FOR JULY 10, 1968

Time (EST)	Wind Speed at Mast (m/sec)	Wind Speed at 100m (m/sec)	Wave ht. (m)	Comment
0000	10.6	——	2.0	
0200	8.5	——	2.0	Anchored at 0230
0400	10.6	——	2.0	
0600	9.6	11.0	2.0	
0800	5.8	13.5	2.0	
1000	5.3	5.5	2.0	
1200	5.3	4.9	2.0	
1400	5.8	13.8	2.0	
1600	6.4	7.7	2.0	
1800	5.3	——	——	
2000	4.7	——	——	

Relative Humidity = 85%

APPENDIX III

CALCULATION DETAILS FOR THE AVERAGE SIZE OF PARTICLES UNDERGOING THERMAL COAGULATION

Derivation of the equations, expressing the number concentration of particles as a function of time, is taken from the work of Higuchi (1959).[1] Considering only Brownian coagulation in the growth of particles, from the kinetic theory of gases the following may be written (Fowler and Guggenheim, 1939).

$$-\frac{dn}{dt} = k_{1,1}\, n_1^2 + k_{1,2}\, n_1 n_2 + k_{1,3}\, n_1 n_3 + \cdots k_{1,m}\, n_1 n_m$$

$$+ k_{2,2} n_2^2 + k_{2,3}\, n_2 n_3 + \cdots\cdots$$

$$+ k_{3,3}\, n_3^2 + \cdots\cdots$$

$$\vdots$$

$$k_{m,m} n_m^2$$

where $n = \sum_{g=1}^{m} n_g$

n_g = concentration of the g-mers

n_m = concentration of the largest particle

and $k_{s,L} = \frac{d_{s,L}^2}{\lambda} \quad 8\pi RT \quad \frac{M_s + M_L}{M_s M_L} \quad 1/2$

T = temperature (absolute)

---

[1] W. I. Higuchi, The agglomeration of Pb and PbO and its importance to lead-alkyl antiknock effectiveness, a theoretical study (unpublished Final Report, Chevron Research Company, 1959) p. IV-1.

$A_1, A_2, \ldots A_g$ = the monomer, dimer, ...g-mer

$M_1, M_2, \ldots M_g$ = the molecular weights of the monomer, dimer, ... g-mer

ρ = the bulk phase density

λ = the symmetry number; $\lambda = 1$ if $s \neq L$, $\lambda = 2$ if $s = L$

$d_{s,L}$ = the collision diameter (cm) for particles A_s and A_L

$$= \frac{3M_1}{4\Pi\rho N}^{1/3} \left(s^{1/3} + L^{1/3} \right)$$

N = Avogadro's number

R = Ideal Gas constant

In calculating average particle size, it is convenient to work with a statistically averaged coefficient of coagulation, i.e.,

$$-\frac{dn}{dt} = k_0 n_1^2 + 2 k_0 n_1 n_2 + 2 k_0 n_1 n_2 + \ldots 2 k_0 n_1 n_m$$
$$+ k_0 n_2^2 + 2 k_0 n_2 n_3 + \ldots$$
$$+ k_0 n_3^2 + \ldots\ldots$$
$$\vdots$$
$$k_0 n_m^2$$

so that $\frac{dn}{dt} = -k_0 n^2$

A statistically averaged k_0 may be written

$$k_0 = Z \frac{\int_{s=L}^{m} \int_{L=1}^{m} n_s n_L \left(s^{1/3} + L^{1/3} \right)^2 \left(\frac{s + L}{sL} \right)^{1/2} ds\, dL}{2 \int_{s=L}^{m} \int_{L=1}^{m} n_s n_L\, ds\, dL}$$

where $$Z = 4\Pi \left(\frac{3M_1}{4\Pi\rho N} \right) \left(\frac{RT}{2\Pi M_1} \right)^{1/2} .$$

Rate laws for three different size distributions were evaluated (After Higuchi, 1959).

TABLE IV-1

RATE LAWS FOR COAGULATION FOR DIFFERENT SIZE DISTRIBUTIONS

n_g	Approximate Rate Law
n_g = constant	$\frac{dn}{dt} = -2.7Z\ (n_0/n)^{1/6}\ n^2$
$n_g \propto g^{-2/3}$	$\frac{dn}{dt} = 2.1Z\ (n_0/n)^{1/3}\ n^2$
$n_g = n$ at $g = n_0/n$	$\frac{dn}{dt} = -2.8Z\ (n_0/n)^{1/6}\ n^2$
$n_g = 0$ elsewhere	This is the usual formula for the collision rate of homogeneous gas.

"On the basis of a preliminary investigation of a more rigorous approach" it was believed that the distribution of a nucleating aerosol lay "somewhere between $n_g \propto g^{-2/3}$ and n_g = constant".[1] An average n value was calculated. Integrating the equation $\frac{dn}{dt} = -k_0 n_2$ for the two distributions, Higuchi obtained

$$n_1^{5/6} = \frac{n_0^{5/6}}{1+2.2Zn_0t} \qquad n_2^{2/3} = \frac{n_0^{2/3}}{1+1.4Zn_0t} .$$

W. I. Higuchi, ibid, p.5.

An average radius was computed statistically

$$\bar{r} = (1/n) \int_{1}^{m} n_g r_g dg \ .$$

With the definition $n = (2n_1 + n_2)/3$ a mean radius was computed as a function of time. The definition $n = (2n_1 + n_2)/3$ was used and the mean radius was

$$\bar{r} = (2\bar{r}_1 + \bar{r}_2)/3$$
$$= 0.89 \ (n_0/n)^{1/3} \ (3M_1/4\Pi\rho N)^{1/3} \ .$$

Using the above equations mean radii were computed for varying temperatures, initial monomer concentrations, lead species, and times.

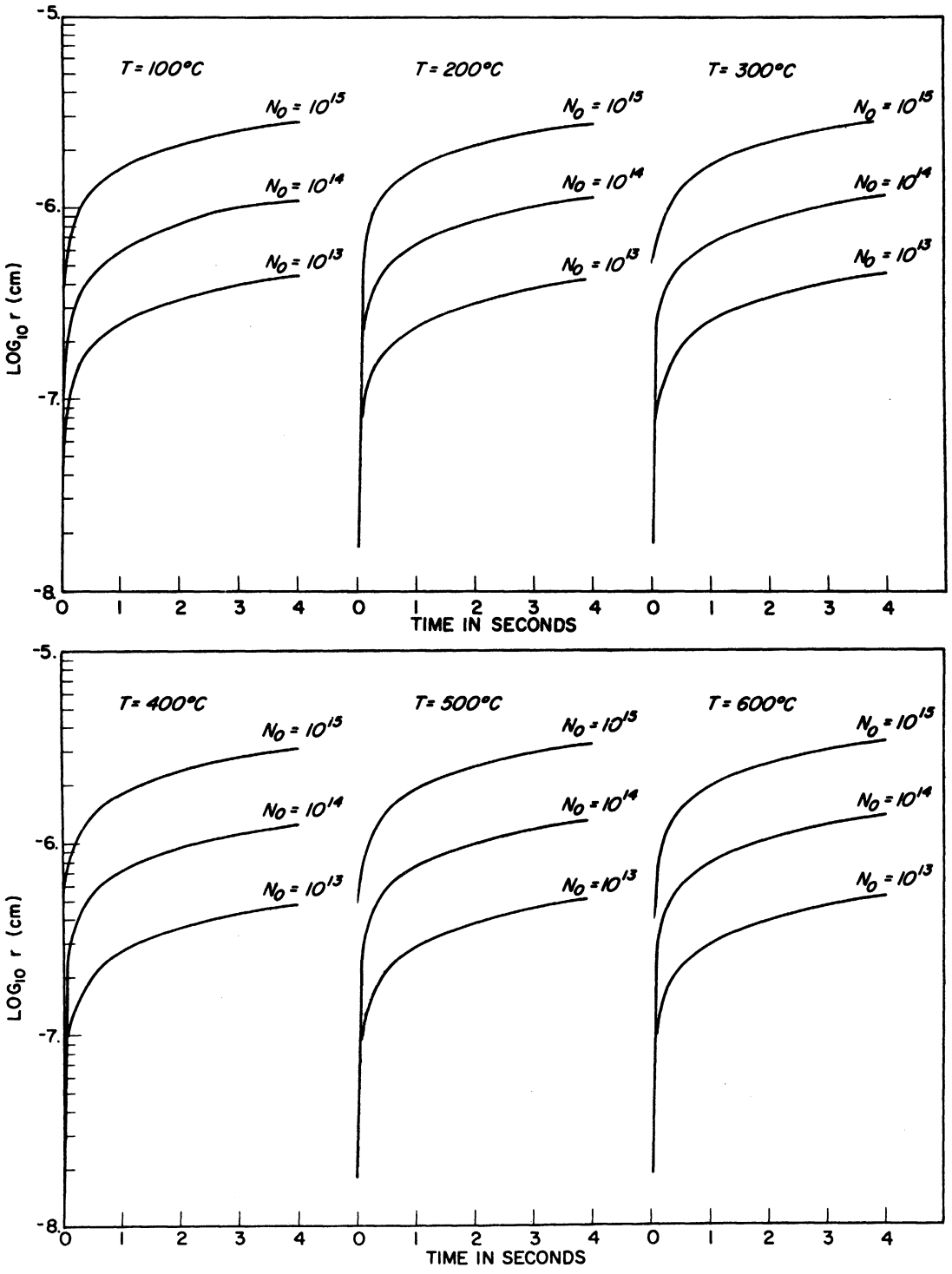

Fig. III-1.--Average radius as a function of time for Pb. N_0 is the initial monomer concentration.

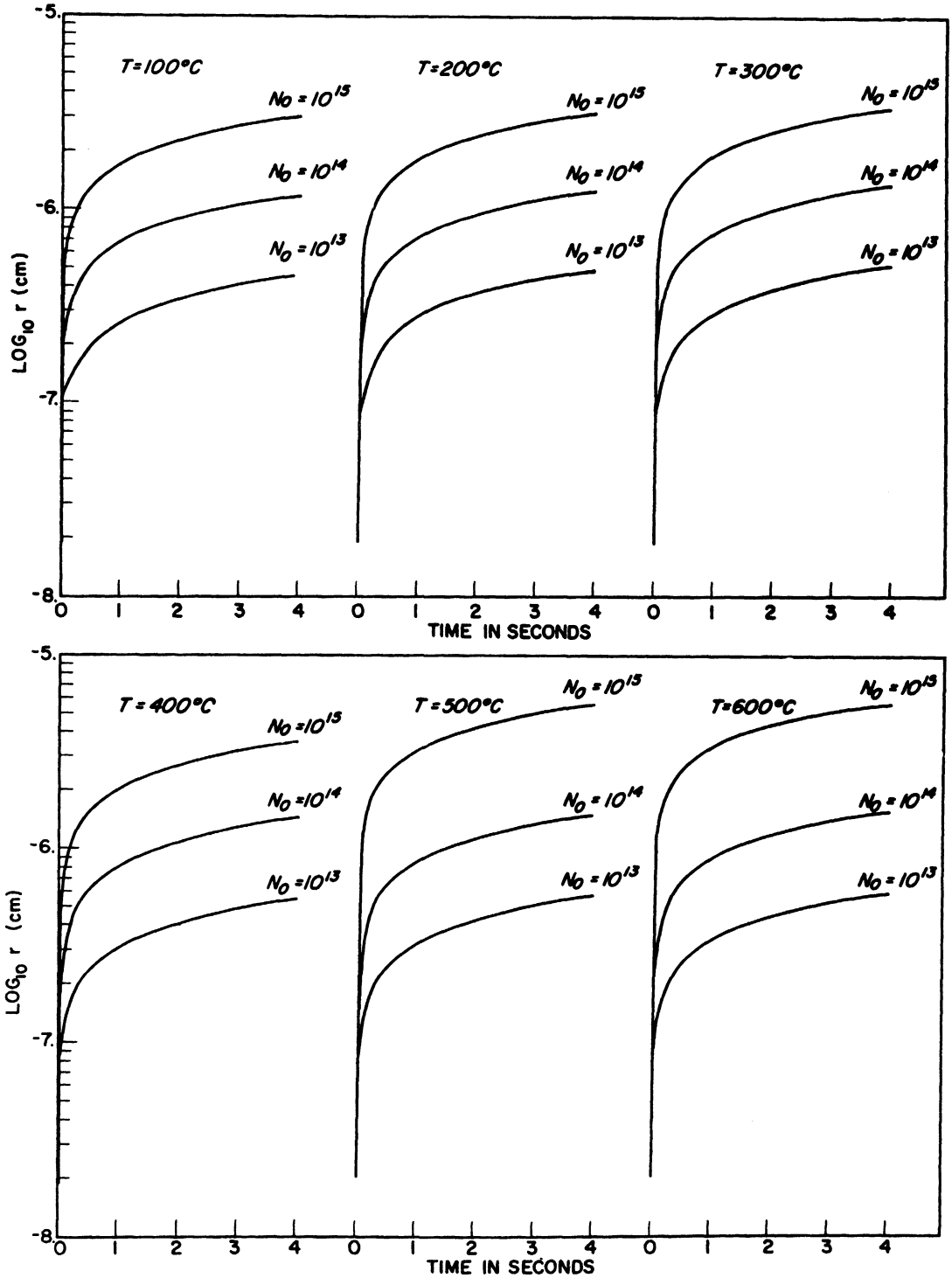

Fig. III-2.--Average radius as a function of time for PbO. N_0 is the initial monomer concentration.

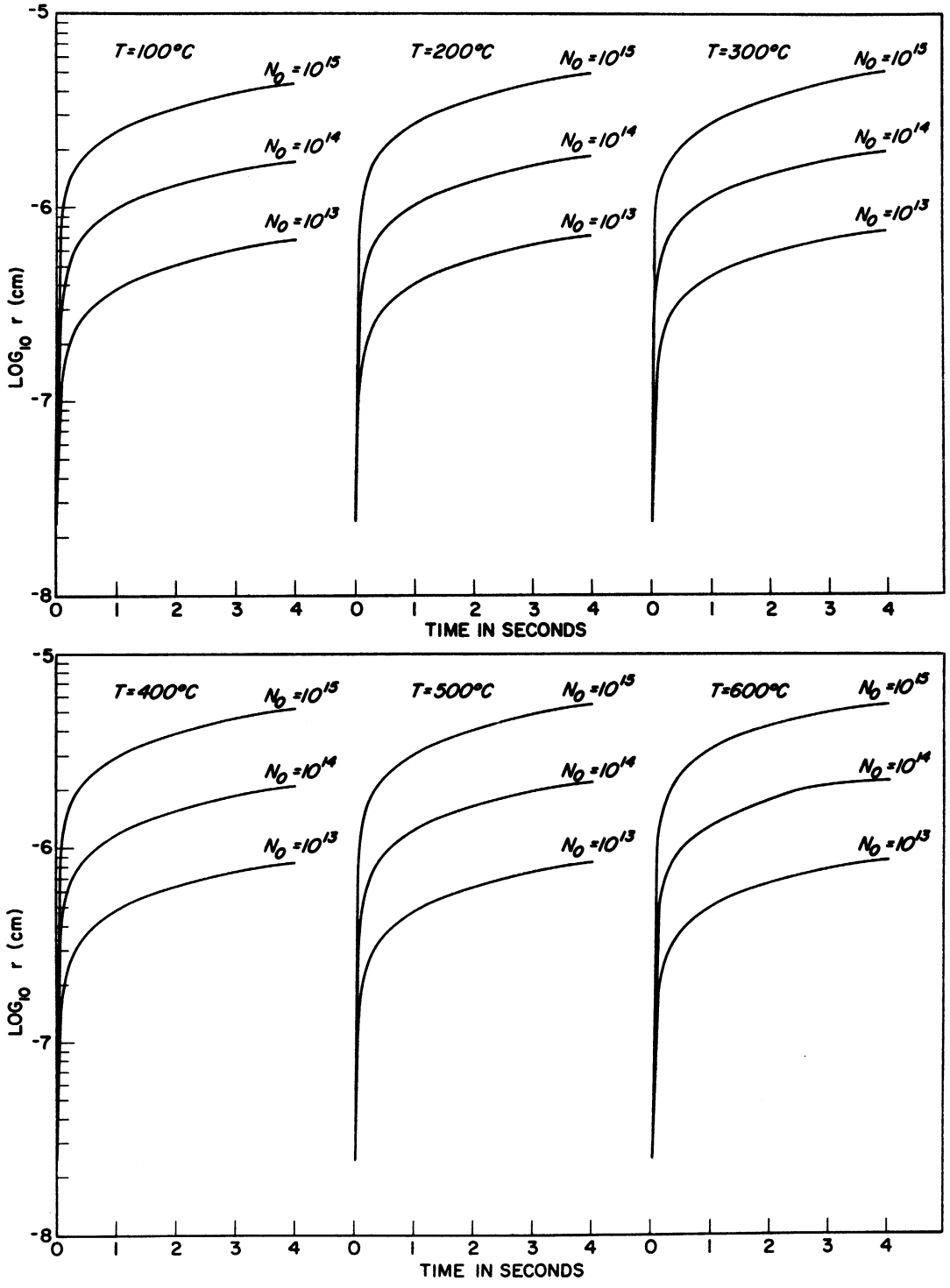

Fig. III-3.--Average radius as a function of time for $PbCl_2$. N_0 is the initial monomer concentration.

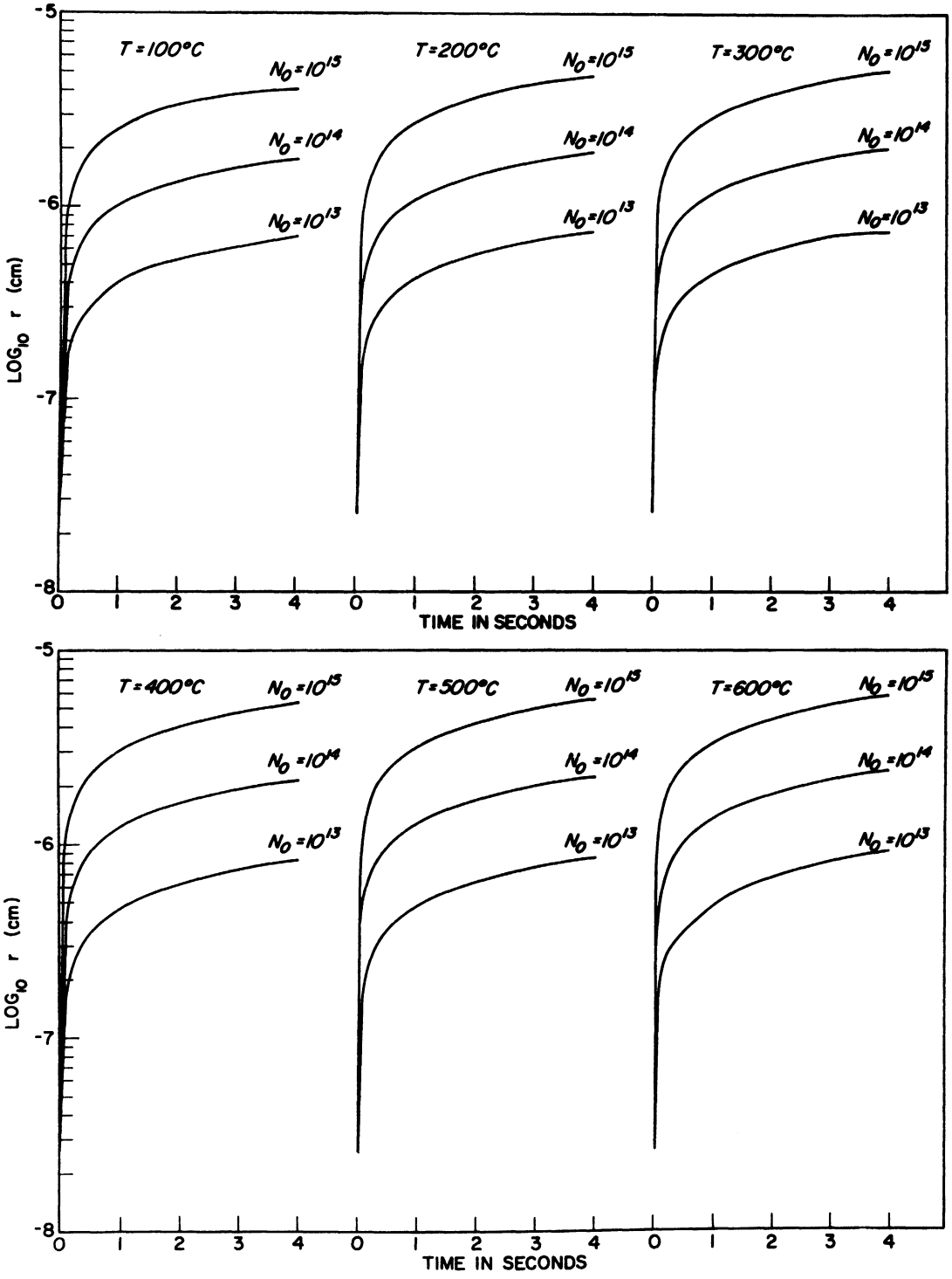

Fig. III-4.--Average radius as a function of time for $PbBr_2$. N_0 is the initial monomer concentration.

In addition, some rates of nucleation were computed based on the Volmer-Becker-Doering-Zeldovitch theory, discussed by Barnard (1953). These rates of homogeneous nucleation, may be regarded as lower limits of nucleation in the engine gas. In most cases the supersaturation ration was between 10 and 100 before significant nucleation took place for temperatures between 400° and 600°C.

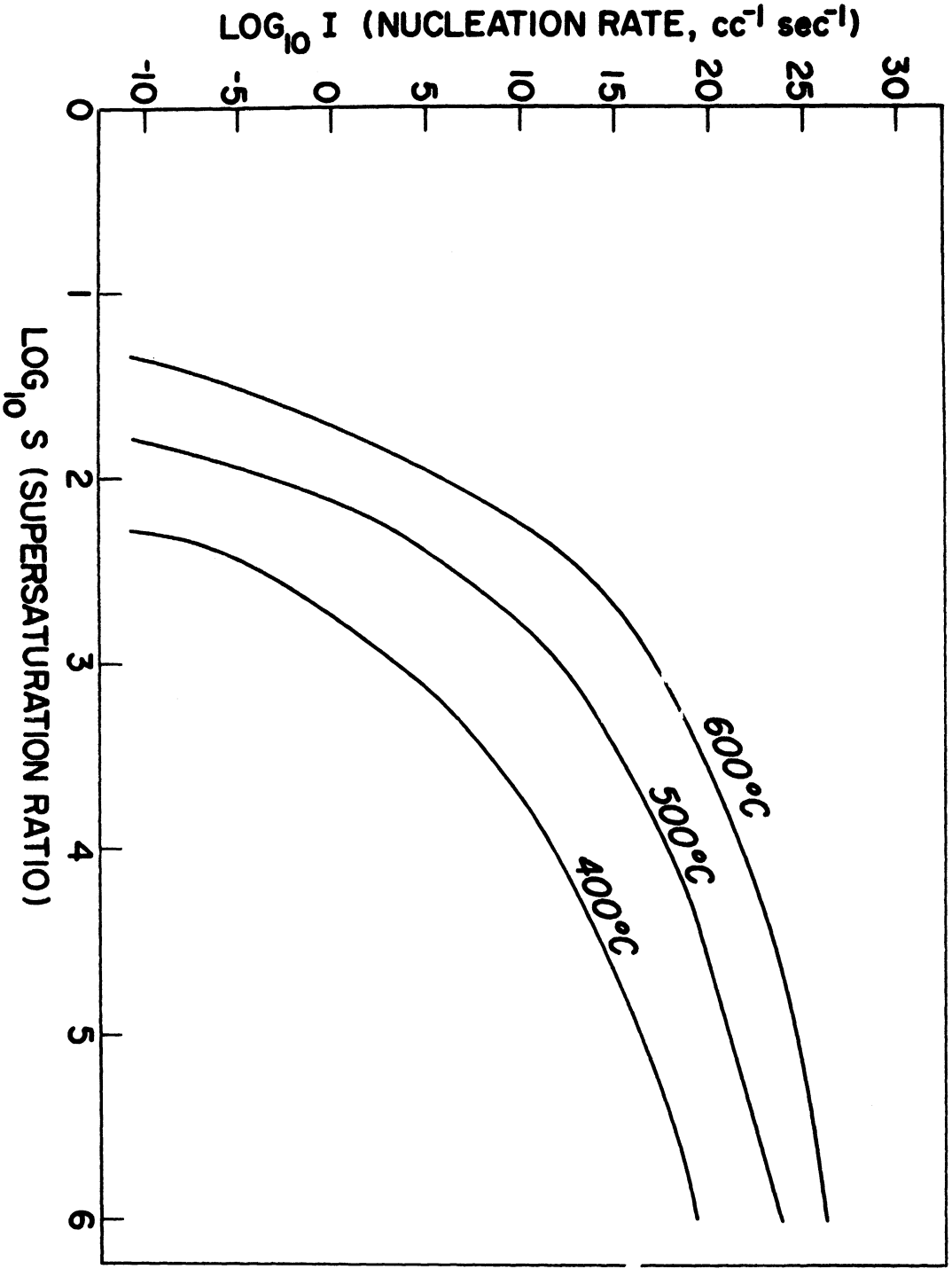

Fig. III-5.--Rate of nucleation vs. supersaturation for Pb.

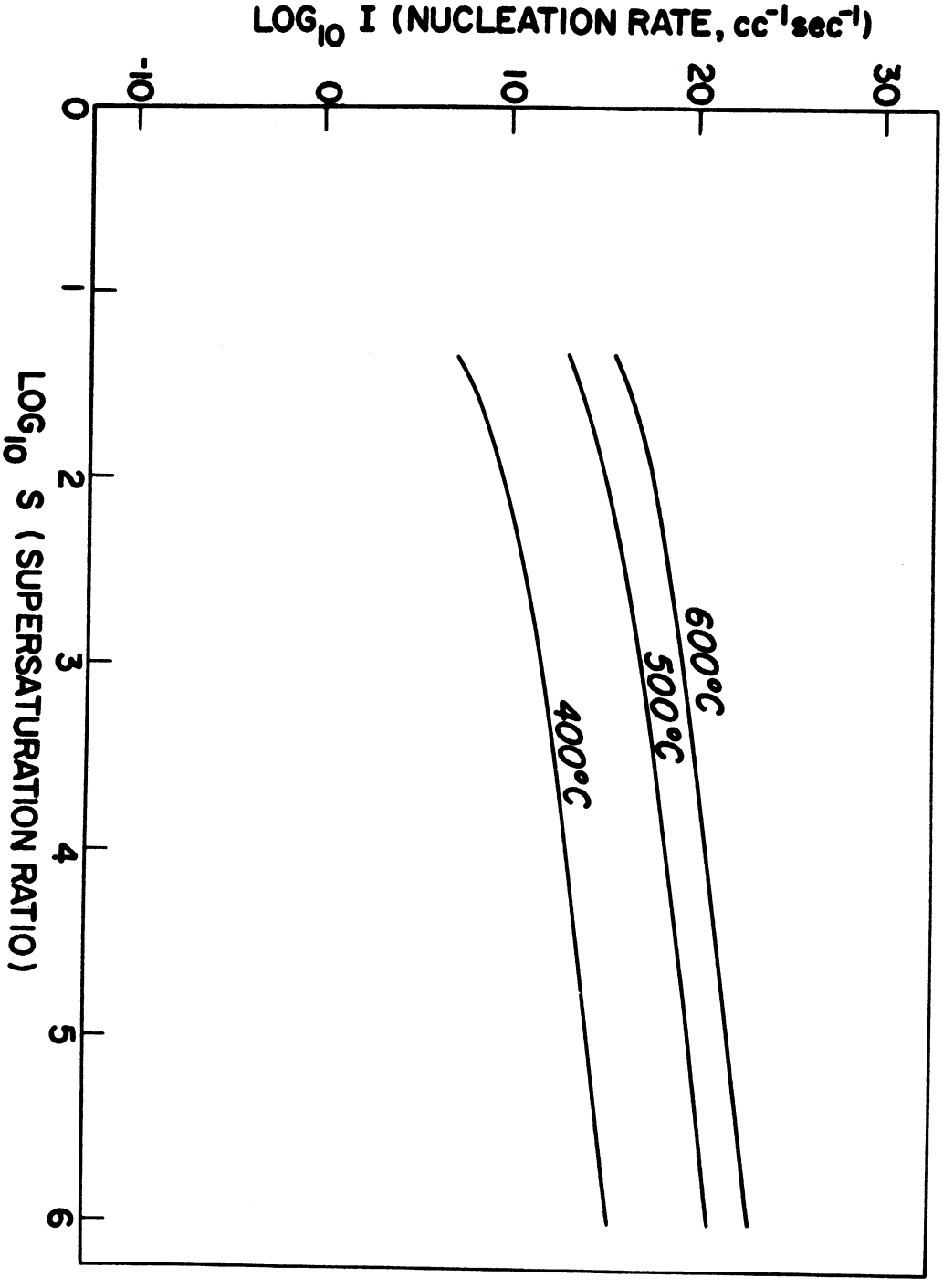

Fig. III-6.--Rate of nucleation vs. supersaturation for PbO.

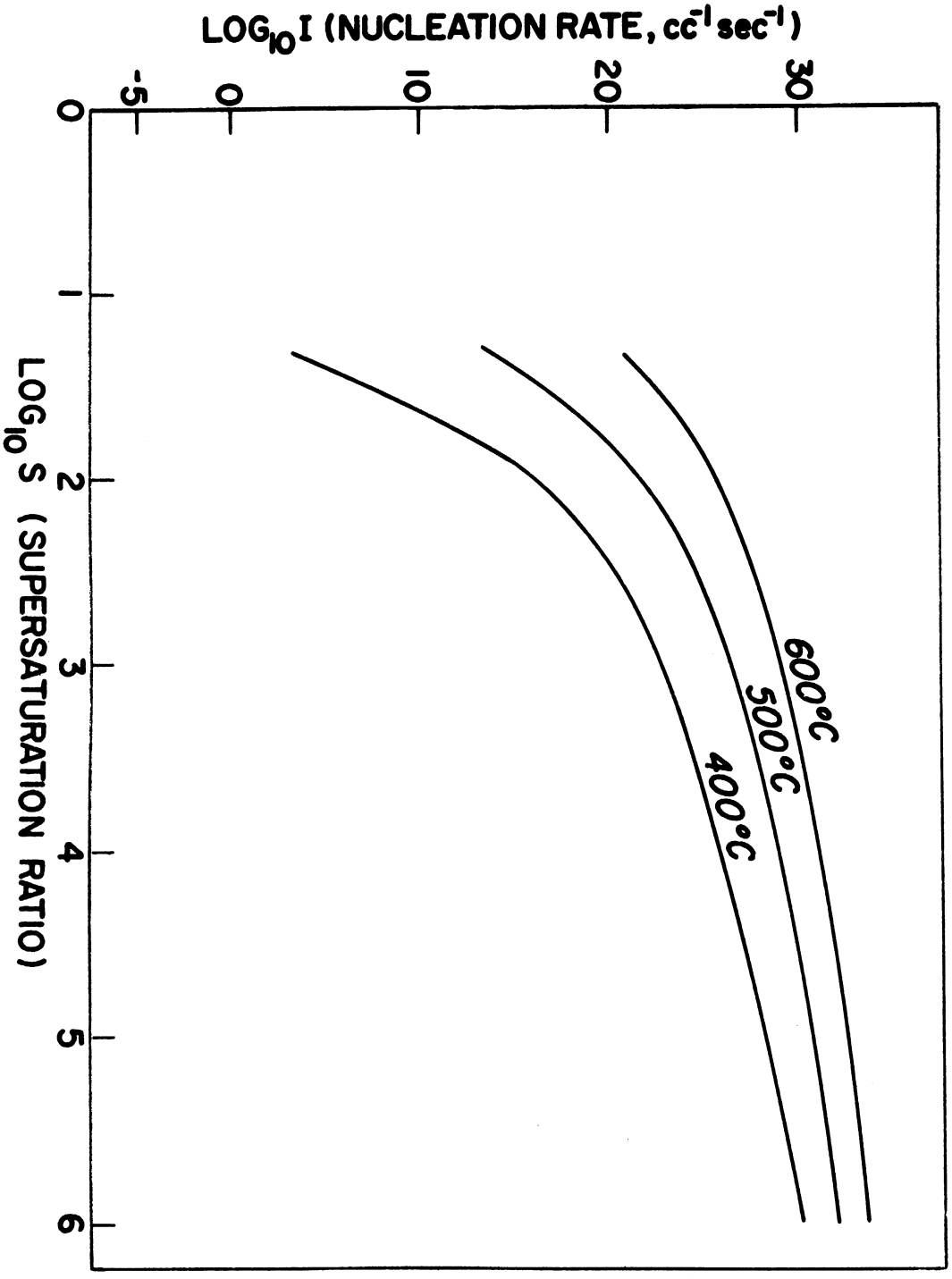

Fig. III-7.--Rate of nucleation vs. supersaturation for $PbCl_2$.

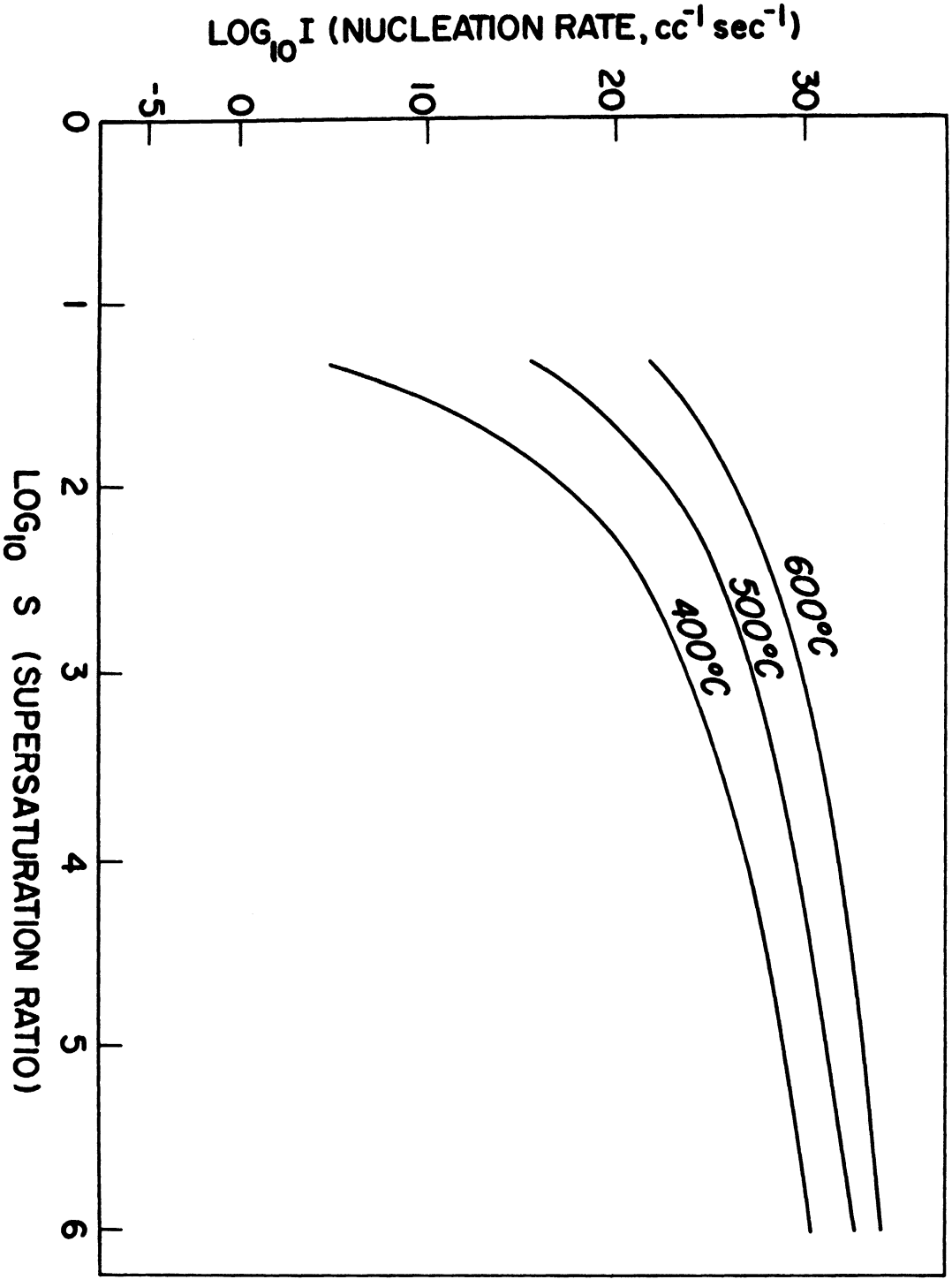

Fig. III-8.--Rate of nucleation vs. supersaturation for $PbBr_2$.

APPENDIX IV

A GENERAL REVIEW OF AEROSOL MECHANICS

A. Motions of Aerosol Particles

The motion of aerosols in the upper size range of the particle spectrum ($r > 0.1$ μm) is governed in the steady rectilinear case by Stokes' formula corrected for slip flow. Stokes' formula gives the drag force on a spherical particle at small Reynolds number (Landau, Lifschitz, 1959).

For steady, incompressible fluid flow, the Navier-Stokes equation is

$$(\vec{U} \cdot \text{grad})\vec{U} = -\left(\frac{1}{\rho_f}\right) \text{grad } p + \left(\frac{\eta}{\rho_f}\right) \nabla^2 \vec{U}$$

where $\vec{U}$ is velocity of the fluid
ρ_f is fluid density
p is pressure
and η is dynamic viscosity.

When viscous and pressure forces dominate inertia forces, the pressure and velocity fields are found for fluid flow around a solid spherical object. The surface drag is then obtained,

$$F_p = 6\Pi\eta\vec{U}a$$

where a is the radius of the sphere and F_p is the surface drag. The Terminal velocity of a freely falling sphere may be determined

gravitational force	buoyant force	net gravitational force
$\frac{4}{3}\Pi a^3 \rho_s g$	$\frac{4}{3}\Pi a^3 \rho_f g$	$\frac{4}{3}\Pi a^3 (\rho_s - \rho_f) g$

At equilibrium, the particle does not accelerate. Surface force = net gravitational force

$$F_p = \frac{4}{3}\Pi a^3(\rho_s - \rho_f)g = 6\Pi\eta\vec{U}a$$

therefore $$\vec{U} = \frac{2}{9}\frac{a^2}{\eta}(\rho_s - \rho_f)g$$

B. Empirical Correction Factor

When the mean free path of the fluid medium (air) is approximately the size of the sphere, Stokes' assumption of a continuous medium is violated. The mean free path at the earth's surface is about $6.5X10^{-6}$cm (Weast, 1968). A "large" particle is about $10^{-5} \leq r \leq 10^{-4}$cm and is only about ten times the mean free path of air. Friction drag and fall velocity for these particles was studied and an empirical equation was given with constants determined by Milliken (1923)

$$\vec{U} = \frac{mg}{6\Pi\eta r}\left(1 + A\frac{\ell}{r} + Q\frac{\ell}{r}\exp(-br/\ell)\right)$$

where $A = 0.864$

$Q = 0.29$

and $b = 1.25$.

Terminal velocities of rigid spheres of unit density in air at 760mm Hg pressure and 20°CC are given in Table Iv-1.

TABLE I v-1

SEDIMENTATION VELOCITY AS A FUNCTION OF PARTICLE DIAMETER

Diameter (μm)	Velocity (cm/sec)	Diameter (μm)	Velocity (cm/sec)
0.1	$8.71X10^{-5}$	4.0	$5.00X10^{-2}$
0.2	$2.27X10^{-4}$	10.0	$3.03X10^{-1}$
0.4	$6.85X10^{-3}$	20.0	1.20
1.0	$3.49X10^{-2}$	40.0	4.71
2.0	$1.29X10^{-1}$	100.0	24.7

C. Deposition of Particles at the Bottom of a Chamber

If $n(r)dr$ is the homogeneous concentration of particles in a chamber with radii between r and r + dr, and V_s is the vertical velocity of sedimentation, the number of particles deposited per second on 1 cm^2 at the bottom of the chamber is $V_s(r)\, n(r)dr$ and the number of particles deposited in a time t is $dN = V_s(r)tn(r)dr$. This formula is applicable only for $t \leq H/V_s(r)$. (H is the height of the chamber) because all particles of the indicated size will settle in a time $H/V_s(r)$.

D. Non-uniform Rectilinear Motion of Aerosol Particles

The general differential equation expressing momentum change for a spherical particle traveling in a straight line through a resisting medium at low Reynolds Number is

$$m\frac{d\vec{U}}{dt} = \vec{F}(t) - \frac{2}{3}\Pi\rho_g r^3 \frac{d\vec{U}}{dt} - 6\Pi\eta r\vec{U}$$

$$- 6r^2\sqrt{\Pi\eta\rho_g}\int_0^t \frac{d\vec{U}}{dx}\frac{dx}{\sqrt{t-x}}$$

where ρ_g = density of gas medium. The first term on the right hand side is the external force acting on the particle, which in general varies with time. The third term is the resistance of the medium for a constant velocity equal to the instantaneous value of the velocity of the particle. The second and last terms express that part of the resistance which is due to the energy expended in setting the medium itself in motion. The second term is the resistance of an ideal fluid to the accelerated motion of a sphere. It is equivalent to an increase in the

mass of the sphere by half of the medium displaced.[1]

Since the density of air is small compared to that of the particle, the second term is neglected. The integral term is usually neglected in published works. Thus

$$\frac{d\vec{U}}{dt} + \frac{\vec{U}}{\tau} - \frac{F}{m} = 0$$

where $\tau = m/6\Pi\eta r$.

When F = mg (where gravity is the external force)

$$V = V_s(1 - \exp(-t/\tau)$$

where V is Velocity of the particle

and V_s is Stokes' flow velocity = τg.

That is, starting from rest, a particle will obtain Stokes' flow exponentially.

E. Impaction Removal of Particles

A simplified two dimensional calculation of impaction efficiency (Fuchs, 1964) is instructive in assessing the importance of impaction in the removal of particles, especially for the small particles in which lead is primarily contained.

Assuming that a stream of particles issues from a slit toward a horizontal impaction plate and that the streamlines of the fluid are approximately circular, the

---

[1] Fuchs, N. A., The Mechanics of Aerosols, McMillan Co., 1964, p.70.

issuing stream will be 2h and the outlet depth d.

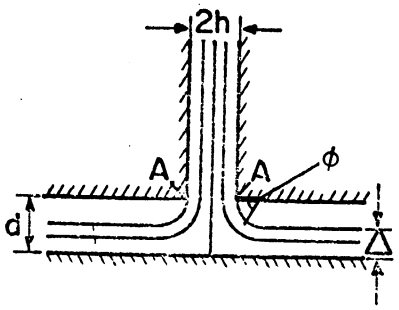

The tangential velocity of particles and stream are practically identical. The radial velocity of the particles is however,

$$v_R = u_0^2 \, \tau / R$$

where τ is the time constant of the particle and R is the radius of curvature of the streamline.

In the time dt the particle is displaced (relative to the medium) the radial distance $dR = v_R \, dt$ and the vertical distance from the impaction plate $dz = v_R \sin \phi \, dt$. If the radius of curvature is large in comparison to the change of the radius due to impaction

$$\Delta z = \int_t \frac{u_0^2 \, \tau \sin \phi \, dt}{R}$$

since

$$u_0 = R \frac{d\phi}{dt}$$

$$dt = R \frac{d\phi}{u_0}$$

and

$$\Delta z = \int_0^{\Pi/2} u_0 \tau \sin\phi \, d\phi$$

$$= u_0 \tau .$$

The efficiency of collection is defined by the ratio of distance a particle moves in the vertical direction to the total width of the issuing stream. Efficiency = $u_0\tau/h$

where τ is a known function of particle size

$\tau(0.01\ \mu m) = 1.4X10^{-9}$

$\tau(0.1\ \mu m) = 2.28X10^{-7}$

$\tau(1\ \mu m) = 1.31X10^{-5}$

and $\tau(10\ \mu m) = 1.23X10^{-3}$.

For particles of 0.1 μm radius and a velocity of 450. cm/sec (about 10 mph) a column of $1.8X10^{-4}$ cm is collected with an efficiency of 50 per cent (i.e. one could expect 1/2 of the particle concentration to impact on one impaction encounter).

F. Other Factors Acting on Aerosol Particles (Ranz and Johnson, 1952)

Electrostatic Force

Electrostatic force may be expressed as charge carried by the particle times the electric field.

$$\vec{F} = q_p\vec{E}$$

The maximum number of charges which can be held by the representative aerosol particle is about 100. If a representative particle (chosen to be 1 μm in diameter, having unit density) has ten unit charges, then an electric field of 32 volts cm will create a force equal to that of gravity.

Thermal Force

Thermal force is directly proportional to the temperature gradient and is directed toward the region of lower

temperature.

$$\vec{F} = -K_T \text{grad } T$$

If the representative particle has a thermal conductivity of 4.0×10^{-4} cal/sec.cm°C, a temperature gradient of 34°C/cm in air at 20°C, 1 atm, the thermal force will be equal to that of gravity.

Magnetic force

If a particle carrying charge q_p is moving at velocity $\vec{U}$ across a magnetic induction $\vec{B}$ the force is

$$F = q_p \vec{U} \times \vec{B}.$$

A particle carrying 10 unit charges moving across a magnetic field of 0.5 gauss (corresponding to the earth's magnetic field) will experience a force equal to that of gravity if it moves 1/5 the speed of light. It is justified to neglect this force under most circumstances.

G. Turbulent Transport of Particles

Turbulent motion, in addition to aiding the coagulation process, is an important process in the diffusion of particles. Often, diffusion of particles is described by the equations of diffusion of gas (e.g. Pasquill's formulation (1962)) with correction for the additional motion of particles relative to the medium. A simplified formula is that of the Fickian expression for the flux of particles.

$$\text{flux} = D_f \frac{dN}{dx_i}$$

$i = 1,2,3$

D_f = diffusion coefficient

N = number of particles/unit volume

H. Scavenging of Particulate Matter by Rain

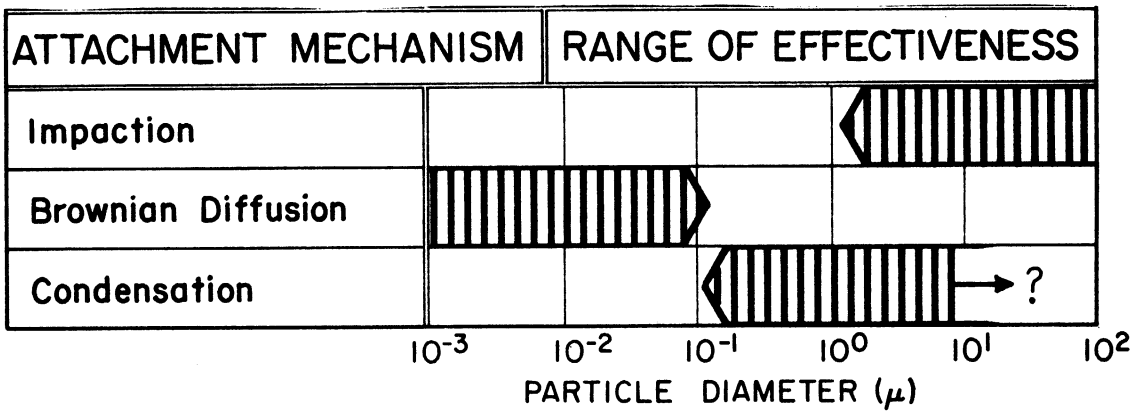

Atmospheric cleaning of particulates (Gatz, 1966) proceeds by five basic mechanisms: 1) Brownian coagulation of particles; 2) turbulent coagulation; 3) impaction; 4) nucleation, in which the aerosol acts as a condensation nucleus for a cloud droplet; and 5) diffusiophoresis, in which aerosol particles are moved toward a condensing droplet by the inward flux of water vapor.

I. Coagulation

The process of coagulation is one in which particles stick together if they come into contact. The process goes on continuously so that the aerosol becomes larger and eventually flocculates out.

The first evidence of coagulation (Green and Lane, 1964) was given by Tolman in 1919. The evidence was the measurement of the intensity of a Tyndall beam in a confined volume of smoke. While the mass concentration of smoke decreased linearly with time, the intensity of the Tyndall beam decreased more rapidly and non linearly. It was possible to correlate the Tyndall meter readings with the mass concentration and with the average size of the particle. It was explained that the decrease of intensity was due to coagulation of particles.

Experiments by Whitlaw Gray showed that coagulation of many smokes follows a simple law

$$\frac{1}{n} - \frac{1}{n_0} = Kt$$

where n is the number of particles per cm^3 at time t, n_0 is the number at time t = 0 and K is a constant.

Differentiation of the above expression shows that the rate at which particles disappear by coagulation depends only on the square of the number present and the constant K

$$\frac{-dn}{dt} = Kn^2.$$

J. Brownian Motion and Diffusion

Particles suspended in fluid move in an irregular manner under the influence of the molecular motion in fluid. If a particle is at the origin of a coordinate system at time t = 0 its subsequent motion may be regarded as a diffusion, in which the concentration is represented by the probability of finding the particle in any particular volume element. If the particles do not affect one another, diffusion in one dimension is analogous to the "random walk" (Chandrasekhar, 1943).

In the random walk all sequences of N steps, each step being a one point progression or regression, have the same probability. To arrive at a point m one must take $(N + m)/2$ steps in the positive direction and $(N - m)/2$ steps in the negative direction. The probability of any sequence of N steps is $(1/2)^N$ and the number of distinct sequences leading to the point m is

$$\frac{N!}{\left[\frac{1}{2}(N + m)\right]! \left[\frac{1}{2}(N - m)\right]!}$$

Hence the probability of arriving at the point m in a sequence of N steps is $w(m,N) =$

$$\frac{N!}{[1/2\ (N + m)]!\ [1/2\ (N - m)]!}(1/2)^N .$$

With Stirling's formula $\log n! =$

$$(n + 1/2)\log n - n + 1/2 \log 2\Pi + 0\ (n^{-1}) \text{ for } n\to\infty$$

for $m \ll N$ and for N very large

$$w\ (m,N) = (2/\Pi N)^{1/2}\ \exp\ (-m^2/2N).$$

If $x = ml$, where l is the length of a step, and the interval Δx is large compared to the length of a step after N displacements $W(x,N)\,\Delta x = W(m,N)\,(\Delta x/2l)$ where $W(x,N)\,\Delta x$ is the probability that the particle is in the interval x, $x + \Delta x$ after N displacements. If a particle undergoes n displacements per unit time then $N = nt$ and

$$w(x,t) = \frac{1}{2(\Pi Dt)^{1/2}} \exp(-x^2/4Dt)$$

where $D = 1/2nl^2$ has the dimensions of a coefficient of diffusion. Although large differences exist between the mechanism of Brownian motion and the "random walk", the expressions derived and expanded to three dimensions for each are analogous. This is due basically to the concept of "apparent mean path" of a particle corresponding to the length of step in "random walk". The forward velocity of a particle from kinetic theory has a mean square velocity of $G^2 = 3\,KT/m$ where m is the particle mass, K is the Boltzmann constant, and T is the absolute temperature. As shown previously the motion of a particle given an impulse at time $t = 0$ is $G = G_0\, e^{-t/\tau}$ where $G_0 = G(t = 0)$ and where τ is the time constant related to friction of the fluid. The "apparent mean free path" is then defined to be $\ell_\beta = \bar{G}\tau$.

The probability equation relating the transition of a particle from position x_0 to position x in a time $t + t'$ shows that a transition from x_0 to any accessible x' in time t must occur and subsequently a transition from x' to x in time t' must occur. The probability of such a pair of transitions is the product of each transition probability if each transition is independent (a condition establishing a Markoff chain for time intervals much larger than the time

constant).

The equation

$$w(x_0, x, t+t') = \int_{x'} w(x_0, x', t)\, w(x', x, t')dx'$$

is integrated over all possible transition pairs leading from x_0 to x.

From this equation the Fokker-Planck equation is derived by expanding all terms in the form of a Taylor series, applying the appropriate statistical integral relations and ignoring terms of second order in the time interval. The equation

$$\frac{\partial w}{\partial t} = \frac{-\partial (V_x w)}{\partial x} + D \frac{\partial^2 w}{\partial x^2}$$

is obtained for one dimension, where D is a diffusion coefficient and V_x is the ordered velocity in the x direction, caused by external forces. The above equation expanded to three dimensions is

$$\frac{\partial w}{\partial t} = \nabla . (\vec{V} w) + D\nabla^2 w$$

The expression for the transition probability $w(x_0, x, t)$ for a particle having no ordered motion was determined by solving the Fokker-Planck equation for one dimension. The result is

$$w(x_0, x, t)dx = \frac{1}{\sqrt{4\Pi Dt}} \exp -(x - x_0)^2/4Dt \quad dx$$

exactly analogous to the "random walk" probability.

An expression for the mean square displacement is

$$\overline{(x-x_0)^2} = \int_{-\infty}^{\infty} (x-x_0)\, w(x_0,x,t)\, dx = 2Dt$$

as given by Einstein.

Transformation of the Fokker-Planck equation (Fuchs, 1964) is employed in finding the particle concentration $N(x,t)$ in the interval x, $x + dx$ at time t. The differential equation obtained is

$$\frac{\partial N}{\partial t} = -\frac{\partial (V_x N)}{\partial x} + D\frac{\partial^2 N}{\partial x^2}$$

The diffusion coefficient D can be calculated from "mobility" of particles suspended in a fluid. In a steady state, the force acting upon each particle must be balanced by the drag. When velocity is small and the particle is spherical Stokes' law is applicable. $V = bf$ where f is the external force, V is velocity, and b is the mobility given by Stokes to be $b = 1/6\Pi\eta r$. Diffusion flux is denoted as $\vec{i}$ and is due to the flux along the concentration gradient and the velocity acquired by the particle due to the external forces. Flux along the concentration gradient is written $-\rho D$ grad c and flux due to the external force is expressed by $\rho c\vec{V}$ where $\vec{V} = fb$ and c is the concentration of particles.

$$\vec{i} = -\rho D \text{ grad } c + \rho\, cbf.$$

In thermodynamic equilibrium $\vec{i} = 0$ and the equilibrium distribution of particles suspended in a fluid, in an external field, is determined by Boltzmann's formula $c = \text{const}(e^{-U/kT})$

where U is the potential energy of the particle in the external field. Since f = -grad U, grad c = $c\vec{f}/kT$. Substituting into the above equations one gets

$$Dcf/kT = cbf$$

$$D = kTb = kT/6\Pi\eta r = kT\tau/m = \overline{G_x^2}\tau = G\ell_\beta\Pi/8$$

since $\overline{G_x^2} = kT/m$

and $\bar{G} = \sqrt{8\bar{G}^2/\Pi 3}$

In these formulae r = a = radius of the particle and b may be the modified (corrected) Stokes' velocity or may need another formulation.

K. Von Smoluchowski's Theory of Rapid Coagulation (Kruyt, 1952)

Coagulation rate is governed by Brownian motion and the interaction of the particles when they are close together. If one postulates that repulsion may be neglected, only London-van der Waals attraction needs to be considered. Further simplified, one can represent the London-van der Waals attraction by a sphere of action surrounding each particle. If another particle enters a particle's sphere of action, the two particles coalesce irreversibly.

If one particle is fixed in the origin and N_0 spherical particles of equal size are initially present per unit volume one can determine how many particles will collide with it in the course of time. The particles not at the origin are in a diffusion field characterized by

$$N = N_0 \text{ for } r > R \text{ at } t = 0$$

$$N = 0 \text{ for } r = R \text{ at } t > 0$$

where r is the distance from the center of coordinates and R is the distance between the centers of two particles at which a lasting contact is formed.

The concentration of particles N (r,t) having no ordered motion is given by the second Fick equation, homogeneous in three dimensions

$$\frac{\partial(rN)}{\partial t} = D \frac{\partial^2(rN)}{\partial r^2}$$

where D is the diffusion constant of the particles. The solution is obtained using Laplace transforms and when subject to the above conditions is

$$N(r,t) = N_0 \frac{R}{r} (1 - \mathrm{erf}((r - R)/2\sqrt{Dt}))).$$

The number, J, of particles diffusing through a closed surface in the direction of the central particle is equal to the number of particles colliding with the central particle. The number J(t) is given by the equation

$$Jdt = 4\Pi DRN_0 (1 + R/\sqrt{\Pi Dt})\, dt.$$

The number of collisions with the central particle is

$$4\Pi DRN_0 (t + \frac{2R\sqrt{t}}{D\sqrt{\Pi}}).$$

However, the central particle is also subject to Brownian motion. The relative displacement of two particles is given by $\vec{r}_1 - \vec{r}_2$ and the relative diffusion constant is

$$D_{12} = \frac{\overline{(r_1 - r_2)^2}}{6t} = \frac{\overline{r_1^2}}{6t} - \frac{\overline{2r_1 r_2}}{6t} + \frac{\overline{r_2^2}}{6t} = D_1 + D_2$$

if the motions of the particles are independent (i.e. correlation zero). If the particles are of equal size then $D_{11} = 2D_1$ and the number of particles colliding with one individual particle for $Dt/R^2 >> 1$ is equal to $8\pi DRN_0$. The number of collisions between particles of type i and type j is $4\pi D_{ij} R_{ij} N_i N_j$. The number of the k-fold particles increases by collisions of i-fold and j-fold particles in which i + j = k and decreases by any collision with the k-fold particles.

$$\frac{dN_k}{dt} = \frac{1}{2} \sum_{\substack{i=1 \\ j=k-i}}^{j=k-1} 4\pi D_{ij} R_{ij} N_i N_j - N_k \sum_{i=1}^{\infty} 4\pi D_{ik} R_{ik} N_i$$

L. Coagulation of Electrically Charged Particles

It can be shown that for the case of small aerosol particles carrying electric charges unipolar charging should cause a marked reduction in the rate of coagulation and that bipolar charging should accelerate coagulation, but to a lesser extent. Experimentally the effect of bipolar charging of particles has not been observed.

The effect of electrical fields was studied experimentally and it was found that a field of 200 V cm^{-1} produced no observable increase of coagulation of an oil mist (Fuchs, 1964). However, in a unipolar mist, a strong electrical field had the effect of increasing the coagulation rate. It was estimated in thunderclouds, where field strength reaches about 1000 V cm^{-1}, polarization coagulation of droplets may be considerable.

M. Correction for Coagulations of Small Particles

If the Knudsen number Kn is defined as the mean free path of the suspending gas divided by the radius of the particle, the Smoluchowski theory can not be applied for Kn greater than unity. That is, one can not apply the above theory to particles smaller than 0.1 μm (Hidy and Brock, 1965).

By the requirements of a Markoff chain on which the equations of coagulations are based, time intervals less than the time τ and distances less than the distance ℓ_β, the "apparent mean free path," can not be applied. A correction utilizing the Smoluchowski formulation, however, can be retained by considering the diffusion of particles toward an absorbing sphere in an established concentration gradient (Fuchs, 1964).

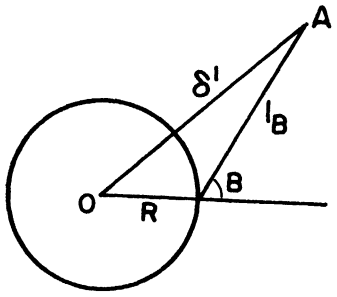

A particle may leave the surface of an absorbing sphere in a random direction. The mean distance δ' from the surface of the sphere reached by the particle after traveling the distance ℓ_β is $\delta' \sim \ell_\beta$ for $\ell_\beta \gg 2r$ and $\delta' \sim \ell_\beta$ for $\ell_\beta \gg 2r$. If a spherical surface of radius $2r + \delta$ exists, concentric with the absorbing sphere, and the concentration is n' at

the outer surface and n_0 at a large distance from the absorbing sphere, then the concentration n is

$$n(r) = n_0 - (n_0 - n') \left(\frac{R + \delta}{r} \right) .$$

The number of particles diffusing inward across the outer surface per unit time is

$$J = 4\Pi(R + \delta)^2 \, 2D \left(\frac{\partial n}{\partial r} \right)_{r = R + \delta}$$

$$= 8\Pi D \, (R + \delta) \, (n_0 - n') .$$

This number may also be determined by kinetic theory of gases which states in part that if the inner sphere were a drop of liquid in equilibrium with its vapor, the number of molecules evaporating from it in unit time and reaching the outer sphere is

$$J_1 = 4\Pi \, R^2 n' \frac{\sqrt{2} \, \bar{G}}{4}$$

Being in equilibrium an equal number of molecules would pass from the outer sphere to the inner. $J_1 = J$ so that

$$8\Pi(R + \delta)D \, (n - n') = \sqrt{2}\Pi R^2 \bar{G} n' .$$

Since $$\ell_\beta \bar{G} = \frac{8}{\Pi} D$$

$$8\Pi(R + \delta)D(n_0 - n') = 8\sqrt{2} \, R^2 D n' / \ell_\beta$$

then $$n' = \frac{n_0}{\frac{\sqrt{2} \, R^2}{\ell_\beta (R + \delta)\Pi} + 1}$$

$$8\Pi(R + \delta)D(n_0 - n') = 8\Pi RDn_0\beta$$

is written to preserve the form of the coagulation equation where β is the correction

$$\beta = \frac{1}{\frac{R}{R + \delta} + \frac{\Pi \ell_\beta}{R\sqrt{2}}}$$

δ' averaged over all directions is given (Fuchs, 1964) as

$$\delta' + \frac{1}{3R\ell_\beta}\left\{(R + \ell_\beta) - (R^2 + \ell_\beta{}^2)^{3/2}\right\} - R.$$

This expression substituted into the correction term β gives an improvement of the basic Smoluchowski equations.

N. Coagulation due to Turbulence

The motion of a suspended particle is made up of the motion of the particle relative to the medium plus the motion of the medium. If the motion of the medium is turbulent, added coagulation would be expected to occur, due to the random motion into which the particle would be set. One would expect turbulent coagulation to be important for larger particles due to their closer response to the larger scale random motion of the medium (i.e. reduced mobility causes consequent reduced response to Brownian motion.) An expression for the disappearance of particles N(r) due to turbulent coagulation is given by Smoluchowski

$$\frac{-dN}{dt} = K_T N(r)N(r')$$

where

$$K_T = 4/3\ w\ (r + r')^3$$

and where w is the velocity gradient normal to the stream line. K_T is plotted and compared to $K_{Brownian}$ for $r = 10$ μm and $0.01\ \mu m \leq 2r' \leq 10\ \mu m$ (Figure IV-1). Three values of the velocity gradient are given: 1) w = 4 (cm/sec)/cm, suggested by Whitlaw-Gray and Patterson, 2) w = 10 (cm/sec)/cm, suggested by Tunitzki's estimate for micro-eddies and 3) w = 30 (cm/sec)/cm, a possible upper limit. As is seen, Brownian motion stops being effective relative to turbulent motion for particles between 0.1 μm and 0.5 μm diameter. Turbulent motion is important for coagulation only when one particle is quite large (greater than 5 μm.)

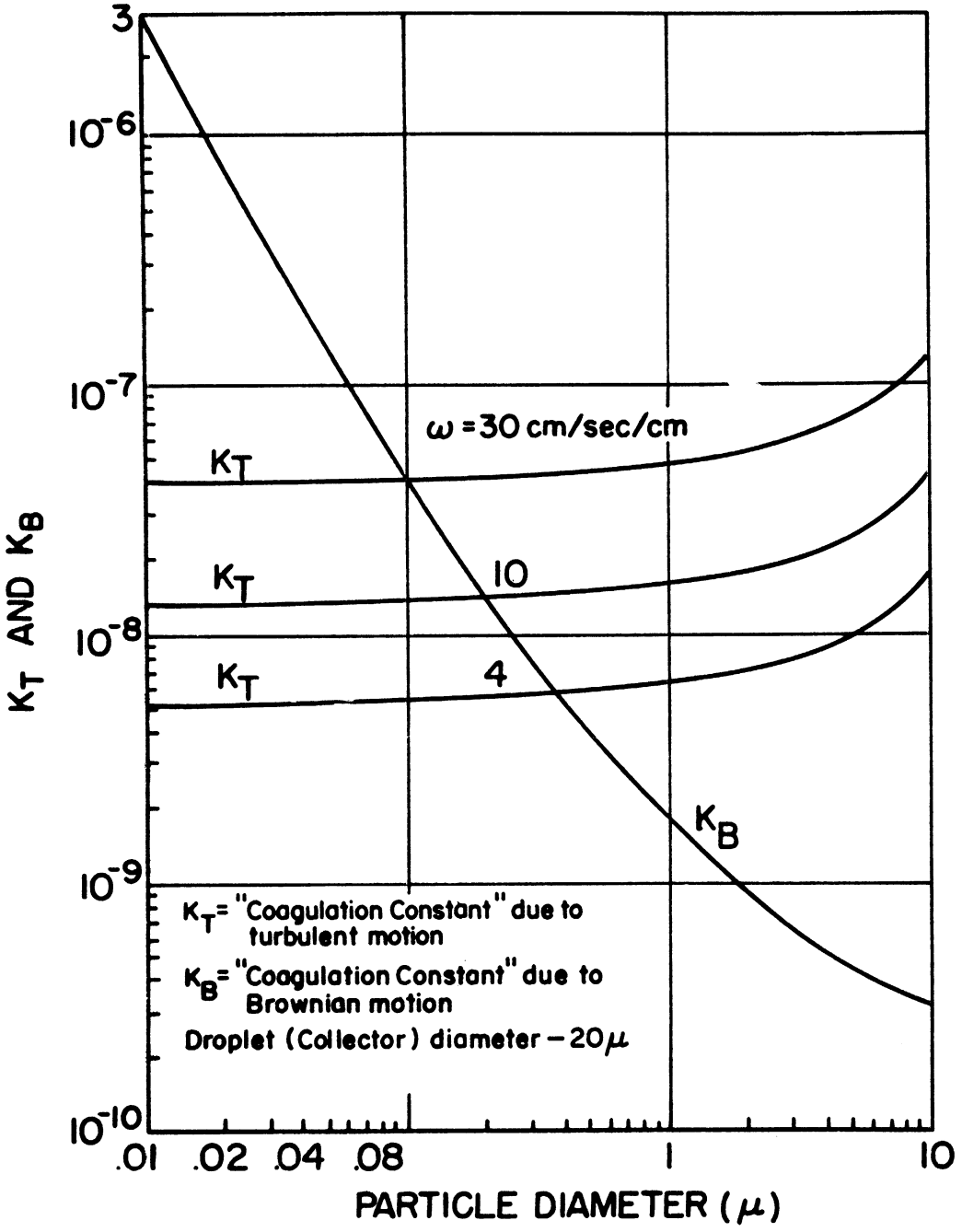

Fig. IV-1.--The coagulation coefficient for turbulent coagulation and Brownian (thermal) coagulation.